A biomechanical analysis of ice hockey skate blade design

Laura Holman

Department of Kinesiology and Physical Education

McGill University, Montreal

April 2024

A thesis submitted to McGill University in partial fulfillment of the requirements of the degree of Master of Science

Table of Contents

Abstract

The longitudinal shape of ice hockey skate blades, known as the blade profile, can be adapted to suit player preferences. The biomechanical effect of blade profile on skating motion and performance is not well understood. Additionally, few studies in ice hockey skating biomechanics have included female participants. This study examined the effect of blade profile on spatiotemporal performance variables, lower limb joint angles, and perception in elite ice hockey players during forward skating and tight turns on ice. The secondary purpose was to compare spatiotemporal performance variables and joint angles between males and females during these tasks. Twenty-six elite ice hockey players (12 male and 14 female) performed trials of a 19.5 m forward skating task and a 23 m 180-degree tight turn task (toward the left and right) on four distinct skate blade profile conditions. Trials were recorded with a video camera for the calculation of task completion times. Lower limb joint angles were measured using an inertial measurement unit-based motion capture system and compared between blade conditions and sexes using Statistical Parametric Mapping. Perception and preference were assessed using a 10 cm visual analog scale. Blade condition had no significant effect on spatiotemporal (task completion time), kinematic, and perception variables across all tasks. Significant differences in joint angles between sexes were revealed, primarily evident in hip adduction and knee flexion during forwards skating, as well as hip internal rotation, knee flexion, and ankle internal rotation during turning. VAS scores showed widespread individual variation in preference. Findings underscore the importance of prioritizing players' subjective experiences when blade profiling. Results have practical implications for training in tight turn technique, as well as female-specific considerations in both on and off-ice training and equipment design. Future research should explore the long-term effect of blade profiles on skating mechanics and examine the relationship between blade preference and individual player characteristics.

Abrégé

La forme longitudinale des lames de patin de hockey sur glace, connu comme la profile de lame, peut être adapté pour répondre aux préférences du joueur (euse). L'effet bioméchanique du profile de lame sur le mouvement de patinage et la performance n'est pas bien connu. En plus, seulement quelques études en hockey sur glace ont inclus des participants femelles. Cette étude à examinée l'effect de profile de lame sur les variables de performances spatio-temporelle, l'angle des joints du bas du corps, et la perception des joueurs (euses) de hockey élites pendant le patinage avant et les virages serrés sur la glace. Le but seconde était de comparer les variables de performances spatio-temporelle et l'angle des joints du bas du corps entre les males et femelles pendant c'est tâches de patinage. Vingt six joueurs (euses) élites de hockey sur glace (12 males et 14 femelles) ont performés des essais de patinage avant de 19.5 m et des virages serrés de 180 degrés sur 23 m (à la gauche et à la droite) avec quatre conditions de profile de lame distinct. Les essais ont étés enregistrés avec un camera vidéo pour la calculation de temps d'achèvement des tâches. Les angles du bas du corps ont étés mesurés en utilisant un système de capture de mouvement basé sur des unités de mesure inertielle et ont comparés les conditions de profile de lame et de sexe avec Statistical Parametric Mapping. La perception et la préférence ont étés évalués en utilisant une échelle visuelle analogique de 10 cm. Les conditions de profile de lame n'ont eu aucun effet significatif sur les variables spatio-temporelle (temps d'achèvement des taches), kinématique, et pour tous les variables de perceptions à travers tous les tâches. Des différences significatives dans les joints du bas du corps entre les sexes ont étés révélés, principalement évident pendant l'adduction des hanches et la flexion des genous pendant la patinage avant, ainsi que la rotation interne des hanches, la flexion des genous, et la rotation interne des chevilles pedant les virages serrés. Les résultats EVA ont démontrés une variation individuelle généralisée des préférences. Les résultats soulignent l'importance de prioriser les expériences subjectives des joueurs (euses) pendant le profilage de lame. Les résultats ont des implications pratiques pour l’entraînement de technique de virage serrés, ainsi que des considérations à l'entraînement sur et hors glace et la conception d’équipment spécifiquement pour les femelles. Le recherche future devrait explorer les effects long-termes des profiles de lames sur les mécaniques de patinages et examiné la relation entre la préférence de lame et les caractéristiques individuel des joueurs (euses).

Acknowledgements

Thank you to my supervisors Dr. Shawn Robbins and Dr. David Pearsall, for accepting me into the Ice Hockey Research Group and supporting me through each stage of my academic journey at McGill. Thank you for providing your valuable insights and feedback while allowing me the space to explore and problem solve independently. I have gained such a positive outlook on the research world and have become a more confident and proficient researcher thanks to your mentorship. Thank you to Phil Renaud, for your help with anything and everything. Your support with brainstorming and problem solving, with data collection and the many, many long hours of data processing, has been instrumental in the progress of this work. It’s been a fun journey, and I appreciate your approachability and sense of humour that made the day-to-day lab experience so enjoyable.

Contributions from Bauer Hockey Ltd. were vital to the success of this project, through financial/material support and research design development. The opportunity to collaborate with them has significantly enriched my academic experience.

Thank you to my lab mates and good friends, Kristin, Cait, Natalie, and Andrew, for making our lab into a second home for me. I am so grateful for the many ways each of you has supported me throughout my project. Those early mornings on the ice collecting data became a highlight of this project for me, thanks to your cheerfulness and humour, even during the unexpected challenges. I’ll never forget the memories we made in our lab, at the arena, during conferences, and on our many adventures. Working alongside you never felt like work at all.

Thank you to my family. Your facetime calls, care packages and letters, and visits to Montreal meant so much to me. Thank you to my parents for the unconditional support you gave to ensure my well-being throughout this experience. Thank you, Sarah, for your guidance with all things science and research related, and Sean, for always knowing how to make me laugh to lighten my stress. I would not have completed this without all your love and support.

Contribution of Authors

Laura Holman, MSc candidate, Department of Kinesiology and Physical Education, McGill University, was responsible for the research design, collection of data, data processing and analysis, and the writing of this thesis. The candidate's supervisors, Shawn M. Robbins, PhD, Associate Professor, School of Physical and Occupational Therapy, McGill University, and David J. Pearsall, PhD, Associate Professor, Department of Kinesiology and Physical Education, McGill University, contributed to the research design and analysis of data.

Phillipe J. Renaud, Department of Kinesiology and Physical Education, McGill University, acted as the lab research assistant, contributing to the research design, collection of data and processing and analysis of data. Richard A. Preuss, PhD, Associate Professor, School of Physical and Occupational Therapy, McGill University, was a member of the thesis committee.

List of Figures

List of Tables

List of Abbreviations

ROH	Radius of Hollow; hollowed curve connecting the blade's edges at the bottom surface of the skate blade
ROC	Radius of Contour; radius of the circle created by the longitudinal curvature of the blade
ROM	Range of Motion
COM	Center of Mass
COD	Change of Direction
IMU	Inertial Measurement Unit
VAS	Visual Analog Scale
ST	Stance phase – the phase during a stride cycle when the blade is in contact with the ice, from the ON event of one skate to the consecutive OFF event of the same skate
SPM	Statistical Parametric Mapping
DS	Double Support; the phase during a stride cycle when two skates are both in contact with the ice at the same time

1. Introduction

Ice hockey is a popular team sport known for its fast pace, physical contact, and skilful puck control. As the hallmark feature of the sport, skating is one of the most important skills to master (Pearsall et al., 2013). Performed on a low-friction ice surface, it requires unique movement adaptations compared to typical gait and specialized equipment to facilitate it. The distinctive frictional properties of the blade/ice interface enable a skater to not only glide over the ice at high speeds but also grip into the ice for push-offs and rapid changes in direction. The skate blade therefore plays a vital role in a player's ability to perform the complex skating skills involved in the game.

The optimization of skate blade design is valuable for skater performance. Typically, three blade features can be adapted to suit the preference of the skater: 1) the radius of hollow (ROH) which affects the depth of edge dig into the ice, 2) the radius of contour (ROC), which affects the longitudinal curvature shape, and 3) the pitch or pivot point, which affects the lean or lie angle of the blade. The radius of contour and the pitch together comprise the *profile* of the blade. When strategically adjusted, these elements can impact factors such as friction, skating speed, control, agility, and perception (Cadeau, 2017; Federolf & Nigg, 2012; Federolf & Redmond, 2010; McKenzie, 2012).

Adapting blade ROH to skater preference is common and is frequently maintained through sharpening. Players can opt for deeper hollows to achieve greater dig and "sharpness", or shallower hollows to achieve more glide and less bite (Lockwood & Frost, 2009). Regarding blade ROC adaptations, players can opt for a shorter ROC to achieve more control, or a longer ROC to achieve more blade contact, and better glide (Lockwood & Frost, 2009). It is also common to adapt one's blade profile beyond the typical single radius shape, as some profile designs now incorporate multiple contour specifications at various sections across the blade (Figure 1). This is thought to allow players to take advantage of the benefits of each size of contour across the blade. Despite these advancements, research and knowledge regarding the effect of blade profiling innovations on performance optimization are limited.

Figure 1

Single radius and multiple radius of contour designs

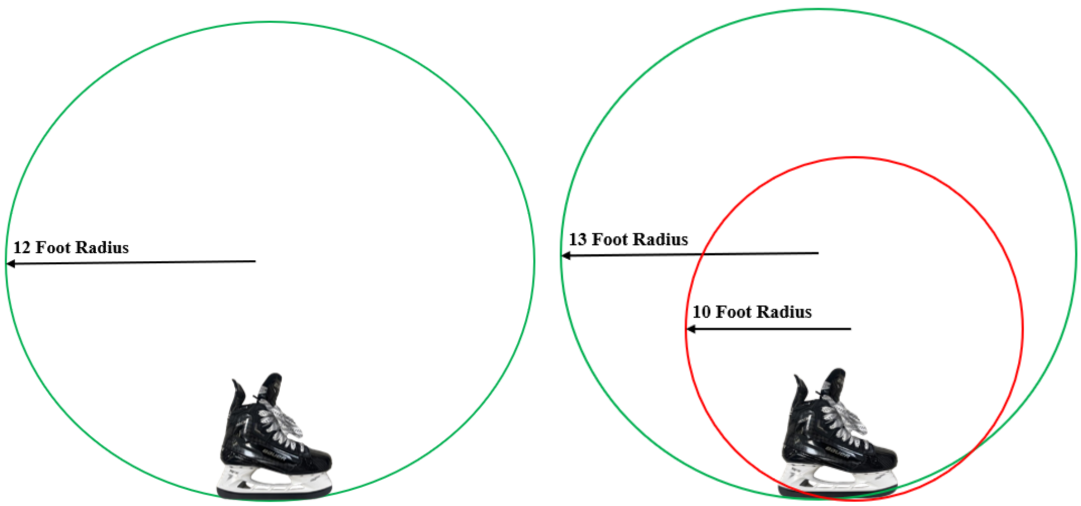

Note. Image is not to scale.

Research in ice hockey skating has made significant strides in characterizing the biomechanical aspects of skating and the effect of skate design on them; however, most of this research focuses exclusively on male participants. Female players are still compelled to adopt training practises and equipment that evolve from male data, which may present potential risks or be unsuitable for enhancing their performance. Previous research findings suggest that there are sex-specific differences in skating technique during forward skating and stopping (Budarick et al., 2020; Hallihan, 2018; Shell et al., 2017). Most prominent of these differences are greater hip and knee joint ranges of motion (ROM) reported in males. No study has analyzed sex differences in tight turn execution, and no study has analyzed the effect of skate or blade design on the biomechanics of female participants.

Current research in ice hockey biomechanics is limited in its examination of the biomechanical impact of skate blade features, particularly regarding the longitudinal shape, or profile, of the blade. There is also a notable gap in comparative analyses between male and female players, with limited focus on the effect of equipment design on female players, and the characterization of skating patterns specific to females. The two purposes of this research project were therefore to 1) compare the effect of four different skate blade profile designs on spatiotemporal variables, lower limb kinematics, and skater perception during forward skating and turning on ice and 2) compare spatiotemporal variables and lower limb kinematics between elite male and female ice hockey players during forward skating and turning on ice. The results of this study have implications for blade profiling and how it may contribute to the optimization of biomechanical factors and skating performance. Additionally, findings will contribute to the limited knowledge of skating mechanics specific to female players, which can inform future design approaches that fit their training and equipment needs.

2. Literature Review

2.1 Skate Blade Design and Characteristics

Ice skating has served as a method of locomotion for many centuries (Formenti & Minetti, 2007). Some of the first skates were developed from animal bones attached beneath boot soles (Formenti & Minetti, 2007; Pearsall & Robbins, 2019). By the 13th century, skating had evolved into an efficient mode of transportation in northern Europe and Russia, facilitating quicker transportation and communication over frozen waterways (Formenti & Minetti, 2007). Over time, skate blade design has undergone numerous modifications to the materials, shape, and design, aiming to improve both speed and metabolic efficiency in ice skating. Such blade shape modifications include features such as blade width, flare angle, edge levelness, hollow shape, contour shape, and pitch, all of which can affect skating performance and perception (Pearsall & Robbins, 2019).

2.1.1 Three Primary Modifiable Blade Shape Features

Three primary ice hockey skate blade shape features can be altered by the user post-manufacturing to match skater preference: depth of edge hollow, longitudinal curvature, and pitch angle. The depth of edge hollow is dictated by the size of the radius that connects the inside and outside edges, known as the ROH. Longitudinal curvature is dictated by the length of the radius of the circle formed by the contour, known as the ROC. Pitch angle is dictated by the difference in height between the fore and aft sections of the blade. The ROC and pitch of the blade together can also be referred to as the *profile* of the blade. These features are displayed in Figure 2.

Figure 2

Three primary ice hockey skate blade characteristics

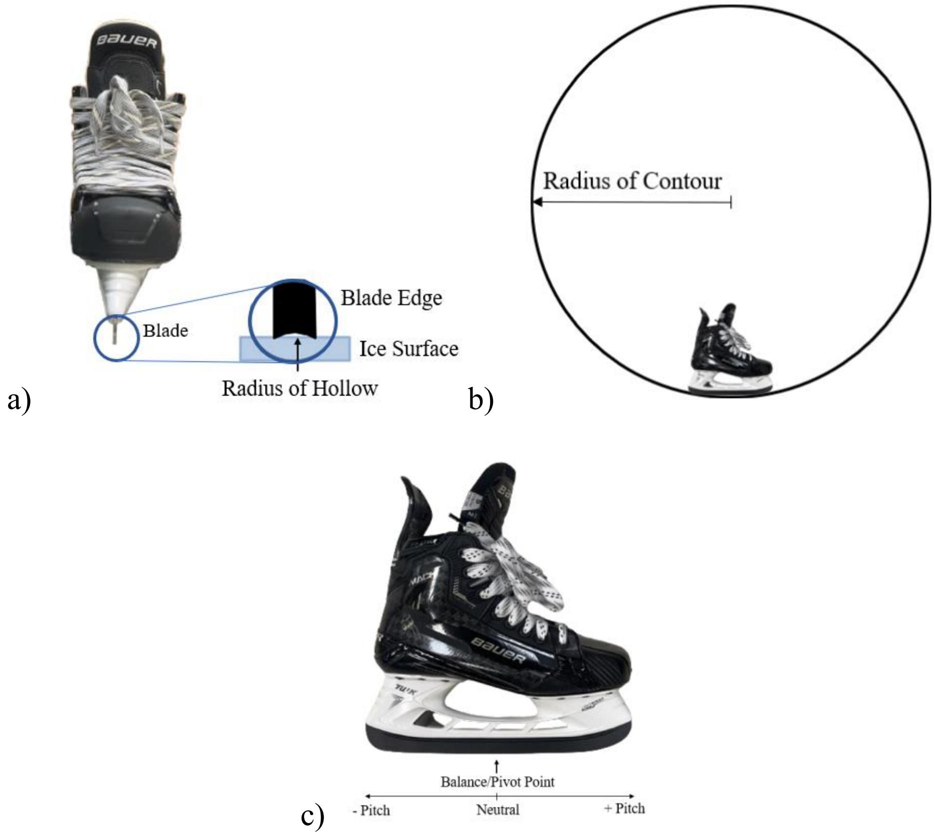

Note. a) Radius of Hollow (front view). b) Radius of Contour c) Pitch.

The ROH affects how deep the edges dig into the ice surface while gliding and pushing off (Lockwood & Frost, 2009). Typical ROH sizes used are 1/2" or 5/8" (12.7 mm or 15.9 mm, respectively) (Lockwood, 2003, as cited in Lockwood & Frost, 2009). Deeper ROH sizes create a deeper groove and are effectively “sharper”, which can result in shorter stopping time but reduced gliding speed due to an increase in friction (Federolf & Redmond, 2010; Gagnon & Dore, 1983; Lockwood & Frost, 2009). This is suggested to increase agility, as the increased “dig” can shorten stop/turn time while maneuvering (Federolf & Redmond, 2010; Gagnon & Dore, 1983; Winchester, 2007). Shallower ROH sizes are thought to increase speed as friction is reduced resulting from less “dig” into the ice (Federolf & Redmond, 2010).

The ROC dictates the amount of blade in contact with the ice. Typical ROC values used by players are between 8 – 12 feet (2.44 m – 3.66 m), but can be adapted beyond these dimensions (Lockwood, 2003, as cited in Lockwood & Frost, 2009). A longer ROC allows for more blade/ice contact which is thought to result in greater skating velocities (Lockwood & Frost, 2009). Conversely, a shorter ROC allows for less blade/ice contact allowing for greater skating agility as it can shorten the radius of a turn itself and may feel easier to control (Lockwood & Frost, 2009). More recently, it has become common for players to use blades with multiple contours at different sections of the blade, as opposed to a standard single radius design. This is thought to allow players to take advantage of both speed and agility benefits through controlled weight shifting toward differently contoured sections of the blade (Lockwood & Frost, 2009; Vienneau et al., 2017).

The pitch of the blade is dictated by the difference in height between the fore and aft segments of the blade which create the pivot/balance point and lie angle. The pitch is typically reported as the distance from the center of the blade to the pivot point, where negative values represent a pivot point that is more towards the heel, positive values represent a pivot point that is more towards the toe, and zero value representing a neutral pitch. Alterations to the pivot point are predicted to cause a forward or backward tilt in the blade and a subsequent shift to the skaters center of mass (COM) (Broadbent, 1985; Lockwood & Frost, 2009).

The ROH, ROC, and pitch of the blade are formed using a mechanized sharpening tool i.e., a high speed grinding stone (McKenzie, 2012). To sharpen the ROH, the stone is first dressed with the appropriate ROH length. The dressed stone is then applied to the blade's surface, spinning at high speed, creating a hollow impression at the bottom (McKenzie, 2012). To profile a blade, the blades are secured in a brace as the bottom surface moves across a grinding stone following a specific template shape running from end to end. This process removes portions of the blade material to create the desired contour and pitch (McKenzie, 2012). Typical profiling machines, such as the Prosharp-Bauer AS1001 and AS2001, apply the profile template to at least 60% of the blade length at the center (Prosharp-Bauer, 2021). The remaining blade ends are often "blended" to create a smooth transition into the profiled section. The blending process is not automated, and the grinding wheel is manually manipulated, which may introduce user-driven variation to the final blade shape.

2.1.2 Blade-Ice Interaction

A widely examined phenomenon in ice skating research is the inherent slipperiness of ice and the mechanisms at play that allow for gliding between ice and blade. Generally speaking, this phenomenon is made possible by a significantly low coefficient of friction resulting when metal interacts with ice (Lockwood & Frost, 2009). Although not conclusive, early and most widely accepted theories center around the presence of a thin liquid film formed between the blade and ice surface, as a result of high pressure and/or frictional heat (Bowden & Hughes, 1939; Lever et al., 2022; Lockwood & Frost, 2009; Reynolds, 1899). Other more recent theories suggest the presence of ice-rich slurries located across high-pressure zones allowing for lubrication of the surface between blade and ice, which enables the slipperiness suited for gliding (Lever & Lines, 2023; Lever et al., 2022). While the exact mechanisms remain inconclusive, the functionality of gliding persists. Skate blade manufacturers continue to innovate blade design features including both shape and material that can influence blade ice interaction. Innovations often incorporate various materials and coatings that claim to achieve lighter weight as well as better edge retention over time and improved glide (Abkowitz et al., 2004).

2.2 Quantitative Factors of Blade Design

2.2.1 Radius of Hollow Investigations

ROH depth can influence the friction dynamics between blade and ice. Federolf and Redmond (2010) tested the effect of ROH depth on friction coefficients using aluminum sled tests. Mounted on different test blade conditions, the sled was accelerated on the ice surface via air compressor, and coefficients of friction were calculated using the mean deceleration of the sled over 8m. They tested three separate ROH depths (6.35mm, 12.70mm, and 19.05mm), and discovered the shallower hollows (12.70mm and 19.05mm) reduced the coefficient of friction during the sled test by 11% and 19% respectively, when compared to the 6.35 mm ROH blade. The deepest hollow proved to exhibit the greatest coefficient of friction, as the edges are subjected to a deeper cut into the ice (Federolf & Redmond, 2010).

Federolf and Redmond (2010) also analyzed whether or not the difference in friction coefficients could lead to meaningful difference for skating performance such as skating task completion time. In this study, 15 participants completed an agility course with a combination of wide and narrow turns on ice, in three separate ROH conditions: 1) their normal hollow, 2) a ROH reduced by 6.35 mm from their normal hollow and 3) a ROH increased by 6.35 mm from their normal hollow. It was found that the deeper hollow condition generally led to an increase in completion times, although these results were non-linear. The majority of participants experienced their slowest run times in the condition that was deeper than their normal hollow.

Other edge related designs apart from the conventional ROH have been explored and subjected to testing. McKenzie (2012) tested the effect of a flat-bottomed hollow shape, as opposed to a rounded hollow, on skating task performance times. The theorized benefit of this blade design is to allow for the bite angle to remain consistent across different hollow depths. A total of 40 varsity and elite midget male hockey players performed several skating skill tasks on a conventional rounded hollow (1.27 cm) and a flat-bottomed hollow blade condition. The flat bottom hollow condition showed subtle improvement in specific performance aspects of the tasks, such as linear speed by 1.13% for varsity players, and 0.72% for midget players; however, it had adverse effects on other measures such as the acceleration and agility portions of the tasks. This indicated that the change in shape did not provide consistent benefit for hockey skating skill performance.

Another edge design investigated is the flared edge design, where the edges of the skate blade lay at an outward angle at the bottom of the blade. Using the aluminum sled test method, Federolf, Mills, and Nigg (2008) tested frictional coefficients of blades with three flared angles (4, 6, and 8 degrees) in comparison to a standard ROH edge design. It was found that the coefficients of friction were reduced from the standard condition by 13%, 21% and 22% for the 4-, 6-, and 8-degree flared blades respectively. This design was taken to the ice by Federolf and Nigg (2012), where they compared skating task completion times on a tight turn course, and straight forward skating task between a flared edge design (ROH 0.08mm and flare angle of 8 degrees) and a normal ROH design (ROH = 0.08mm). It was found that run times on the tight turn course, and straight skating task were improved by 1.3% and 1.0% respectively, in the flared design compared to the normal design.

2.2.2 Radius of Contour and Blade Profile Investigations

Some researchers have theorized the biomechanical impact of ROC and blade profile design. Broadbent (1985, as cited in Cadeau, 2017) developed mathematical models that suggest an increase in the pitch angle of the blade at the heel will lead to a forward shift in the player's center of mass (COM). It was also proposed that a player's point of balance on their feet changes as a function of both the pitch and the ROC of the blade. Lockwood and Frost (2009) suggest that blade design can affect lower extremity alignment. For example, a more backward leaning pitch can act to raise the front of the foot, dorsiflex the ankle, and flex the knee. Holding this posture for a prolonged period throughout a game may continually stretch the plantar flexors and put greater stress on the quadriceps which could increase the risk of injuries such as patellofemoral syndrome and Achilles tendinitis (Lockwood & Frost, 2009).

Various studies have analyzed the impact of ROC during on-ice studies. McKenzie (2012) investigated the effect of various ROC profiles on the time to completion of a linear acceleration course and a combination multi-skill course that included various change in direction and pivot tasks. Three different blade profiles were compared: 1) the player's current ROC and ROH (used as a baseline), 2) a moderate triple contoured blade i.e., a profile incorporating three contours, with increasing radius size from front to back of blade with a moderate difference between each contour (2.74 m – 5.08 m – 3.05 m from front to back), and 3) a triple contoured blade, with increasing radius size from front to back of blade and a more substantial difference between each contour (2.13 m – 5.08 m – 3.96 m from front to back). The ROH for the two triple contour conditions was kept consistent at 1.27 cm. Varsity male players showed significant improvement in their completion time of the combination multi-skill course and the linear acceleration course with condition 2, the moderate triple contour profile when compared to the baseline ROC profile. Overall time on the combination agility and linear speed test was reduced by an average of 1.47% when using the moderate triple contour compared to baseline. Their increase in speed may have been due to the increased amount of blade in contact with the ice from the flat transition area that lengthened the radius at the back of the blade. Players also tended to prefer the feel of the moderate triple contour – as their familiarity, comfort, and confidence may have been compromised while in condition 3, the more radical triple contour profile (McKenzie, 2012).

Only one known study has empirically analyzed the effect of ROC on bodily factors such as joint angles and foot plantar pressure. Vienneau et al. (2017) analyzed the impact of blade ROC on hip range of motion and plantar pressure patterns during backwards skating. Three different blade contour profiles were compared including a standard single radius, a short single radius (i.e., the agility profile) and a combination profile which consisted of a short radius at the anterior portion of the blade and a longer radius at the posterior portion of the blade. Specific radii measures were not disclosed by the authors. During the backwards crossovers task, the fastest performance times were seen with the agility profile, followed by the standard and then the combination profile. The greatest hip extension angle at push-off was seen with the standard profile. The agility profile showed the greatest hip flexion/extension range of motion. More plantar force was produced in the agility and standard profile compared to the combination profile. Overall, completion time for the backwards crossover task was 2.3% faster in the agility profile compared to the standard longer single radius (Vienneau et al., 2017).

Quantifying the impact of individual blade alterations is challenging, as each blade factor (such as ROC) when altered independently, may yield different effects when combined with other adaptations (such as pitch or ROH). Cadeau (2017) investigated this complexity by analyzing the effect of recommended ROH, ROC, and pitch conditions combined, based on player weight and position. Lighter players were recommended shorter contours and deeper hollows, and vice versa for heavier players. The pitch was recommended based on position where forwards were given a pivot point that centered further towards the heel compared to defenders. 40 elite male hockey players performed eight skating tasks including skills such as forward skating, backward skating, cross overs, and stop and starts. Performance variables such as completion time and movement initiation time were compared between the players current blades and the new recommended blade condition. Significant differences were found in movement initiation time and total time in four of the eight skating tasks assessed, revealing that players exhibited faster times in the recommended blade condition as opposed to their current blade conditions. The average reduction in skating time for isolated skill tasks was 0.0011 s/kg for movement initiation time, and 0.0012 s/kg for total time. Average reduction in skating time for the combined skating drill was 0.0052 s/kg for movement initiation time, and 0.0032 s/kg for total time. While statistically significant, the observed differences are subtle. Overall, the results of this study highlight the challenge of determining optimized blade conditions for individual players and indicate the need for further investigation.

2.3 Qualitative Factors of Blade Design

Personal preference, comfort and "feel" are major factors that drive a player's choice in skate blade characteristics (Pearsall & Robbins, 2019). Blade preference can be impacted by factors such as weight or position (Lockwood & Frost, 2009). Heavier players typically lean toward longer ROC and shallower ROH whereas lighter players tend to prefer a shorter ROC and deeper ROH (Lockwood, 2003). This is possibly due to the increase in bite a lighter player can achieve with a deeper hollow, and a more controlled feel with a shorter ROC (Lockwood & Frost, 2009). Blade pitch adjustments may also improve "feel" based on the demands of a player's position, as defenders may prefer their pivot point to facilitate backward skating movements, and attackers may seek a more forward leaning pitch to feel more on their toes (Lockwood & Frost, 2009). Level of familiarity can also impact blade preference especially when experimenting with more extreme styles of ROC and profiles that are much different from the standard single ROC design (McKenzie, 2012).

Donnelly (2010) tested players subjective observations from ROH, ROC, and pitch conditions that were both greater and less than their normal conditions. In shorter ROC and deeper ROH compared to their normal blades, participants reported difficulty stopping and discomfort from the limited blade-ice contact. In longer ROC and shallower ROH, participants reported difficulty turning but an improvement in gliding. Pitch angle created discomfort with too much forward or backward lean, which led some participants to experience lower back pain and an unbalanced feeling. Some comparative blade perception studies analyze player capacity to accurately distinguish between blade condition and the effects on their performance. Federolf and Redmond (2010) found players struggled to identify the ROH conditions they were skating on and performed best on. Cadeau (2017) discovered that players did not necessarily prefer the blade condition that resulted in shorter skating times. A blade with an enhanced sense of feel has the potential to, but may not always, enhance performance, and therefore both factors need careful consideration when choosing blade specifications.

2.4 Sex Differences in Ice Hockey Skating Mechanics

Much of prior ice hockey biomechanics research involved male participants only. Inappropriately excluding females from research participation can lead to unequal distribution of benefits or cause harm if concepts discovered from male data are applied improperly to female populations. Injury mechanisms and risk factors often present differently in male and female athletes, which may be due to differences in body segment parameters, muscle strength and stiffness, joint laxity, or training techniques (Bonci, 1999; Panagodage Perera et al., 2018). In ice hockey specifically, female athletes tend to experience concussions and lower body injuries such as adductor strains and ankle sprains most frequently, whereas males tend to experience upper body injuries most frequently (MacCormick et al., 2014; Schick & Meeuwisse, 2003). Previous research findings suggest that there are sex-specific differences in skating technique during forward skating starts, full strides, and a stop-and-go task (Budarick et al., 2020; Hallihan, 2018; Shell et al., 2017).

2.4.1 Forward Skating Starts

Using 3-D motion capture cameras on ice, Shell (2017) analyzed joint angular motion on ice during the first seven steps of forward skating starts in elite male and female ice hockey players. Males were able to reach greater peak speeds by the seventh step and displayed significantly wider stride widths compared to the female players. Males tended to exhibit greater hip flexion/extension during the final two steps of the skating sequence, and greater hip abduction at all steps by an average of 10 degrees. Males also exhibited greater knee flexion by about 10 degrees during the 4^{th} and 6^{th} step (Shell et al., 2017).

2.4.2 Forward Skating Maximal Speed

Similarly, during maximal speed strides, Budarick (2020) analyzed joint angle differences between male and female elite skaters on ice using 3D motion capture. Greater hip abduction was reported in males by about 7 degrees compared to females, and greater knee flexion was displayed by males throughout the stride. A more prominent knee extension plateau was discovered in females, where the phase of knee extension upon blade contact was lengthened in comparison to male skaters. Females also displayed a tendency for greater pre-extension of the knee, as their skate met the ice with each stride. Sex differences in stride width were not found to be significant at maximal speed, as they were during skating starts (Budarick et al., 2020; Shell et al., 2017).

2.4.3 Stop-and-go

Sex-specific differences were also detected during a more agility-type task, a stop-and-go. Specifically, joint angles and center of mass (COM) movement were compared between elite male and female hockey players using 3D motion capture cameras on ice as players performed a full-stop and 180 degree turn (Hallihan, 2018). Female players tended to skate into the stop with more upright body positioning, less forward trunk lean, less hip flexion, and less knee flexion compared to male players. Males maintained a relatively stable COM position for a longer period of time before rapidly dropping it just before entering the stop, whereas females tended to lower their COM more slowly prior to the stop phase. This plyometric technique used by males may have allowed them to exit the stop more rapidly, and likely produce more force and generate greater accelerations out of the stop (Hallihan, 2018) .

Of the presented studies that do involve female participants, none include an analysis of skate or blade design. There is currently a lack of knowledge regarding how this equipment performs with or is perceived by female players, whether it suits their needs or if it is beneficial to them and how it compares with the experience of male skaters.

2.5 Knowledge Gaps

In examining the current state of ice hockey skate blade research, several gaps exist. Numerous studies delve into the effects of ROH, ROC, and pitch alterations particularly on factors like friction, skating task completion time, skating speed and player perception; however, there is a lack of research exploring their impact on overall bodily motion and mechanics. As the blade profiling industry continues to market and cater to athletes for performance improvement, understanding the benefits of blade design modification is becoming increasingly more valuable for coaches and players. The scientific impact of skate blade adaptations remains relatively unexplored. Additionally, despite the extensive participation of females in ice hockey globally, a significant gap persists, with limited research focusing on the male/female comparison in skating biomechanics. Sex-specific differences exist during forward skating starts, full strides, and stopping tasks; however, other skating tasks remain unexplored. Also, no known study has yet examined the biomechanical effect of equipment design on female ice hockey players.

2.6 Objectives and Hypotheses

The primary objective of this research project was to investigate how four specific ROC profiles affect spatiotemporal variables, lower limb joint angles (hip, knee, and ankle), and skater perception during forward skating and turning on ice in elite ice hockey players. Blade conditions being compared in this study vary in their longitudinal contour shape, as well as the number and size of contours throughout the blade. The secondary objective was to compare males and females in spatiotemporal variables and lower limb joint angles during forward skating and turning on ice.

Hypotheses for blade condition effects include: 1) Profiles with less blade contact at the toe region (i.e., Triple Radius and Quadruple Radius profiles) will lead to less hip flexion and greater ankle dorsiflexion angles at end-stride. 2) Profiles with greater ice contact (i.e., Single Radius and Ellipse profiles) will result in faster forward skating completion times, but slower turn task completion times when compared to profiles with less blade contact. Hypotheses for the effect of sex include: 1) Males will complete the forward skating and turning tasks in less time compared to female participants. 2) Males will display greater hip and knee flexion and hip abduction angles, during forward skating and turning, when compared to females.

3. Methods

3.1 Participants

Twenty-six elite male (n=12) and female (n=14) ice hockey players were recruited for this study (Table 1). Participants were free from serious injuries of any type at the time of testing that could have prevented them from practicing or playing. Participants were excluded if they did not use Bauer Ltd. brand skates as they would not be compatible with the blades used in the study. Participants were primarily recruited from the McGill University men's and women's varsity ice hockey teams; however, participants were also recruited from outside the McGill community from a slightly lower caliber, to broaden the pool of eligible participants with the appropriate skate type. Elite was defined as having previously played at the AAA level or higher. Of the 26 participants, 18 were currently competing at the Canadian USports level, 5 participants had previously competed at this level, and 3 had previously competed at the AAA level. All skater positions were included, except goaltending.

Table 1

Participant demographics

Measure	Male (mean (SD))	Female (mean (SD))
Height (m)	183.5 (4.3) *	168.2 (6.1) *
Weight (kg)	86.0 (9.2) *	65.0 (8.0) *
Age (yrs)	26 (6) *	20 (2) *
Hockey Playing Experience (yrs)	19 (4) *	14 (2) *

Note. * Indicates a significant difference between males and females ($p < 0.01$).

The sample size was determined appropriate through an a priori power analysis using G*power (Faul et al., 2007) considering a significance level of 0.05, statistical power of 0.80, and an estimated medium-large effect size (effect size of f = 0.5). The estimated mean effect size was determined from previous studies comparing skating kinematics between males and females on ice, particularly the effect sizes for variables showing significant differences in hip adduction and knee flexion (Budarick et al., 2020; Shell et al., 2017).

3.1.1 Ethical Considerations

A certificate of approval for research involving human participants was granted by the McGill University Research Ethics Board II after an application was submitted (File #: 22-08-025) (Appendix A). All participants provided their informed consent before participating by signing a written consent form clearly outlining the procedure, compensation, potential risks and benefits, and the voluntary nature of the study (Appendix B).

3.2 Location

The study took place at the McConnell Arena on the McGill University main campus in Montreal, Quebec, Canada. Testing occurred between November 2022 to February 2023.

3.3 Instrumentation

The Xsens MVN Link (Xsens, Enschede, Netherlands) inertial motion capture system was used to collect kinematic data. This portable system contains a collection of 17 Inertial Measurement Unit (IMU) sensors. Each IMU contained a 3D linear accelerometer, 3D gyroscope, 3D magnetometer, and a barometer. The sensors were connected to each other via wires and were attached to the participant’s body segments at 17 locations including the head, sternum, pelvis, shoulders, upper arms, forearms, hands, upper legs, lower legs, and feet (Figure 3). This system collected data at a sampling frequency of 240 Hz.

Figure 3

IMU sensors and placement locations on human figure and live participant

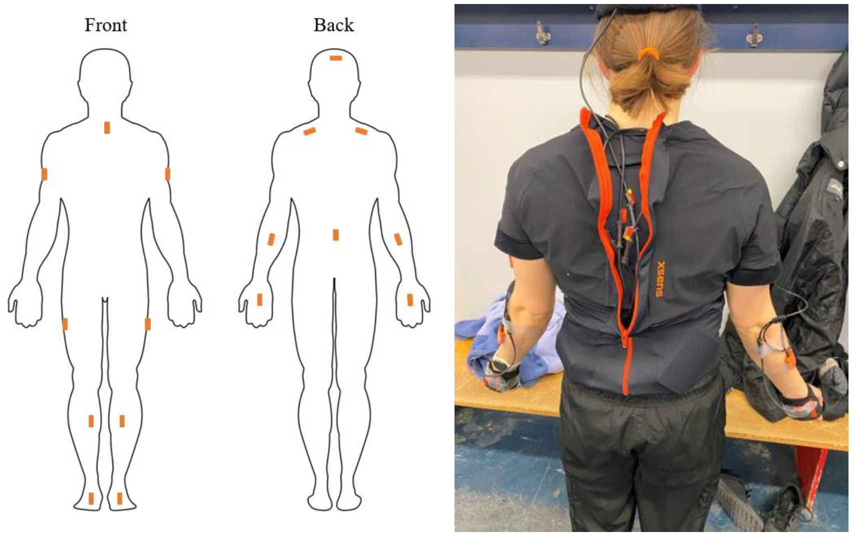

Note. Sensor placement image has been adapted from Denroche (2020).

The Dell UltraSharp Webcam camera was used to video record the trials which was used for post-hoc visual analysis and calculation of task completion times. The camera was set up stationary in the arena by the testing area and was synchronized to record simultaneously with the Xsens MVN Link system. Video data were recorded at a sampling frequency of 60 Hz.

3.4 Experimental Protocol

3.4.1 Off-Ice Prep

The participants were prepped for the data collection session in a private changeroom in the arena building. Each participant filled out an information form to provide information about their hockey playing experience, age, the equipment they use (i.e., skate model, sharpening characteristics of their current blades etc.) and their injury history (Appendix C and Appendix Table D1). Current skate blade characteristics were self-reported by participants. The participant was weighed with a scale and their body measurements were taken with a flexible ruler and inputted into the Xsens MVN system for calibration. Body measurements included total height, shoulder height, hip height, knee height, ankle height, arm span, wrist span, elbow span, shoulder width, hip width, and foot length.

The IMU system (XSens, Enschede, Netherlands) was placed on the participant. If the participant was female, they were accompanied by a female researcher, and vice versa for males. The 17 IMU sensors were placed on various body segments (Figure 3). The sensors were placed directly on the participant's skin (with the exception of the head, feet, and hand sensors), secured with double sided tape and a layer of medical tape overtop. The sensor on the head was secured in a headband worn by the participant. The sensors on the feet were secured with duct tape to the laces of the skate (Figure 4). The sensors on the hands were secured with Velcro inside small gloves worn by the participant. The sensors were attached with wires to a body pack fastened in the back pocket of the Xsens shirt worn by the participant. The body pack communicated wirelessly with the computer using a Wi-Fi connection access point, allowing the participant to skate freely. A battery pack was fastened in a back pocket of the shirt and connected via wire to the body pack. The pockets, holes, and zippers on the back of the Xsens shirt organized the wires to avoid having loose wire slack that could disrupt the participant's movement. Excess wire slack from outside the shirt was taped down with medical tape to the skin. The participants wore track pants and a long sleeve top over the sensors and Xsens shirt. Body segment measurements taken were entered into the Xsens software system to prepare for calibration.

Figure 4

Xsens IMU sensor secured to skate

3.4.2 On-Ice Calibration

The participant was calibrated to the Xsens MVN Link system by performing a short calibration trial to ensure the virtual body model was rendered correctly. This involved standing in an initial static neutral pose, walking 4 m in one direction, turning, and walking back to the original static position. This took place on a carpet on the ice surface. The computer and Wi-Fi access point were set up on the ice near the participant where the researcher recorded the trials.

3.4.3 Blade Conditions

Participants performed trials of skating tasks in four different blade conditions. The blade conditions studied were profiles specific to Prosharp-Bauer (Table 2). Four categories of blade profiles were studied which included the Single Radius, Triple Radius, Quadruple Radius, and Ellipse profiles. The Single Radius profile contained one single radius (10 ft.) that acted like a control condition. This radius corresponds to the standard out-of-box condition of Bauer Hockey Ltd. Blades. The Triple Radius profile contained three differently contoured regions, intended to increase agility. The Quadruple Radius profile contained four differently contoured regions across the blade, intended to increase the contact surface and provide a more balanced feel. The

Ellipse profile contained one ellipse-shaped contour (rather than circular), intended to provide a seamless feel and optimal ice contact during any skating task.

The Triple, Quadruple, and Ellipse Profiles encompass Prosharp-Bauer's "Performance Profiles". These blade conditions were chosen as they represent common variations in skate blade profiles involved in current industry practice. Specific radii of the contoured regions and the pitches of each blade type were proportionally different depending on the size of the skate/blade holder used by the participant, consistent with the current recommendations of the manufacturer. All blade conditions were sharpened to the same ROH of 5/8".

Table 2

Blade condition specifications

Profile Type	**Profile Size**	**Skate Size**	**Radius of Contour Specifications (ft)**	**Pitch (mm)**
Single Radius 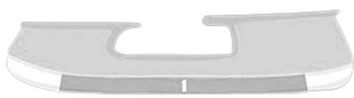	N/A	4-12	10	0 (Neutral)
Triple Radius 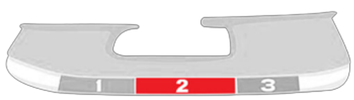	XXS	4	5 – 10 – 13	-15
	XS	5-6	5 – 11 – 13	-17
	S	7-8	6 – 12 – 20	-20
	M	9-10	6 – 13 – 20	-20
	L	11-12	6 – 14 – 20	-20
Quadruple Radius 	XXS	4	5 – 7 – 9 – 11	-15
	XS	5-6	6 – 8 – 11 – 12	-17
	Zero	7-8	6 – 9 – 11 – 13	-20
	I	9-10	6 – 9 – 12 – 15	-20
	II	11-12	7 – 10 – 13 – 16	-20
Ellipse 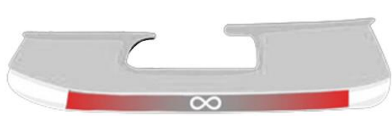	XXS	4	N/A	-15
	XS	5-6	N/A	-17
	Zero	7-8	N/A	-20
	I	9-10	N/A	-20
	II	11-12	N/A	-20

Note. Pitch values represent the distance from the pivot point to the center of the blade, with 0mm representing a pivot point at the center line, and negative values representing a pivot point more toward the heel. Blades with multiple contours show from left to right the contours from the front to back sections of the blade. Blade and holder images are taken from Prosharp-Bauer.

Each set of blades was re-sharpened and re-profiled after every three participant's use to maintain the ROH depth and the profile shape of each blade. This corresponded to approximately 30 minutes of use between each sharpening/profiling. The blades were sharpened and profiled by the blade manufacturers using the same mechanized machines (AS2001, Prosharp-Bauer). These machines were cared for and serviced by the manufacturers. The AS2001 is pre-programmed to form the blades into their respective profiles based on the desired parameters. To sharpen or profile, the blades were secured into a holder and moved across a grinding wheel to form the desired profile or hollow shape. For profiling, a physical template matching the shape of the profile was used to guide the wheel to grind the blade to the appropriate specs. Separate grinding wheels are typically used to profile and to sharpen the blades within the machines.

3.4.4 Skating Tasks

Three skating tasks were performed by the participant (Figure 5):

1) <u>Forward Skating:</u> Starting at the goal line, the participant accelerated forward on the researchers "go" command at full speed until they passed the first blue line (~19.5 m).

2) <u>Right Tight Turn:</u> Starting at the blue line, the individual skated forward on the researcher's "go" command at full speed toward the opposite blue line, performed as tight of a turn as possible toward the right (clockwise 180˚) around a cone at the opposite blue line without stopping and skated back to the center red line (~22.86 m).

3) <u>Left Tight Turn:</u> Starting at the blue line, the individual skated forward on the researcher's "go" command at full speed toward the opposite blue line, performed as tight of a turn as possible toward the left (counterclockwise 180˚) around a cone at the opposite blue line without stopping and skated back to the center red line (~22.86 m).

Figure 5

Skating task trajectories

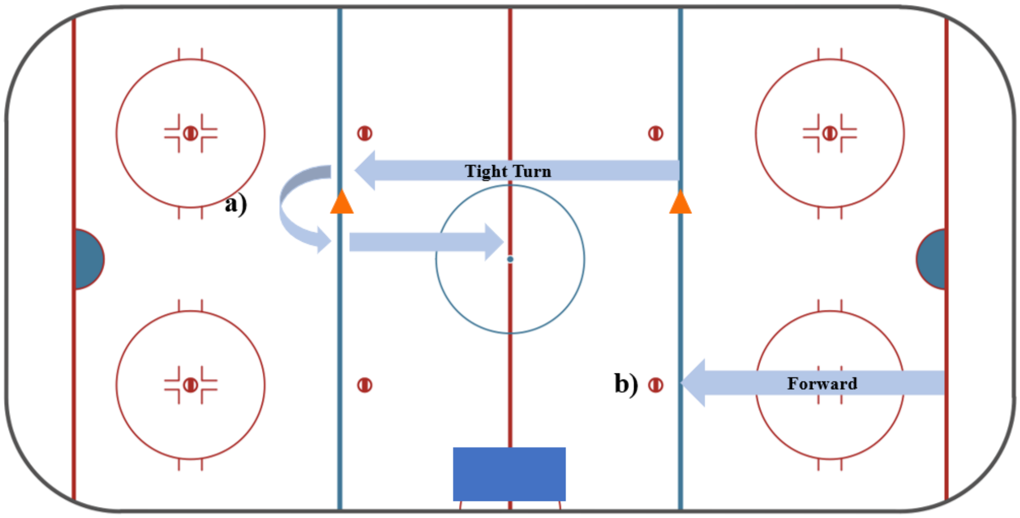

Note. a) Tight turn skating task trajectory (only the right turn direction is shown). b) Forward skating task trajectory. Blue arrows represent the direction of movement. Orange triangles represent cones placed on the ice to mark the target turning point. The blue rectangle represents the researcher's computer and camera set-up area.

Pylons were used to mark the target turning points on the ice. Participants performed three trials of each task in four different blade conditions, for a total of 36 tasks. Participants took approximately 30 seconds of rest between trials of the same task to re-set for the next trial. Additional rest and/or water breaks were provided whenever necessary. A five-minute period of warm-up time was given at the start of the trials and between blade conditions to freely skate, to get acquainted with the feel of the new blade condition. Participants were blinded to the blade condition. The blade order and task order were randomized for each participant using a random number order generator. Each individual participant performed their tasks in the same order for each blade type, but the task order was different for each participant.

To maintain optimal ice quality and minimize the effect of damaged ice, the task course set up was moved to fresh ice periodically throughout the testing session. Participants wore their familiar skates, the ones they used regularly during practise and in competition. The skates were

Bauer Ltd. brand with the blade releasing trigger technology, which allowed for easy removal of the blade from the blade holder when changing blade conditions.

Participants carried a stick to maintain skating mechanics as close to their true nature as possible. Participants were instructed to skate through the end point (blue line for forward skating, red line for tight turns). Participants were told to perform each task as they felt most comfortable and were not restricted to any specific step sequence or pattern; however, they were instructed to perform a front facing start (not a crossover start). Participants were told to skate as fast as possible within control, to mimic game-like intensity during each skating task.

3.4.5 Participant Feedback Perception Scores

After completing three trials for each task in a given blade condition, participants completed a feedback questionnaire containing four questions about their subjective perception of the blade condition. They rated the blades on three factors – forward performance (Figure 6), turn performance, and an overall rating, using a 10 cm Visual Analog Scale (VAS) (Appendix E). Participants placed a vertical mark along each line to rate the blade condition from "least ideal" to "most ideal" regarding each factor. Participants were told to consider all significant factors for task performance, such as their perception of speed, balance, stability, and confidence to provide a holistic rating on how ideal the blade condition felt. Participants were also able to provide written comments if they felt necessary, for supplemental subjective feedback.

The distance in millimeters from the left anchor of the VAS scale to the mark made by the participant on each line was measured with a ruler and recorded as a numeric score. Each participant therefore had a score for each questionnaire item (i.e., forward score, turning score, and overall preference rating score) on a scale from 0-100 mm.

Figure 6

10 cm Visual Analog Scale for forward skating rating

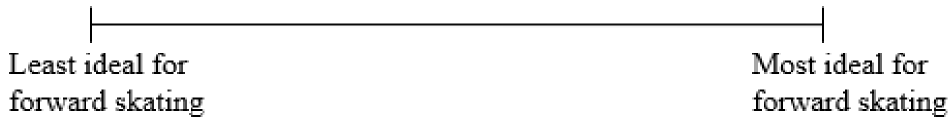

3.5 Data Processing

Data from the Xsens MVN system were exported to Visual3D x64 Professional software (version 2023.03.1, C-Motion, Germantown, MD, USA) for calculation of joint angles and stride event detection. This allowed the researcher to identify when skate ON and OFF events occurred for each trial. This was used to separate trials into stance phases, and to calculate metrics such as double support phase time and turn time.

Joint angles were first calculated in Visual 3D software from segment orientations measured by the Xsens system. The joint reference frame axis system was defined as follows: X-rotation signified sagittal plane rotation, Y-rotation signified frontal plane rotation, and Z-rotation signified transverse plane rotation, to align with the previous lab-standard axes system. Joint angle calculation followed the Euler X, Y, Z order of rotation. Hip flexion, adduction, and internal rotation were positive, knee flexion and internal rotation were positive, and ankle dorsiflexion, inversion, and internal rotation were positive. Sagittal, frontal, and transverse planes were analyzed for both the hip and ankle, and only sagittal and transverse planes were analyzed for the knee. Calculated joint angles from Visual3D were further processed using the BiomechZoo toolbox (Dixon et al., 2017) which occurred after event detection and labelling, in MATLAB (version 2017b, Mathworks, Natick, MA, USA). Trials were normalized to 101 data points. A mean trial was calculated for each participant using all three trials within each task and blade condition.

Skate ON and OFF events were determined using sagittal plane knee angle and vertical foot acceleration signals. This method of event detection was based on the work of Khandan et al. (2022), which validated event detection from vertical foot acceleration against events detected from instrumented force sensing insoles in skates. Vertical foot acceleration signals were filtered using a lowpass Butterworth filter with a cutoff frequency of 15 Hz. First, local maxima in sagittal plane knee angle were identified, which occurred approximately midway through the swing phase. A frame window of 50 frames and threshold value of 60 degrees were used to ensure that only the local maxima representative of peak knee flexion during the swing phase were identified. Second, the filtered vertical acceleration signal of the foot sensor was used to identify specific frames where skate ON and OFF events occurred. OFF events were defined as the final local maximum prior to the peak in sagittal plane knee angle. ON events were defined as the first local minimum after the peak in sagittal plane knee angle. An investigator visually confirmed all events visually and made adjustments if the algorithm failed to accurately identify any ON or OFF events. These parameters were used for both forward and turn trials. For turn trials, an additional "turn event" was designated which marked the start of the turn and occurred at the last ON event before the two-footed turn entrance.

3.5.1 Stance Labelling

Data were then imported into MATLAB for further labelling using the BiomechZoo toolbox (Dixon et al., 2017). Forward and turn trials were processed similarly, but each task consisted of different events so were labelled in two separate processes.

Forward Trials. Leg sides for the forward trials were named to side 1 i.e., the leg side that took the first step, and side 2 i.e., the leg side that took the second step, based on which leg initiated the task, irrespective of left or right. Using identified ON and OFF events, stance phases

(ST) were identified and labelled. A stance phase refers to the duration the skate is on the ice within a single stride cycle, defined from the ON of one skate to the consecutive OFF of the same skate.

For each forward trial, eight stances were identified and labelled from ST0 to ST7. The side 1 leg performed ST1, ST3, ST5, and ST7, while the side 2 leg performed ST0, ST2, ST4, and ST6. ST0 covered the time from the start of the trial (initial side 1 OFF) to the first side 2 OFF, representing a stance-like phase before the first true stance (ST1) of the task. The tasks conclusion was marked by the final side 1 ON event. Since the final side 2 stance therefore did not conclude with a side 2 OFF event, signifying it was not a true stance, it was identified as a pseudo-stance and left unlabelled.

Turn Trials. Leg sides for the turn trials were labelled with I (inside) and O (outside). The inside leg was defined as the leg closest to the cone being turned around. For right turns the inside leg was the right leg. For left turns, the inside leg was the left leg. Only the turn event and stances post-turn were analyzed, all stances that occurred prior to the turn were excluded from analysis. Four stance phases were identified and labelled from ST1-ST4. The outside leg performed ST1 and ST3 while the inside leg performed ST2 and ST4. The turn task began at the point when two feet came into contact with the ice to begin the two-footed tight turn. ST1 occurred from the start of the turn to the first OFF of the outside leg. ST2 occurred from the start of the turn to the first OFF of the inside leg. ST3 and ST4 occurred consecutively as normal stances after the turn by the side 1 and side 2 legs respectively. The task's end was marked by the final inside leg ON event. Therefore, another pseudo-stance was identified for the outside leg at the end of the task, as this pseudo-stance did not conclude with the OFF of the outside leg.

3.5.2 Double Support Phase and Turn Time

Once events were identified and labelled appropriately, spatiotemporal variables of interest could be calculated including double support phase times and turn time, using BiomechZoo (Dixon et al., 2017). Double support phases occur throughout skating when there is ice contact of both skates at the same time. Double support phase time was defined from the ON of one skate to the consecutive OFF of the opposite skate. Eight double support phases were identified for forward trials. Three double support phase times were identified for both left and right turn tasks. Turn time was defined from the ON event that initiated the two-footed turn to the first outside leg OFF event out of the two-footed turn.

3.5.3 Total Task Completion Time

Forward task completion time, left turn task, and right turn task completion time were determined using video analysis. Video captures were exported into video viewing software Media Player Classic Home Cinema (MPC-HC). Task completion time was calculated by subtracting the time at which the participant's first step blade came off the ice, to the point in time at which their blade touched the end line. These events were identified visually by an investigator. For forward tasks, the end line was the blue line. For the turn tasks, the end line was the red line.

All dependent variables of interest were grouped into three categories which include: spatiotemporal, kinematic, and perception (Table 3).

Table 3

List of dependent variables

Variable Type	Variable Name	Description
Spatiotemporal	Forward task completion time	Completion time of the entire forward task
	Left turn task completion time	Completion time of the entire left turn task
	Right turn task completion time	Completion time of the entire right turn task
	Left turn time	Time to completion of the left turn – from two-foot contact to first push-off out of turn
	Right turn time	Time to completion of the right turn – from two-foot contact to first push-off out of turn
	Double Support Phase Times (all tasks)	Time duration for all phases with simultaneous two-foot contact
Kinematic	Hip Angle	Sagittal plane angle (flexion (+)/extension (–)) Frontal plane angle (adduction (+)/abduction (–)) Transverse plane angle (internal (+)/external (–) rotation)
	Knee Angle	Sagittal plane angle (flexion (+)/extension (–)) Transverse plane angle (internal (+)/external (–) rotation)
	Ankle Angle	Sagittal plane angle (dorsi (+)/plantar (–) flexion) Frontal plane angle (inversion (+)/eversion (–)) Transverse plane angle (internal (+)/external (–) rotation)
Perception	Forward rating	Score (from 0-100mm) on the forward performance VAS
	Turn rating	Score (from 0-100mm) on the turn performance VAS
	Overall preference rating	Score (from 0-100mm) on the overall preference rating VAS

3.6 Statistical Analysis

Demographic data (i.e., height, weight, age and playing experience) were compared between males and females using independent samples t-tests. Perception scores were compared between blade conditions using a Friedman Test for within-subjects. These tests were performed using IBM SPSS Statistics for Windows Version 27 (IBM Crop., Armonk, N.Y., USA). Statistical significance was set at $p < 0.05$.

Spatiotemporal discrete variables were compared using two separate analysis of variance (ANOVA) designs. Double support phase times were compared across double support phase, blade condition, and sex using a three-way mixed ANOVA with double support phase and blade condition as within-subjects factors, and sex as the between-subjects factor. Task completion times were compared across blade conditions (within-subject) and sex (between-subject) using a two-way mixed ANOVA. For both tests, if Mauchly's Test of Sphericity was violated, a Greenhouse-Geisser correction was applied. Pairwise comparisons were conducted based on estimated marginal means with 95% confidence intervals (CI), and Bonferroni corrected p-values were used for multiple comparisons. Partial eta squared was calculated to evaluate effect size. These tests were performed using SPSS.

Statistical parametric mapping (SPM) was used for the analysis of the normalized kinematic joint angle waveforms to analyze the effect of both sex and blade condition. This allowed for a complete waveform analysis of the joint angle curves rather than a comparison of only discrete points. All SPM tests and corrections were performed using the open-source code from spm1d toolbox (version M.0.4.10, 2022) in MATLAB (Pataky, 2012).

To compare males to females, SPM two-sample t-tests were used. A statistical parametric map was created from a calculated scalar output statistic (SPM{t}) for each individual time point in the normalized waveform of each joint angle (Pataky, 2012). This was done for only the kinematic variables of the Single Radius blade condition only, for all tasks. A critical threshold value was calculated, for which only statistically significant t-statistics surpassed. When multiple adjacent points of the scalar statistic surpassed the critical threshold, this was referred to as a "supra-threshold cluster" (Pataky, 2012). A *p*-value was calculated for each supra-threshold cluster to determine the probability that this result was a product of a random process. If the *p*-value was less than 0.05, this was deemed statistically significant.

To compare blade conditions, SPM one-way repeated measures ANOVAs were used. A statistical parametric map was created from a calculated output statistic (SPM{F}) for each individual time point in the normalized waveform of each joint angle (Pataky, 2012). This was done for male and female data combined, for all tasks. A mean curve was calculated separately for each blade condition for a given joint angle combining all participant mean trials. A critical threshold value was calculated, for which only statistically significant F-statistics surpassed. Similar to the t-test, when supra-threshold clusters surpassed the critical threshold, this signified a significant difference between blade conditions. Where necessary, post hoc tests were conducted using pair-wise comparisons (SPM paired-sample t-tests) with a Bonferroni correction to determine which blade conditions were different from each other at each supra-threshold cluster in the timeseries curve.

4. Results

After trial inspection, specific trials were excluded from analyses due to factors such as falls or stumbles, technical sensor issues, or missing event data. In the SPM t-test analysis, only the Single Radius blade condition was examined and therefore significantly fewer trials were included in comparison to the SPM ANOVA analysis, which included all blade types. Table 4 and Table 5 summarize the trial count for each specific analysis. Of the 26 participants, only one currently skated with a Prosharp-Bauer profile – the Quadruple Radius. The remaining 25 participants had not altered their blade ROC/profile from the manufacturers standard form and had very little previous exposure to profiles beyond a single radius design (Appendix Table D1).

Table 4

Number of trials and participants for spatiotemporal analyses

		Task Completion			Double support and Turn Time		
		Male	Female	**Total**	Male	Female	**Total**
Forward	Total Participants	12	14	26	11	14	25
	Number of Trials	143	169	312	130	167	297
Left Turn	Total Participants	12	14	26	10	14	24
	Number of Trials	144	169	313	114	158	272
Right Turn	Total Participants	11	14	25	11	14	25
	Number of Trials	141	169	310	127	161	288

Table 5

Number of trials and participants for SPM analyses on kinematic variables

		SPM t-test			SPM repeated measures ANOVA		
		Male	Female	**Total**	Male	Female	**Total**
Forward	Total Participants	12	14	25	11	14	25
	Number of Trials	35	41	76	130	167	297
Left Turn	Total Participants	12	14	24	10	14	24
	Number of Trials	31	39	70	114	158	272
Right Turn	Total Participants	12	14	25	11	14	25
	Number of Trials	32	39	71	127	161	288

Note. SPM t-tests were conducted on the Single Radius blade condition only and therefore included a significantly fewer number of total trials.

4.1 Spatiotemporal Variables

4.1.1 Forward Skating Task

Task Completion Time. For forward task completion time, there was no significant main effect of blade, and no significant blade*sex interaction (Appendix Table F1). A significant main effect of sex was observed, with a large effect size ($\eta^2 = 0.625$), indicating that males completed the task faster than females by 0.37 seconds (95% CI = 0.25, 0.48) (Appendix Table F1). Mean completion times and standard deviations are displayed in Table 6.

Table 6

Means (standard deviations) for forward skating task completion time

		Blade Condition			
Variable	**Sex**	**Single**	**Triple**	**Quadruple**	**Ellipse**
Forward task completion time (s)	F	3.65 (0.14)	3.66 (0.14)	3.68 (0.14)	3.64 (0.15)
	M	3.30 (0.19)	3.29 (0.16)	3.29 (0.18)	3.30 (0.18)

Note. F represents Female, M represents Male.

Double Support Phase Time. Levene's test of homogeneity was violated for DS3 in the Triple Radius condition (F = 6.535, $p = 0.018$) as well as DS4 in the Single Radius condition (F = 6.124, $p = 0.021$). As the sample sizes were not vastly different and only two conditions out of 32 violated the assumption, the regular ANOVA results were interpreted (van den Berg, 2023). The three-way mixed ANOVA revealed only a significant main effect of DS phase. Double support phase time displayed a gradual increase in duration during the forward skating task, with later phases showing a more extended period of double support (Table 7). Pairwise comparisons revealed several significant differences in DS phase time between DS phases (Appendix Table F3). There were no significant main effects of sex or blade condition, and no significant interactions involving sex, blade condition or DS phase (Appendix Table F2).

Table 7

Means (standard deviations) for double support phase times for the forward skating task

		Time (seconds)			
		Blade Condition			
Phase	**Sex**	**Single**	**Triple**	**Quadruple**	**Ellipse**
1	F	0.08 (0.06)	0.07 (0.06)	0.07 (0.05)	0.06 (0.05)
	M	0.05 (0.06)	0.04 (0.05)	0.05 (0.05)	0.04 (0.06)
2	F	0.04 (0.04)	0.05 (0.04)	0.05 (0.04)	0.05 (0.04)
	M	0.02 (0.04)	0.04 (0.04)	0.02 (0.04)	0.03 (0.04)
3	F	0.07 (0.04)	0.07 (0.04)	0.06 (0.06)	0.07 (0.04)
	M	0.04 (0.02)	0.05 (0.02)	0.04 (0.03)	0.04 (0.03)
4	F	0.08 (0.05)	0.07 (0.04)	0.07 (0.04)	0.08 (0.04)
	M	0.06 (0.02)	0.06 (0.03)	0.05 (0.04)	0.06 (0.03)
5	F	0.09 (0.05)	0.08 (0.04)	0.09 (0.05)	0.08 (0.05)
	M	0.08 (0.03)	0.07 (0.02)	0.07 (0.04)	0.07 (0.03)
6	F	0.08 (0.06)	0.08 (0.05)	0.09 (0.04)	0.08 (0.05)
	M	0.08 (0.04)	0.08 (0.04)	0.08 (0.05)	0.07 (0.04)
7	F	0.10 (0.05)	0.10 (0.05)	0.09 (0.04)	0.09 (0.05)
	M	0.09 (0.03)	0.08 (0.03)	0.09 (0.04)	0.09 (0.04)
8	F	0.10 (0.05)	0.09 (0.06)	0.11 (0.05)	0.10 (0.05)
	M	0.10 (0.07)	0.10 (0.06)	0.09 (0.02)	0.10 (0.05)

Note. F represents Female, M represents Male.

4.1.2 Left Turn Task

Task Completion and Turn Time. For the left turn task completion time, there was no significant main effect of blade or a significant blade*sex interaction (Appendix Table F1). A significant main effect of sex was observed with a large effect size ($\eta^2 = 0.396$), indicating that males completed the task faster than females by 0.42 seconds (95% CI = 0.20, 0.64) (Appendix Table F1).

For left turn time, there was no significant main effect of blade, no significant main effect of sex, and no significant blade*sex interaction (Appendix Table F1). Table 8 displays the means and standard deviations for left turn task completion time and turn time.

Table 8

Means (standard deviations) for task completion time and turn time for the left turn task

		Blade Condition			
Variable	**Sex**	**Single**	**Triple**	**Quadruple**	**Ellipse**
Task completion time (s)	F	5.39 (0.25)	5.38 (0.27)	5.44 (0.25)	5.37 (0.23)
	M	5.02 (0.36)	4.95 (0.31)	4.96 (0.28)	4.98 (0.29)
Turn time (s)	F	1.19 (0.24)	1.21 (0.23)	1.19 (0.29)	1.26 (0.31)
	M	1.27 (0.34)	1.23 (0.19)	1.24 (0.29)	1.16 (0.22)

Note. F represents Female, M represents Male.

Double Support Phase Time. A significant main effect of DS phase was observed (Appendix Table F2). Pairwise comparisons revealed several significant differences in DS phase time between DS phases (Appendix Table F4). Overall, there was a noticeable increase in double support phase duration over time. The second DS phase typically showed the longest duration, followed by the third DS phase, and the first DS phase consistently having the shortest duration (Table 9). There was no significant main effect of sex, or blade condition, and no significant interactions (Appendix Table F2).

Table 9

Means (standard deviations) for double support phase times for the left turn task

		Double Support Phase Time (seconds)			
		Blade Condition			
Phase	**Sex**	**Single**	**Triple**	**Quadruple**	**Ellipse**
1	F	0.06 (0.04)	0.06 (0.06)	0.07 (0.06)	0.05 (0.05)
	M	0.01 (0.04)	0.04 (0.04)	0.04 (0.06)	0.04 (0.05)
2	F	0.10 (0.03)	0.09 (0.03)	0.16 (0.19)	0.10 (0.04)
	M	0.09 (0.04)	0.10 (0.05)	0.10 (0.05)	0.09 (0.05)
3	F	0.10 (0.08)	0.10 (0.07)	0.09 (0.07)	0.10 (0.06)
	M	0.11 (0.09)	0.09 (0.07)	0.09 (0.06)	0.08 (0.07)

Note. F represents Female, M represents Male.

4.1.3 Right Turn Task

Task Completion and Turn Time. For the right turn task completion time, there was no significant main effect of blade, and no significant blade*sex interaction (Appendix Table F1). For the Single Radius blade condition, the assumption of homogeneity of variance was violated (F = 5.869, p = 0.024). Despite the significant Levene's test, a significant main effect of sex was observed ($p < 0.001$) with a large effect size ($\eta^2 = 0.528$), indicating that males completed the task faster than females by 0.49 seconds (95% CI = 0.29, 0.68). Given the highly significant p value and effect size for this main effect, and the relatively balanced sample sizes, it was deemed appropriate to interpret this effect (van den Berg, 2023).

For right turn time, there were no significant main effects of blade or sex, and no significant blade*sex interaction (Appendix Table F1). Means and standard deviations for task completion and turn time for the right turn task are shown in Table 10.

Table 10

Means (standard deviations) for task completion time and turn time for the right turn task

		Blade Condition			
Variable	**Sex**	**Single**	**Triple**	**Quadruple**	**Ellipse**
Task completion time (s)	F	5.39 (0.15)	5.45 (0.30)	5.50 (0.23)	5.41 (0.21)
	M	4.99 (0.29)	4.94 (0.30)	4.96 (0.31)	4.91 (0.24)
Turn Time (s)	F	1.29 (0.28)	1.32 (0.35)	1.32 (0.25)	1.27 (0.23)
	M	1.22 (0.24)	1.20 (0.17)	1.23 (0.17)	1.20 (0.22)

Note. F represents Female, M represents Male.

Double Support Phase Time. A significant main effect of DS phase was observed (Appendix Table F2). Pairwise comparisons revealed several significant differences in DS phase time between DS phases (Appendix Table F4). Overall, there was a noticeable increase in double support phase duration over time. The second DS phase typically showed the longest duration, followed by the third DS phase, and the first DS phase consistently having the shortest duration

(Table 11). There was no significant main effect of sex or blade condition, and no significant interactions (Appendix Table F2).

Table 11

Means (standard deviations) for double support phase times for the right turn task

		Double Support Phase Time (seconds)			
		Blade Condition			
Phase	**Sex**	**Single**	**Triple**	**Quadruple**	**Ellipse**
1	F	0.07 (0.05)	0.07 (0.05)	0.06 (0.05)	0.05 (0.03)
	M	0.03 (0.05)	0.02 (0.05)	0.05 (0.04)	0.03 (0.05)
2	F	0.10 (0.03)	0.10 (0.04)	0.10 (0.03)	0.11 (0.03)
	M	0.08 (0.05)	0.09 (0.03)	0.10 (0.04)	0.09 (0.04)
3	F	0.10 (0.07)	0.08 (0.07)	0.08 (0.06)	0.10 (0.08)
	M	0.09 (0.06)	0.08 (0.06)	0.07 (0.04)	0.08 (0.06)

Note. F represents Female, M represents Male.

4.2 Joint Angles

Significant results from the SPM analysis on kinematic variables are described below, with representative figures (Figure 7-25).

4.2.1 Forward Skating Task

Sex Comparison. For side 1 hip adduction angle, there were six suprathreshold clusters that exceeded the critical threshold (t = 3.466). The clusters occurred during the swing phase prior to ST1, during ST1, ST3, ST5 and ST7, and during the swing phase after ST7 (Figure 7C – 7D). At each cluster, males were significantly more abducted at the hip.

For side 1 knee flexion angle, there were three suprathreshold clusters that exceeded the critical threshold (t = 3.732). The clusters occurred during ST1, ST5 and ST7 (Figure 9A – 9B). At each cluster, males were significantly more flexed at the knee.

For side 2 knee flexion angle, there were four suprathreshold clusters that exceeded the critical threshold (t = 3.787). The clusters occurred just prior to and during ST2, as well as twice during the ending pseudo-stance (Figure 10A – 10B). At each cluster, males were significantly more flexed at the knee.

Blade Comparison. No variables showed suprathreshold clusters exceeding the critical threshold for the forward skating task, suggesting that there were no significant differences between blade conditions for any joint angle waveform (Appendix Figure G1 – G6).

Figure 7

Side 1 leg hip flexion/extension, adduction/abduction, and internal/external rotation angles during forward skating

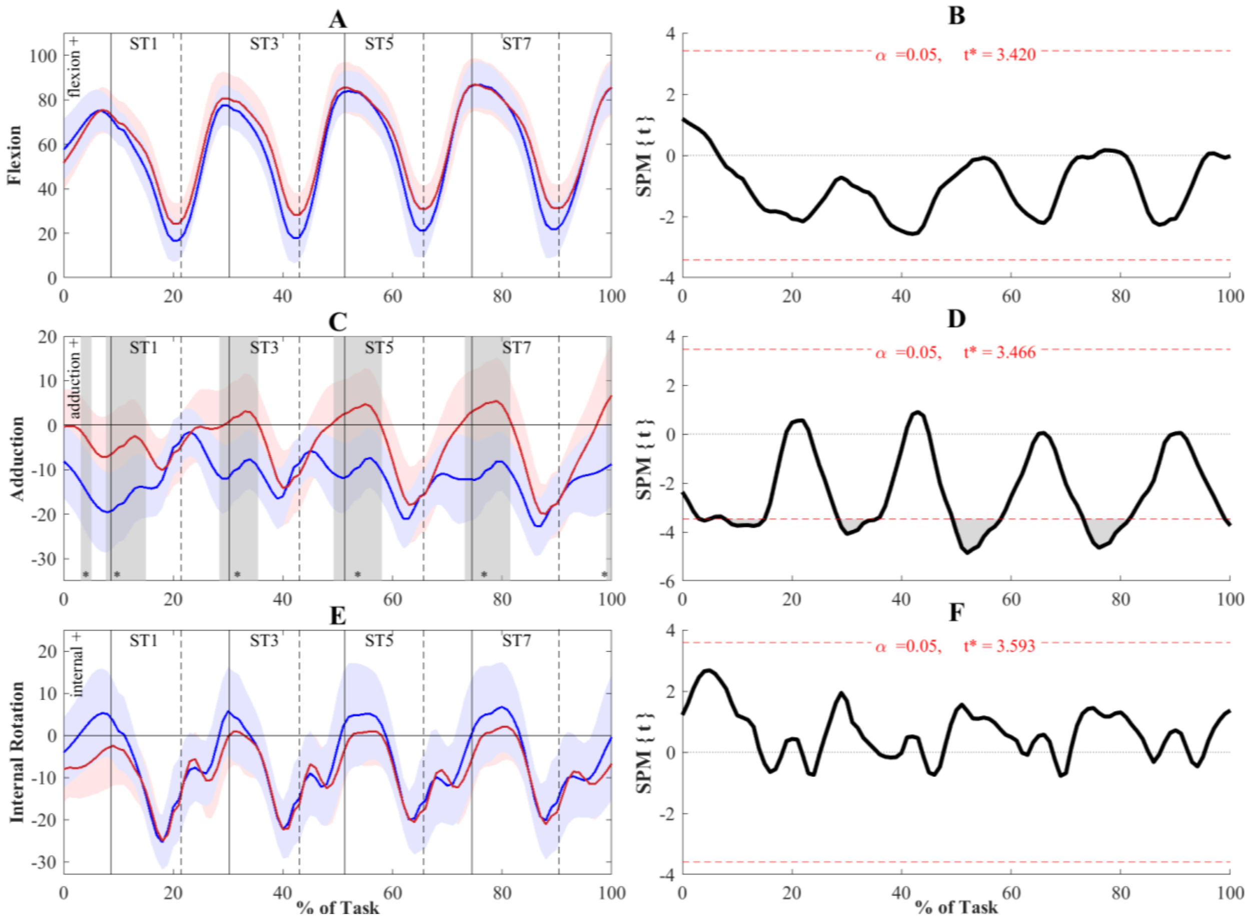

Note. (A) Hip flexion/extension, (C) hip adduction/abduction, (E) hip internal/external rotation for the side 1 leg. Angles are represented in degrees, where flexion, adduction and internal rotation are positive. Angles are expressed as a percentage of the forward skating task. Associated SPM plots are positioned to the right of each joint angle waveform graph ((B), (D), (F)). Red lines represent mean angle for females, blue lines represent mean angle for males. Red (female) and blue (male) shaded regions denote standard deviations. Vertical lines indicate skate ON (solid) and skate OFF (dotted) events. Stance phases are labelled within their respective skate ON and OFF events. Regions where the scalar output statistic (SPM{t}) surpassed the critical threshold (t*) indicate a significant difference in joint angle between males and females. These regions are shaded in grey with significance levels marked as * $p < 0.05$.

Figure 8

Side 2 leg hip flexion/extension, adduction/abduction, and internal/external rotation angles during forward skating

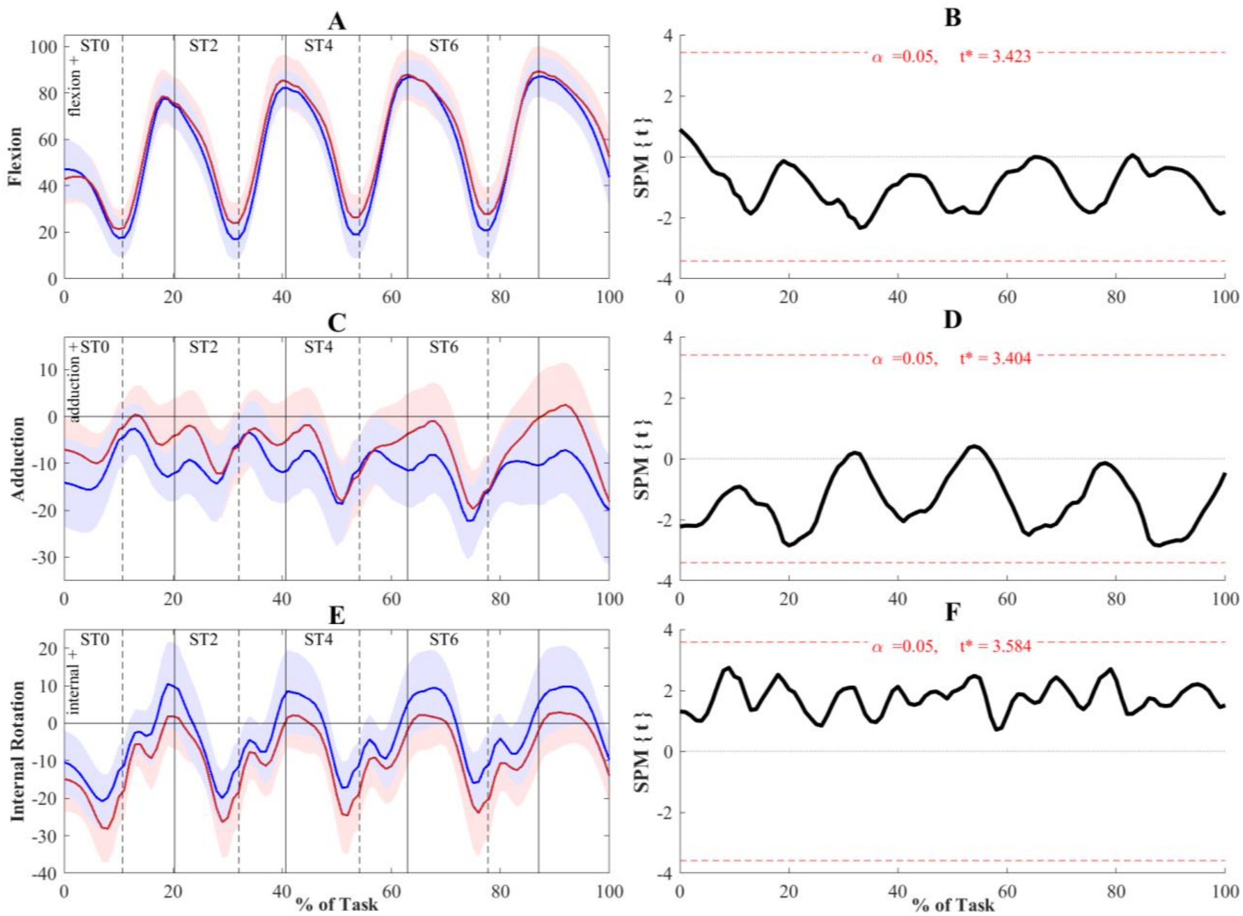

Note. (A) Hip flexion/extension, (C) hip adduction/abduction, (E) hip internal/external rotation for the side 2 leg. Angles are represented in degrees, where flexion, adduction, and internal rotation are positive. Angles are expressed as a percentage of the forward skating task. Associated SPM plots are positioned to the right of each joint angle waveform graph ((B), (D), (F)). Red lines represent mean angle for females, blue lines represent mean angle for males. Red (female) and blue (male) shaded regions denote standard deviations. Vertical lines indicate skate ON (solid) and skate OFF (dotted) events. Stance phases are labelled within their respective skate ON and OFF events. Regions where the scalar output statistic (SPM{t}) surpassed the critical threshold (t*) indicate a significant difference in joint angle between males and females. These regions are shaded in grey with significance levels marked as * $p < 0.05$.

Figure 9

Side 1 knee flexion/extension and internal/external rotation angles during forward skating

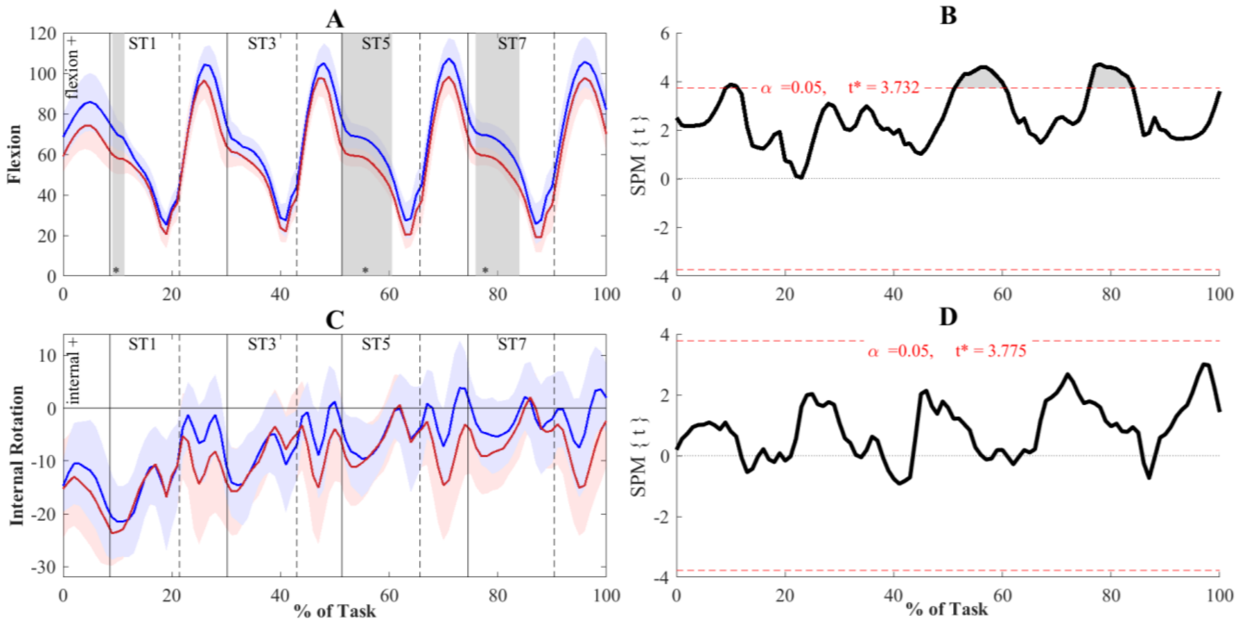

Note. (A) Knee flexion/extension, (C) knee internal/external rotation for the side 1 leg. Angles are represented in degrees, where flexion and internal rotation are positive. Angles are expressed as a percentage of the forward skating task. Associated SPM plots are positioned to the right of each joint angle waveform graph ((B), (D)). Red lines represent mean angle for females, blue lines represent mean angle for males. Red (female) and blue (male) shaded regions denote standard deviations. Vertical lines indicate skate ON (solid) and skate OFF (dotted) events. Stance phases are labelled within their respective skate ON and OFF events. Regions where the scalar output statistic (SPM{t}) surpassed the critical threshold (t*) indicate a significant difference in joint angle between males and females. These regions are shaded in grey with significance levels marked as * $p < 0.05$.

Figure 10

Side 2 knee flexion/extension and internal/external rotation angles during forward skating

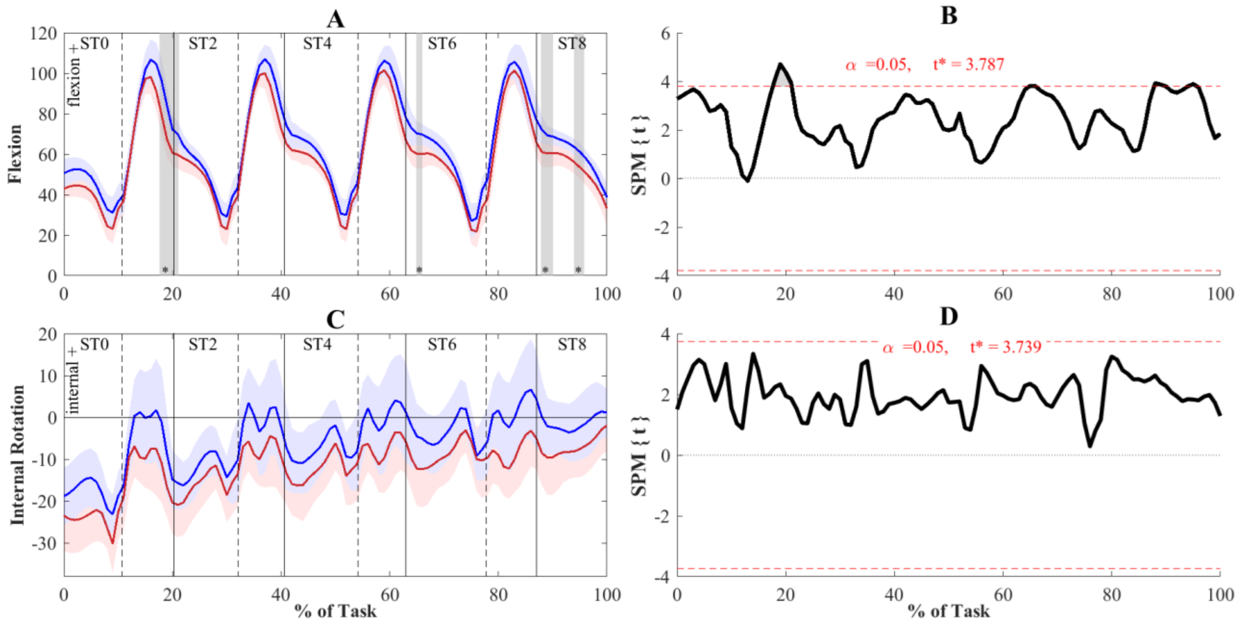

Note. (A) Knee flexion/extension, (C) knee internal/external rotation for the side 2 leg. Angles are represented in degrees, where flexion and internal rotation are positive. Angles are expressed as a percentage of the forward skating task. Associated SPM plots are positioned to the right of each joint angle waveform graph ((B), (D)). Red lines represent mean angle for females, blue lines represent mean angle for males. Red (female) and blue (male) shaded regions denote standard deviations. Vertical lines indicate skate ON (solid) and skate OFF (dotted) events. Stance phases are labelled within their respective skate ON and OFF events. Regions where the scalar output statistic (SPM{t}) surpassed the critical threshold (t*) indicate a significant difference in joint angle between males and females. These regions are shaded in grey with significance levels marked as * $p < 0.05$.

Figure 11

Side 1 ankle dorsi/plantar flexion, inversion/eversion, and internal/external rotation angles during forward skating

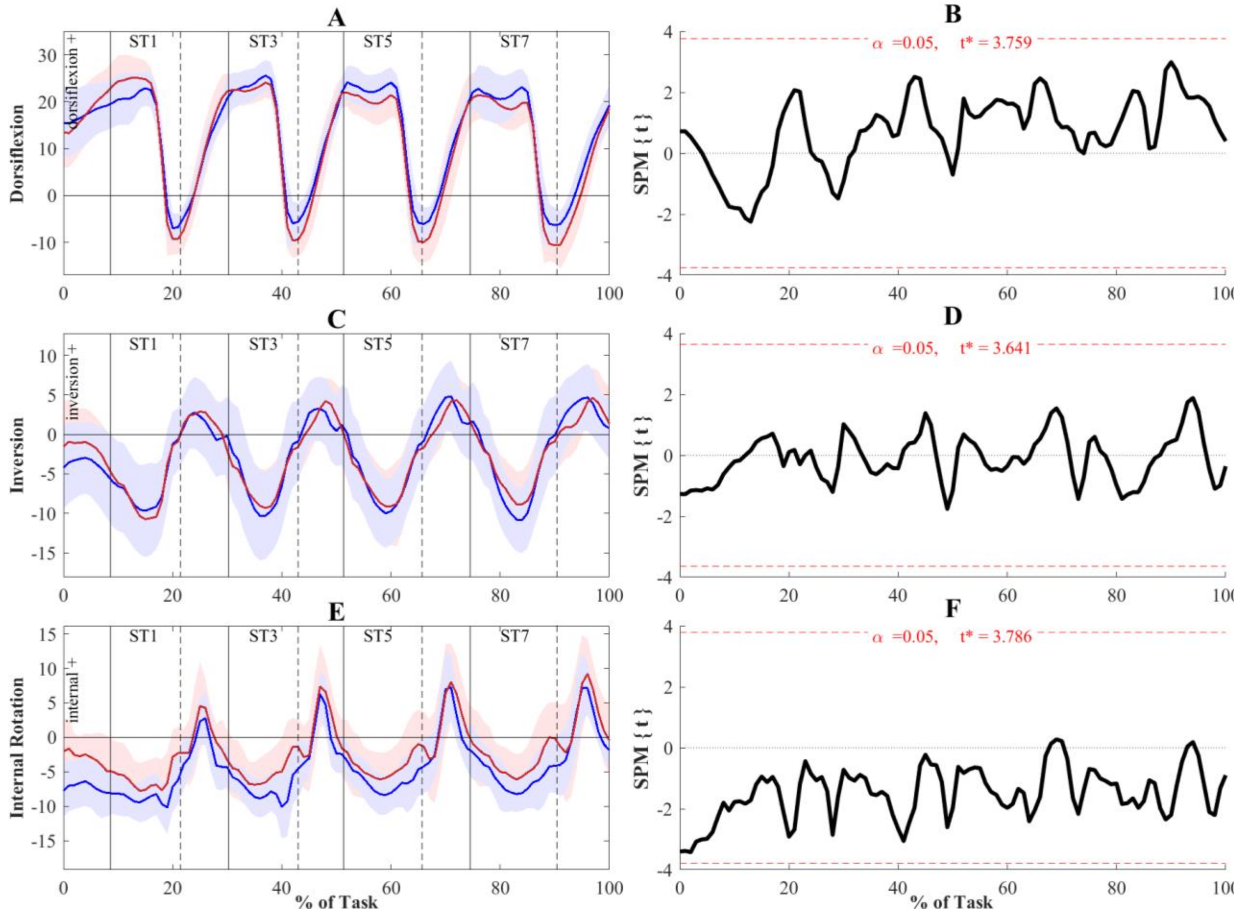

Note. (A) Ankle dorsi/plantar flexion, (C) ankle inversion/eversion, (E) ankle internal/external rotation for the side 1 leg. Angles are represented in degrees, where dorsiflexion, inversion, and internal rotation are positive. Angles are expressed as a percentage of the forward skating task. Associated SPM plots are positioned to the right of each joint angle waveform graph ((B), (D), (F)). Red lines represent mean angle for females, blue lines represent mean angle for males. Red (female) and blue (male) shaded regions denote standard deviations. Vertical lines indicate skate ON (solid) and skate OFF (dotted) events. Stance phases are labelled within their respective skate ON and OFF events. Regions where the scalar output statistic (SPM{t}) surpassed the critical threshold (t*) indicate a significant difference in joint angle between males and females. These regions are shaded in grey with significance levels marked as * $p < 0.05$.

Figure 12

Side 2 ankle dorsi/plantar flexion, inversion/eversion, and internal/external rotation angles during forward skating

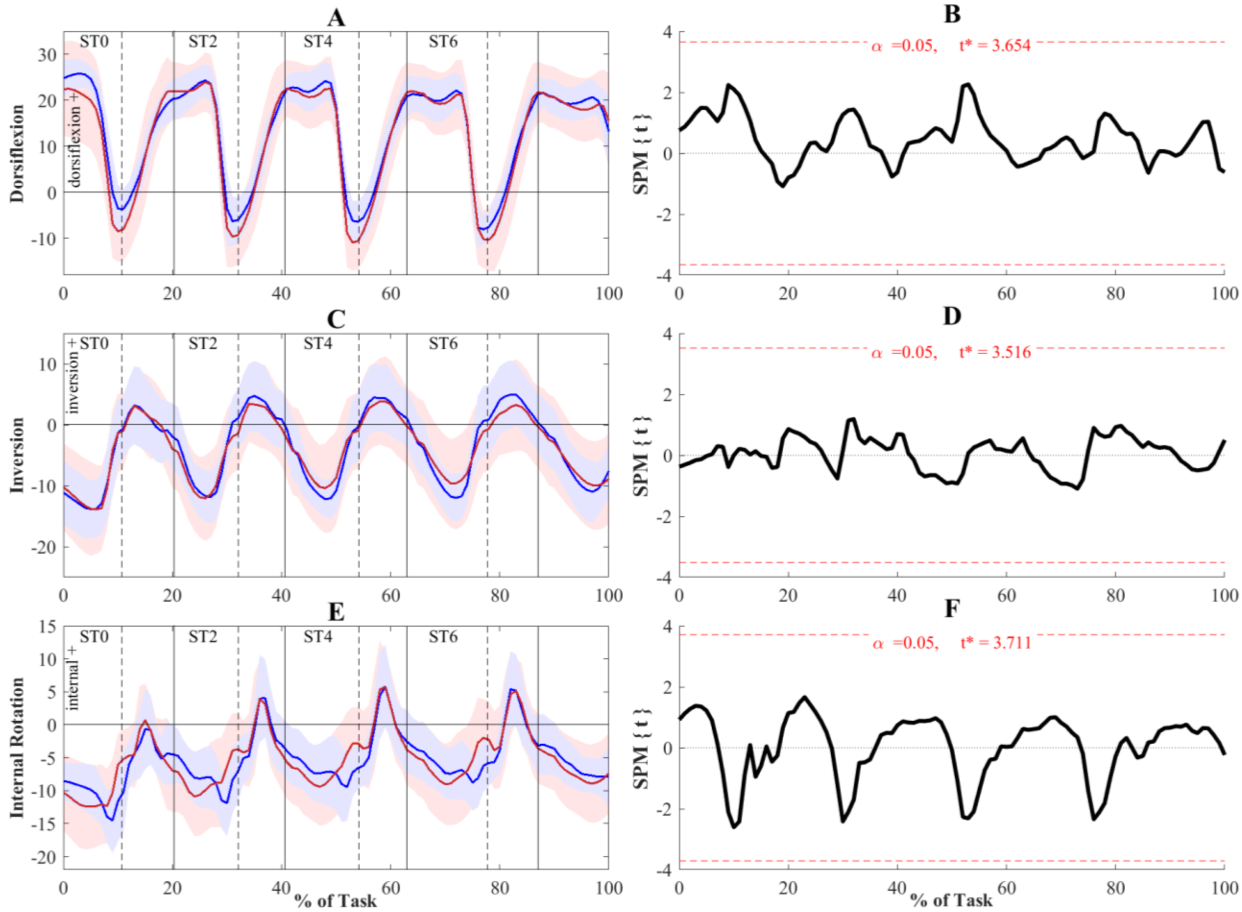

Note. (A) Ankle dorsi/plantar flexion, (C) ankle inversion/eversion, (E) ankle internal/external rotation for the side 1 leg. Angles are represented in degrees, where dorsiflexion, inversion, and internal rotation are positive. Angles are expressed as a percentage of the forward skating task. Associated SPM plots are positioned to the right of each joint angle waveform graph ((B), (D), (F)). Red lines represent mean angle for females, blue lines represent mean angle for males. Red (female) and blue (male) shaded regions denote standard deviations. Vertical lines indicate skate ON (solid) and skate OFF (dotted) events. Stance phases are labelled within their respective skate ON and OFF events. Regions where the scalar output statistic (SPM{t}) surpassed the critical threshold (t*) indicate a significant difference in joint angle between males and females. These regions are shaded in grey with significance levels marked as * $p < 0.05$.

4.2.2 Left Turn Task

Sex Comparison. For the outside leg hip internal rotation angle, there was one suprathreshold cluster that exceeded the critical threshold (t = 3.339). The cluster began at the very end of ST1 and continued for 8.21 % of the task into the swing phase after ST1 (Figure 13E – 13F). At this cluster, males were significantly more internally rotated at the hip.

For the outside leg knee flexion angle, there were six suprathreshold clusters that exceeded the critical threshold (t = 3.520). These clusters occurred at the very start of ST1/turn phase, during the swing phase after ST1, during ST3, and lastly during the ending pseudo-stance (Figure 15A – 15B). At each cluster, males were more flexed at the knee.

For the outside leg knee internal rotation angle, there was one suprathreshold cluster that exceeded the critical threshold (t = 3.550). This cluster occurred during the swing phase after ST3 (Figure 15C – 15D). At this cluster, males were more internally rotated at the knee.

For the inside knee flexion angle, there was one suprathreshold cluster that exceeded the critical threshold (t = 3.446). This cluster occurred during ST4, where males were more flexed at the knee (Figure 16A – 16B).

For the inside ankle internal rotation angle, there was one suprathreshold cluster that exceeded the critical threshold (t = 3.533). This cluster occurred at the start of ST4, coinciding with the skate ON event beginning ST4 (Figure 18E – 18F). At this cluster, females were more internally rotated at the ankle.

Blade Comparison. No variables showed suprathreshold clusters exceeding the critical threshold for the left turn task, suggesting that there were no significant differences between blade conditions for any joint angle waveform (Appendix Figure G7 – G12).

Figure 13

Outside leg hip flexion/extension, adduction/abduction, and internal/external rotation angles during left turns

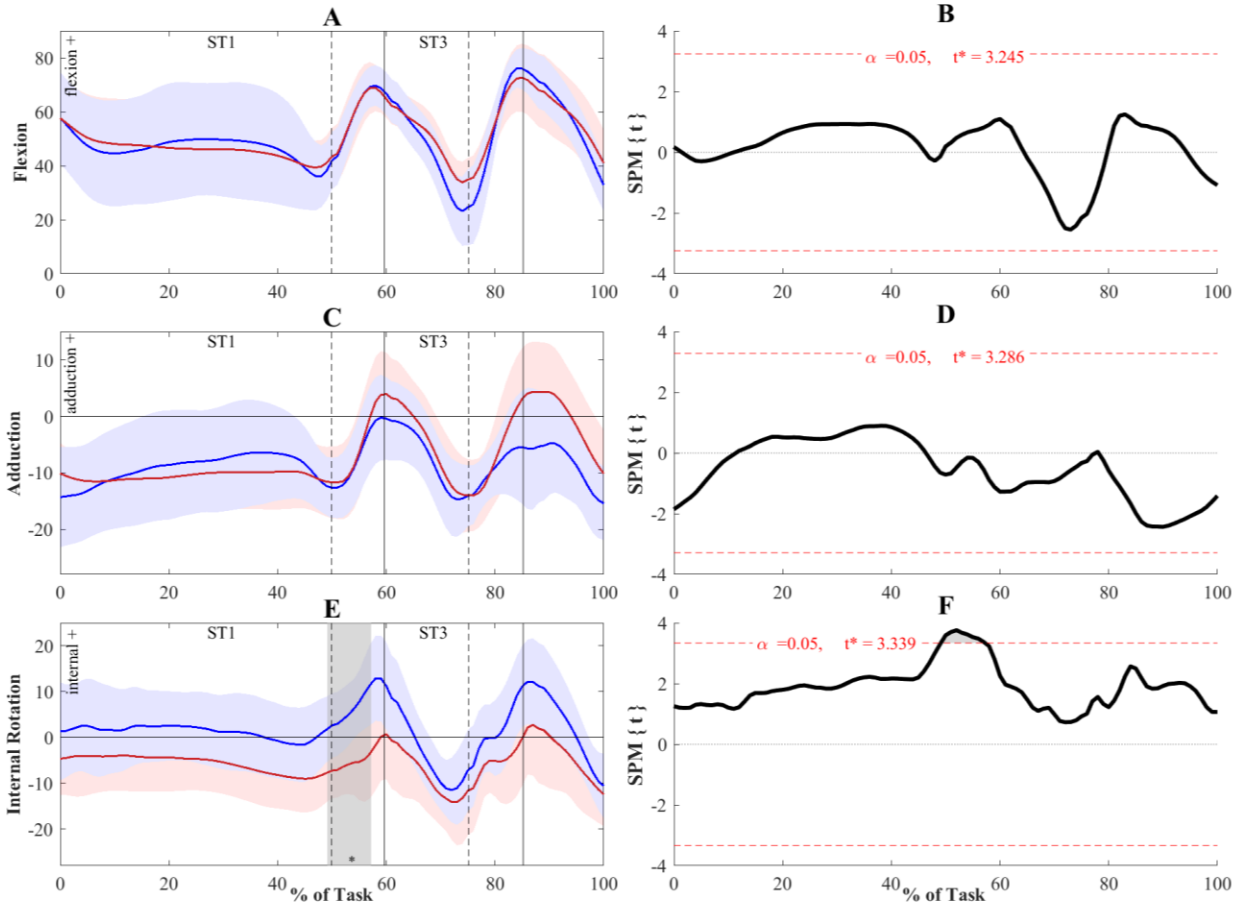

Note. (A) Hip flexion/extension, (C) hip adduction/abduction, (E) hip internal/external rotation for the outside leg. Angles are represented in degrees, where flexion, adduction, and internal rotation are positive. Angles are expressed as a percentage of the left turn task, where 0% represents the start of the turn event. Associated SPM plots are positioned to the right of each joint angle waveform graph ((B), (D), (F)). Red lines represent mean angle for females, blue lines represent mean angle for males. Red (female) and blue (male) shaded regions denote standard deviations. Vertical lines indicate skate ON (solid) and skate OFF (dotted) events. Stance phases are labelled within their respective skate ON and OFF events. Regions where the scalar output statistic (SPM{t}) surpassed the critical threshold (t*) indicate a significant difference in joint angle between males and females. These regions are shaded in grey with significance levels marked as * $p < 0.05$.

Figure 14

Inside leg hip flexion/extension, adduction/abduction, and internal/external rotation angles during left turns

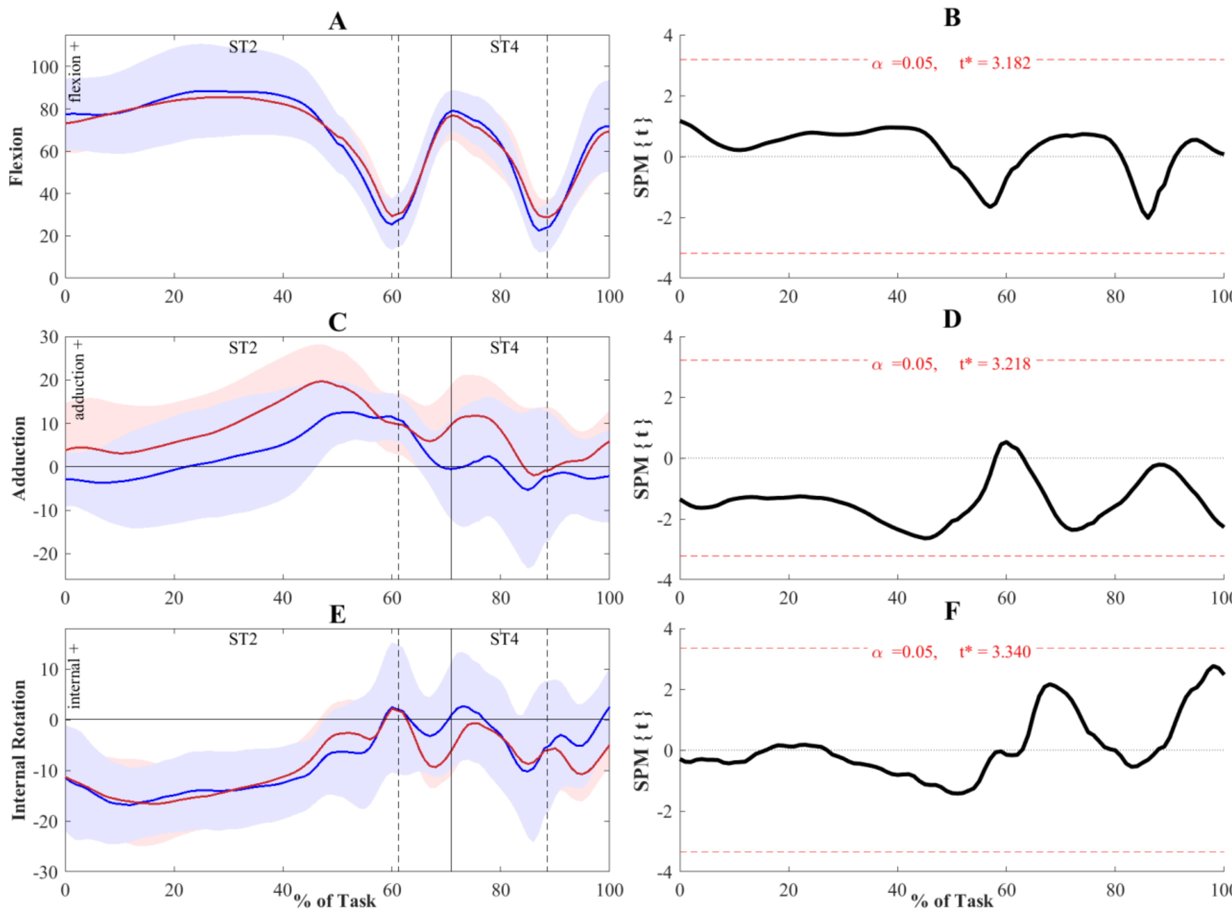

Note. (A) Hip flexion/extension, (C) hip adduction/abduction, (E) hip internal/external rotation for the inside leg. Angles are represented in degrees, where flexion, adduction, and internal rotation are positive. Angles are expressed as a percentage of the left turn task, where 0% represents the start of the turn event. Associated SPM plots are positioned to the right of each joint angle waveform graph ((B), (D), (F)). Red lines represent mean angle for females, blue lines represent mean angle for males. Red (female) and blue (male) shaded regions denote standard deviations. Vertical lines indicate skate ON (solid) and skate OFF (dotted) events. Stance phases are labelled within their respective skate ON and OFF events. Regions where the scalar output statistic (SPM{t}) surpassed the critical threshold (t*) indicate a significant difference in joint angle between males and females. These regions are shaded in grey with significance levels marked as * $p < 0.05$.

Figure 15

Outside leg knee flexion/extension and internal/external rotation angles during left turns

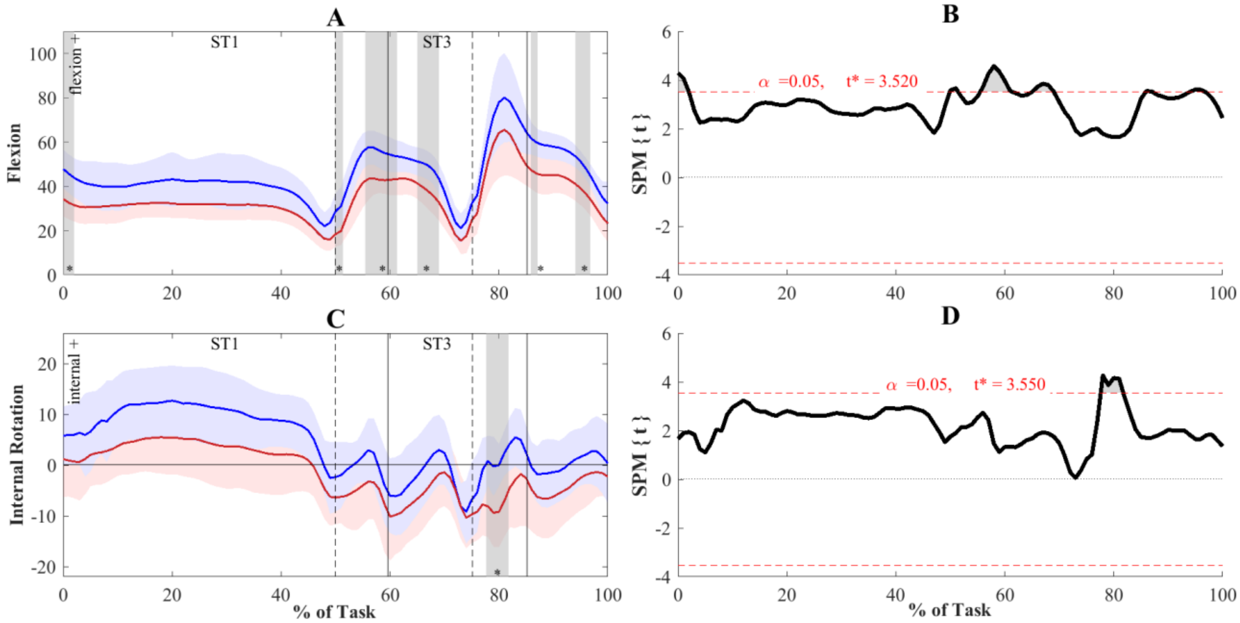

Note. (A) Knee flexion/extension, (C) knee internal/external rotation for the outside leg. Angles are represented in degrees, where flexion and internal rotation are positive. Angles are expressed as a percentage of the left turn task, where 0% represents the start of the turn event. Associated SPM plots are positioned to the right of each joint angle waveform graph ((B), (D)). Red lines represent mean angle for females, blue lines represent mean angle for males. Red (female) and blue (male) shaded regions denote standard deviations. Vertical lines indicate skate ON (solid) and skate OFF (dotted) events. Stance phases are labelled within their respective skate ON and OFF events. Regions where the scalar output statistic (SPM{t}) surpassed the critical threshold (t*) indicate a significant difference in joint angle between males and females. These regions are shaded in grey with significance levels marked as * $p < 0.05$.

Figure 16

Inside leg knee flexion/extension and internal/external rotation angles during left turns

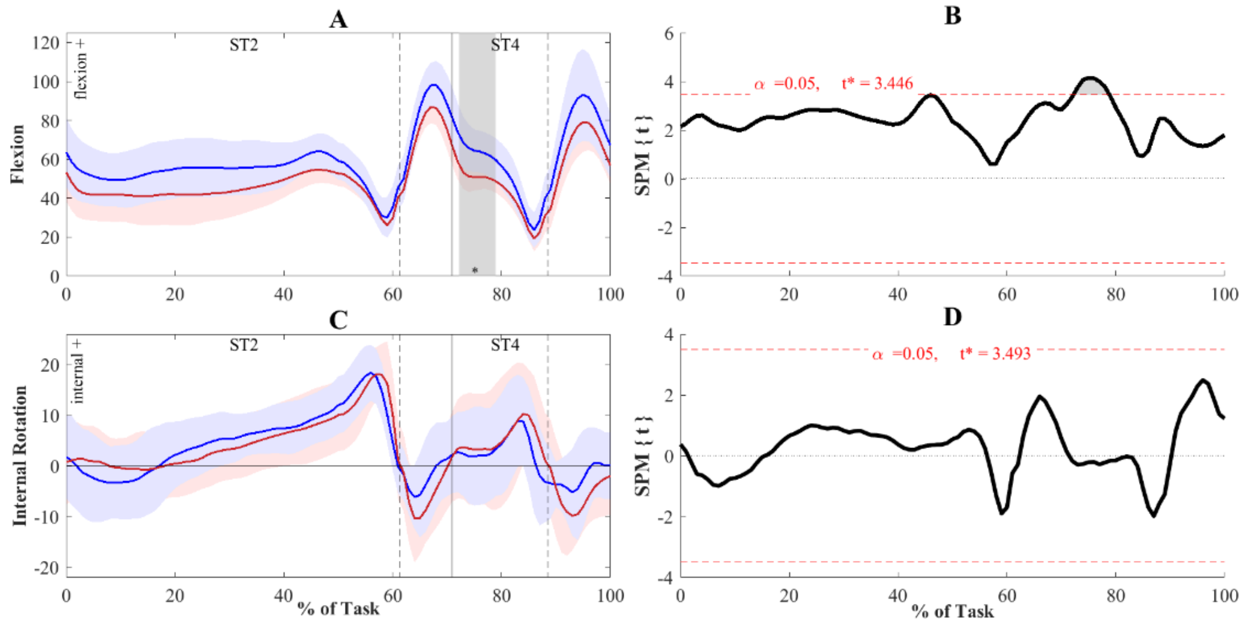

Note. (A) Knee flexion/extension, (C) knee internal/external rotation for the inside leg. Angles are represented in degrees, where flexion and internal rotation are positive. Angles are expressed as a percentage of the left turn task, where 0% represents the start of the turn event. Associated SPM plots are positioned to the right of each joint angle waveform graph ((B), (D)). Red lines represent mean angle for females, blue lines represent mean angle for males. Red (female) and blue (male) shaded regions denote standard deviations. Vertical lines indicate skate ON (solid) and skate OFF (dotted) events. Stance phases are labelled within their respective skate ON and OFF events. Regions where the scalar output statistic (SPM{t}) surpassed the critical threshold (t*) indicate a significant difference in joint angle between males and females. These regions are shaded in grey with significance levels marked as * $p < 0.05$.

Figure 17

Outside leg ankle dorsi-plantar flexion, inversion/eversion, and internal/external rotation angles during left turns

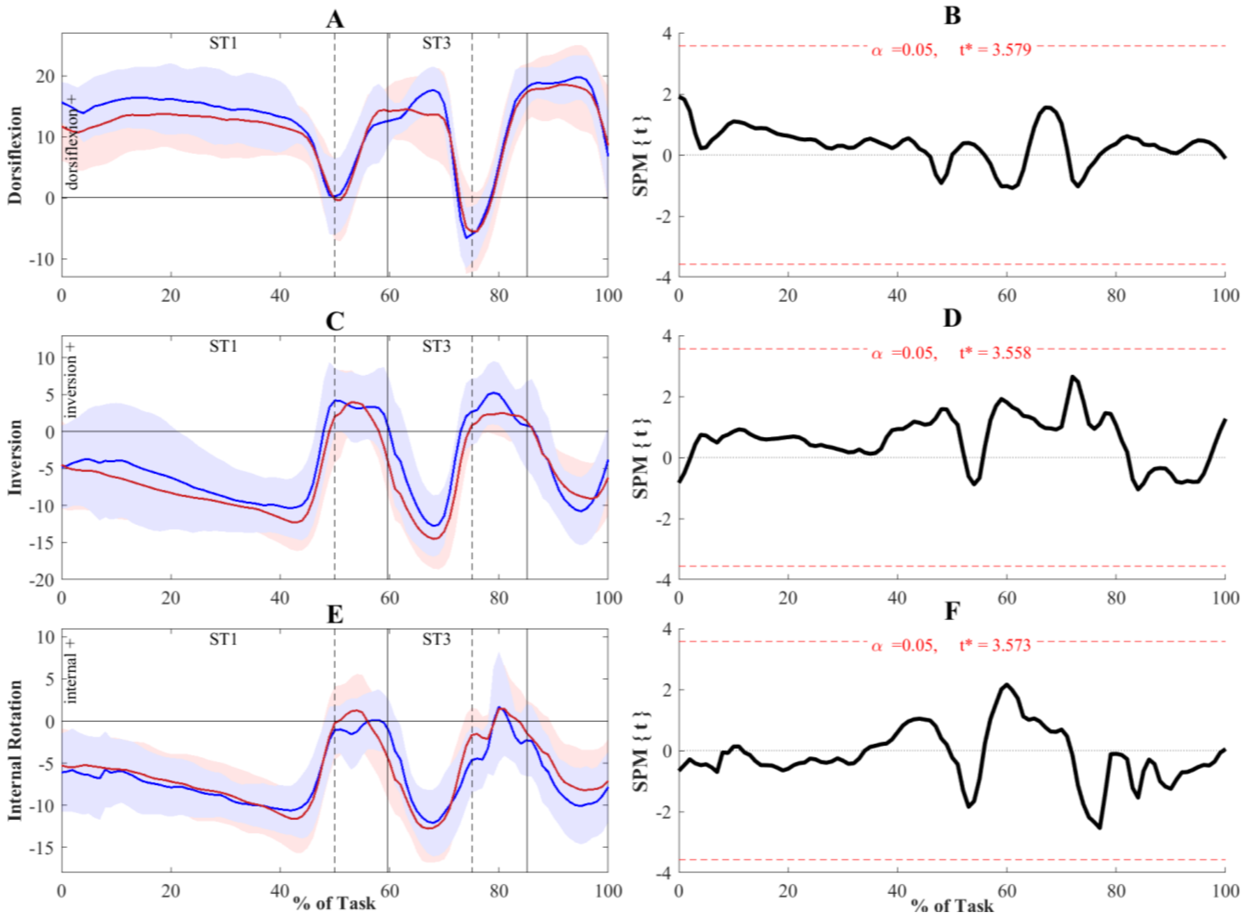

Note. (A) Ankle dorsi/plantar flexion, (C) ankle inversion/eversion, (E) ankle internal/external rotation for the outside leg. Angles are represented in degrees where dorsiflexion, inversion, and internal rotation angles are positive. Angles are expressed as a percentage of the left turn task, where 0% represents the start of the turn event. Associated SPM plots are positioned to the right of each joint angle waveform graph ((B), (D), (F)). Red lines represent mean angle for females, blue lines represent mean angle for males. Red (female) and blue (male) shaded regions denote standard deviations. Vertical lines indicate skate ON (solid) and skate OFF (dotted) events. Stance phases are labelled within their respective skate ON and OFF events. Regions where the scalar output statistic (SPM{t}) surpassed the critical threshold (t*) indicate a significant difference in joint angle between males and females. These regions are shaded in grey with significance levels marked as * $p < 0.05$.

Figure 18

Inside leg ankle dorsi-plantar flexion, inversion/eversion, and internal/external rotation angles during left turns

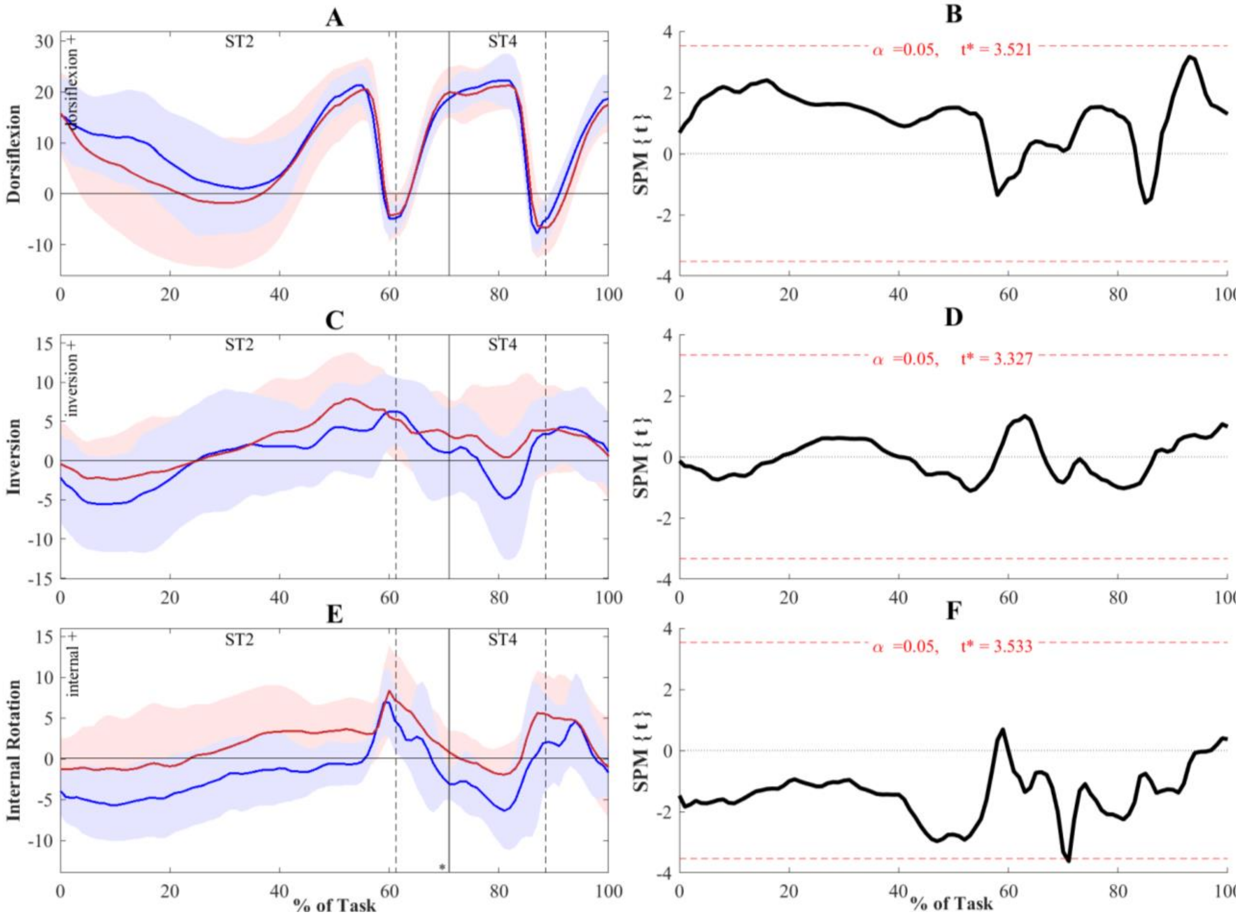

Note. (A) Ankle dorsi/plantar flexion, (C) ankle inversion/eversion, (E) ankle internal/external rotation for the inside leg. Angles are represented in degrees where dorsiflexion, inversion, and internal rotation angles are positive. Angles are expressed as a percentage of the left turn task, where 0% represents the start of the turn event. Associated SPM plots are positioned to the right of each joint angle waveform graph ((B), (D), (F)). Red lines represent mean angle for females, blue lines represent mean angle for males. Red (female) and blue (male) shaded regions denote standard deviations. Vertical lines indicate skate ON (solid) and skate OFF (dotted) events. Stance phases are labelled within their respective skate ON and OFF events. Regions where the scalar output statistic (SPM{t}) surpassed the critical threshold (t*) indicate a significant difference in joint angle between males and females. These regions are shaded in grey with significance levels marked as * $p < 0.05$.

4.2.3 Right Turn Task

Sex Comparison. For the outside hip internal rotation angle, there was one suprathreshold cluster that exceeded the critical threshold ($t = 3.336$). This cluster began at the end of ST1 and continued into the swing phase after ST1 (Figure 19E – 19F). At this cluster, males were more internally rotated at the hip.

For the inside hip adduction angle, there was one suprathreshold cluster that exceeded the critical threshold ($t = 3.241$). This cluster occurred at the end of the swing phase after ST2 and continued into ST4 (Figure 20C – 20D). At this cluster, males were more abducted at the hip.

For the outside knee flexion angle, there were three suprathreshold clusters that exceeded the critical threshold ($t = 3.512$). These clusters occurred at ST1, the swing phase after ST1, and during the ending pseudo-stance (Figure 21A – 21B). At each cluster, males were more flexed at the knee.

For the inside knee flexion angle, there was one suprathreshold cluster that exceeded the critical threshold ($t = 3.497$). This cluster occurred during the swing phase after ST2 and continued into ST4 (Figure 22A – 22B). At this cluster, males were more flexed at the knee.

For the inside ankle internal rotation angle, there were three suprathreshold clusters that exceeded the critical threshold ($t = 3.465$). These clusters occurred during ST2, the swing phase after ST2, and ST4 (Figure 24E – 24F). For all clusters, females were more internally rotated.

Blade Comparison. For the inside ankle internal rotation angle, there was one suprathreshold cluster that exceeded the critical threshold ($t = 5.388$). This cluster occurred towards the end of ST2, during the turn (Figure 25E – 25F). Post hoc analysis using SPM paired sample t-tests revealed one suprathreshold cluster that exceeded the critical threshold ($t = 3.717$), suggesting greater internal rotation for the Quadruple Radius compared to the Triple Radius ($p =$

0.048). However, this result did not remain significant after applying a Bonferroni correction for multiple comparisons ($p = 0.257$). All other blade comparisons resulted in no significant clusters for any joint angle (Appendix Figure G13 – G17).

Figure 19

Outside leg hip flexion/extension, adduction/abduction, and internal/external rotation angles during right turns

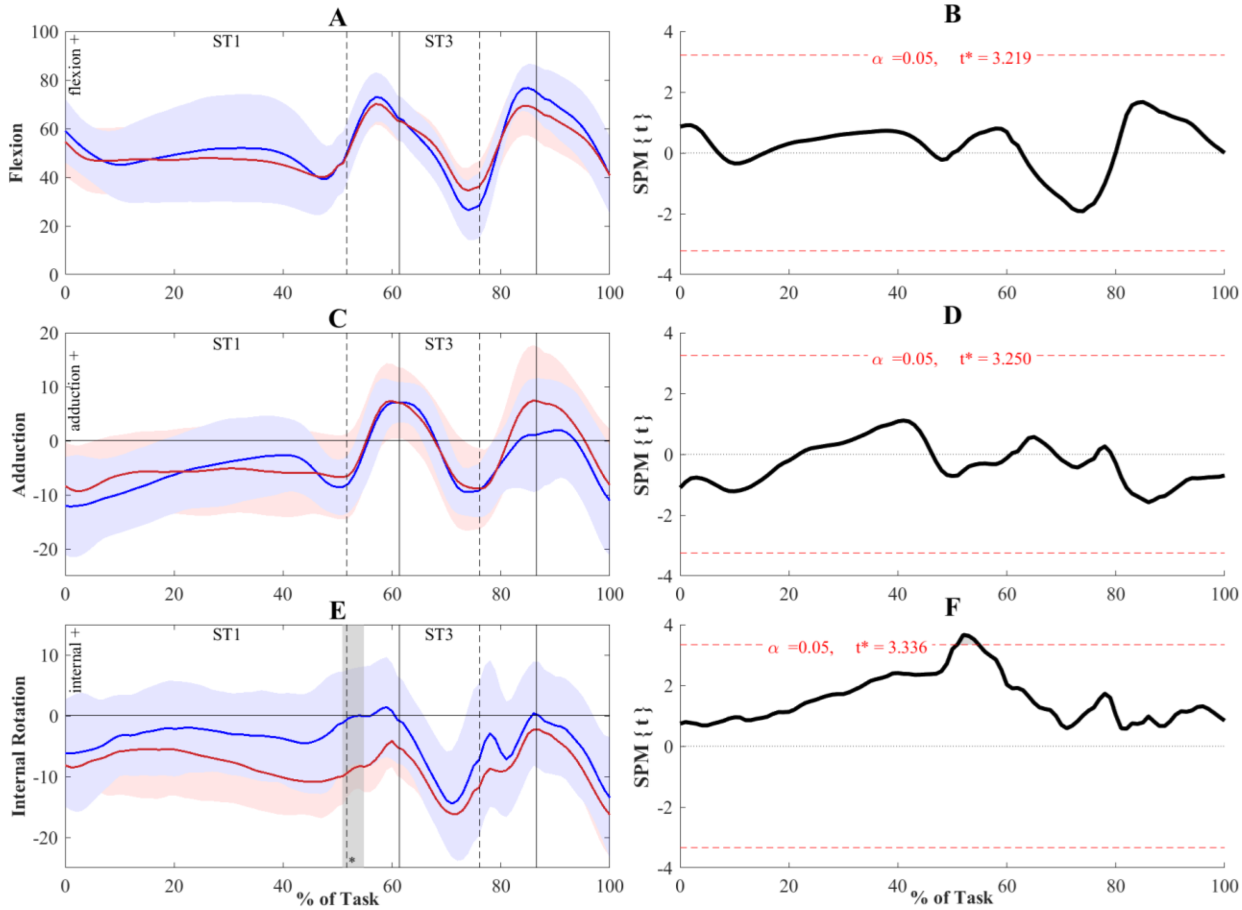

Note. (A) Hip flexion/extension, (C) hip adduction/abduction, (E) hip internal/external rotation for the outside leg. Angles are represented in degrees, where flexion, adduction, and internal rotation are positive. Angles are expressed as a percentage of the right turn task, where 0% represents the start of the turn event. Associated SPM plots are positioned to the right of each joint angle waveform graph ((B), (D), (F)). Red lines represent mean angle for females, blue lines represent mean angle for males. Red (female) and blue (male) shaded regions denote standard deviations. Vertical lines indicate skate ON (solid) and skate OFF (dotted) events. Stance phases are labelled within their respective skate ON and OFF events. Regions where the scalar output statistic (SPM{t}) surpassed the critical threshold (t*) indicate a significant difference in joint angle between males and females. These regions are shaded in grey with significance levels marked as * $p < 0.05$.

Figure 20

Inside leg hip flexion/extension, adduction/abduction, and internal/external rotation angles during right turns

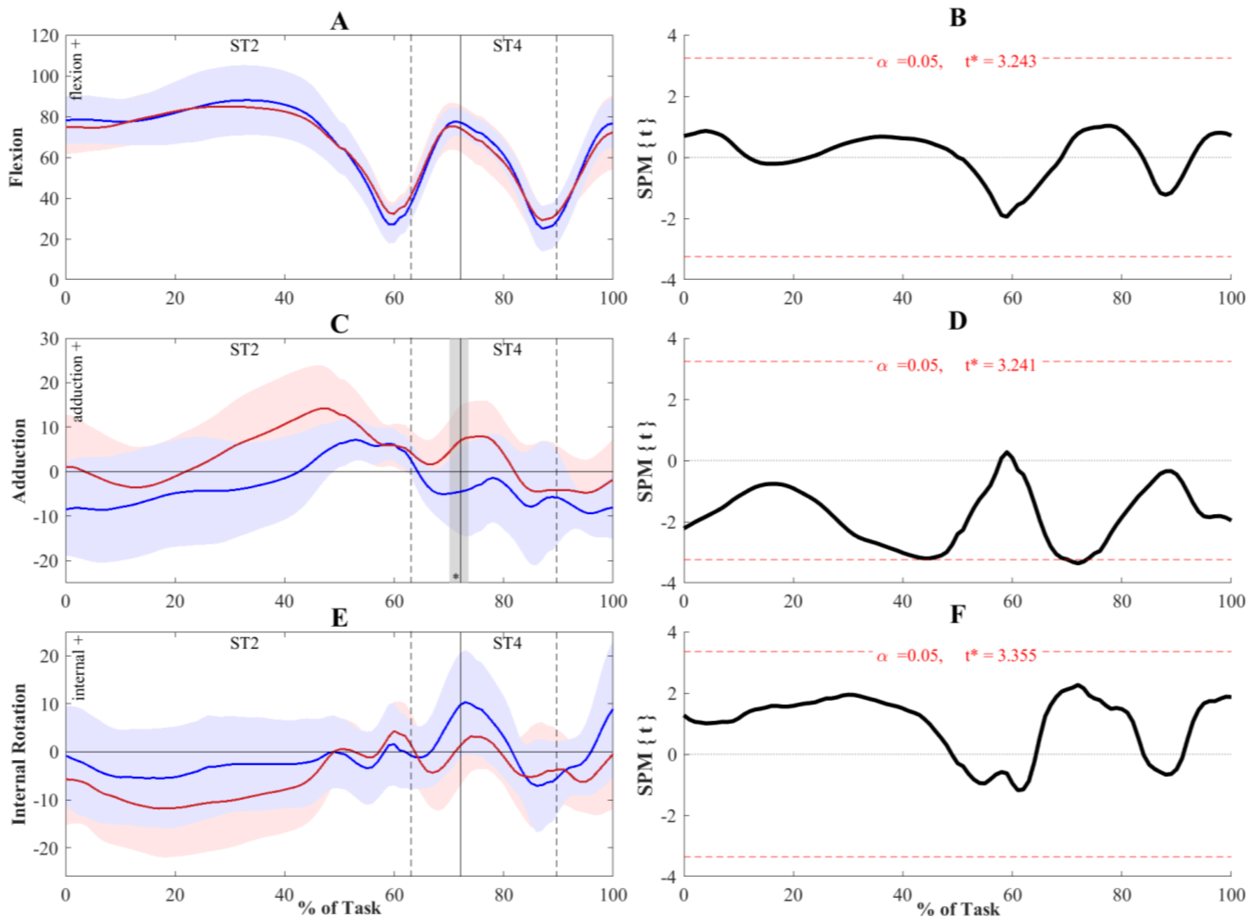

Note. (A) Hip flexion/extension, (C) hip adduction/abduction, (E) hip internal/external rotation for the inside leg. Angles are represented in degrees, where flexion, adduction, and internal rotation are positive. Angles are expressed as a percentage of the right turn task, where 0% represents the start of the turn event. Associated SPM plots are positioned to the right of each joint angle waveform graph ((B), (D), (F)). Red lines represent mean angle for females, blue lines represent mean angle for males. Red (female) and blue (male) shaded regions denote standard deviations. Vertical lines indicate skate ON (solid) and skate OFF (dotted) events. Stance phases are labelled within their respective skate ON and OFF events. Regions where the scalar output statistic (SPM{t}) surpassed the critical threshold (t*) indicate a significant difference in joint angle between males and females. These regions are shaded in grey with significance levels marked as * $p < 0.05$.

Figure 21

Outside leg knee flexion/extension and internal/external rotation angles during right turns

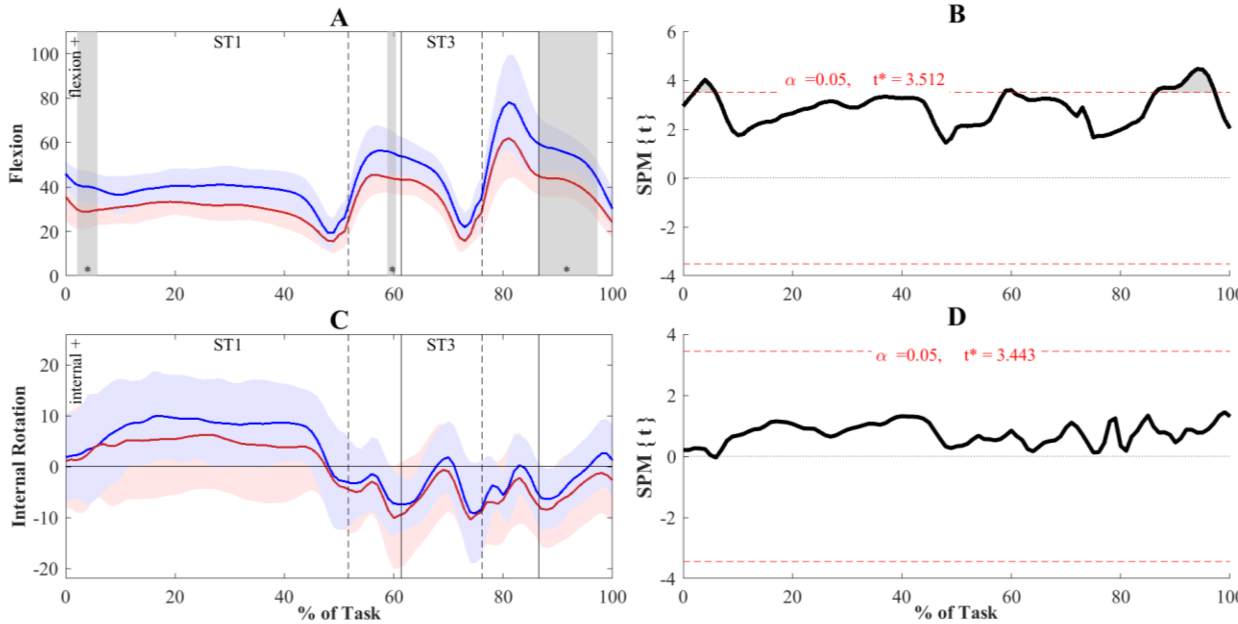

Note. (A) Knee flexion/extension, (C) knee internal/external rotation for the outside leg. Angles are represented in degrees, where flexion and internal rotation are positive. Angles are expressed as a percentage of the right turn task, where 0% represents the start of the turn event. Associated SPM plots are positioned to the right of each joint angle waveform graph ((B), (D)). Red lines represent mean angle for females, blue lines represent mean angle for males. Red (female) and blue (male) shaded regions denote standard deviations. Vertical lines indicate skate ON (solid) and skate OFF (dotted) events. Stance phases are labelled within their respective skate ON and OFF events. Regions where the scalar output statistic (SPM{t}) surpassed the critical threshold (t*) indicate a significant difference in joint angle between males and females. These regions are shaded in grey with significance levels marked as * $p < 0.05$.

Figure 22

Inside leg knee flexion/extension and internal/external rotation angles during right turns

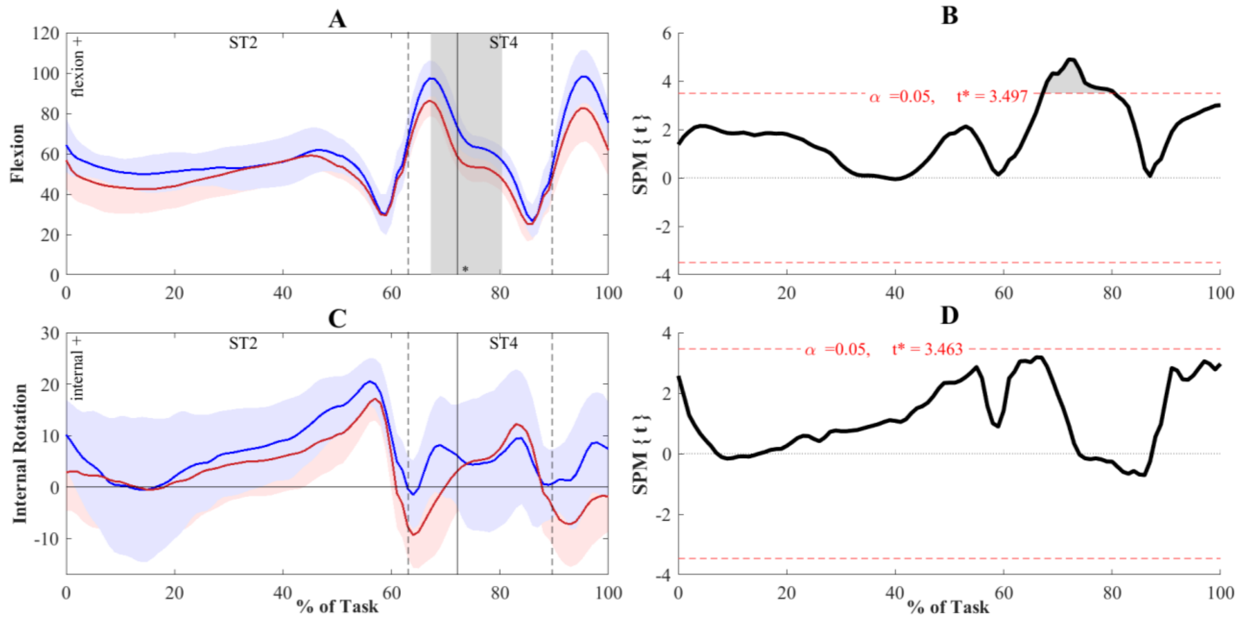

Note. (A) Knee flexion/extension, (C) knee internal/external rotation for the inside leg. Angles are represented in degrees, where flexion and internal rotation are positive. Angles are expressed as a percentage of the right turn task, where 0% represents the start of the turn event. Associated SPM plots are positioned to the right of each joint angle waveform graph ((B), (D)). Red lines represent mean angle for females, blue lines represent mean angle for males. Red (female) and blue (male) shaded regions denote standard deviations. Vertical lines indicate skate ON (solid) and skate OFF (dotted) events. Stance phases are labelled within their respective skate ON and OFF events. Regions where the scalar output statistic (SPM{t}) surpassed the critical threshold (t*) indicate a significant difference in joint angle between males and females. These regions are shaded in grey with significance levels marked as * $p < 0.05$.

Figure 23

Outside leg ankle dorsi/plantar flexion, inversion/eversion, and internal/external rotation angles during right turns

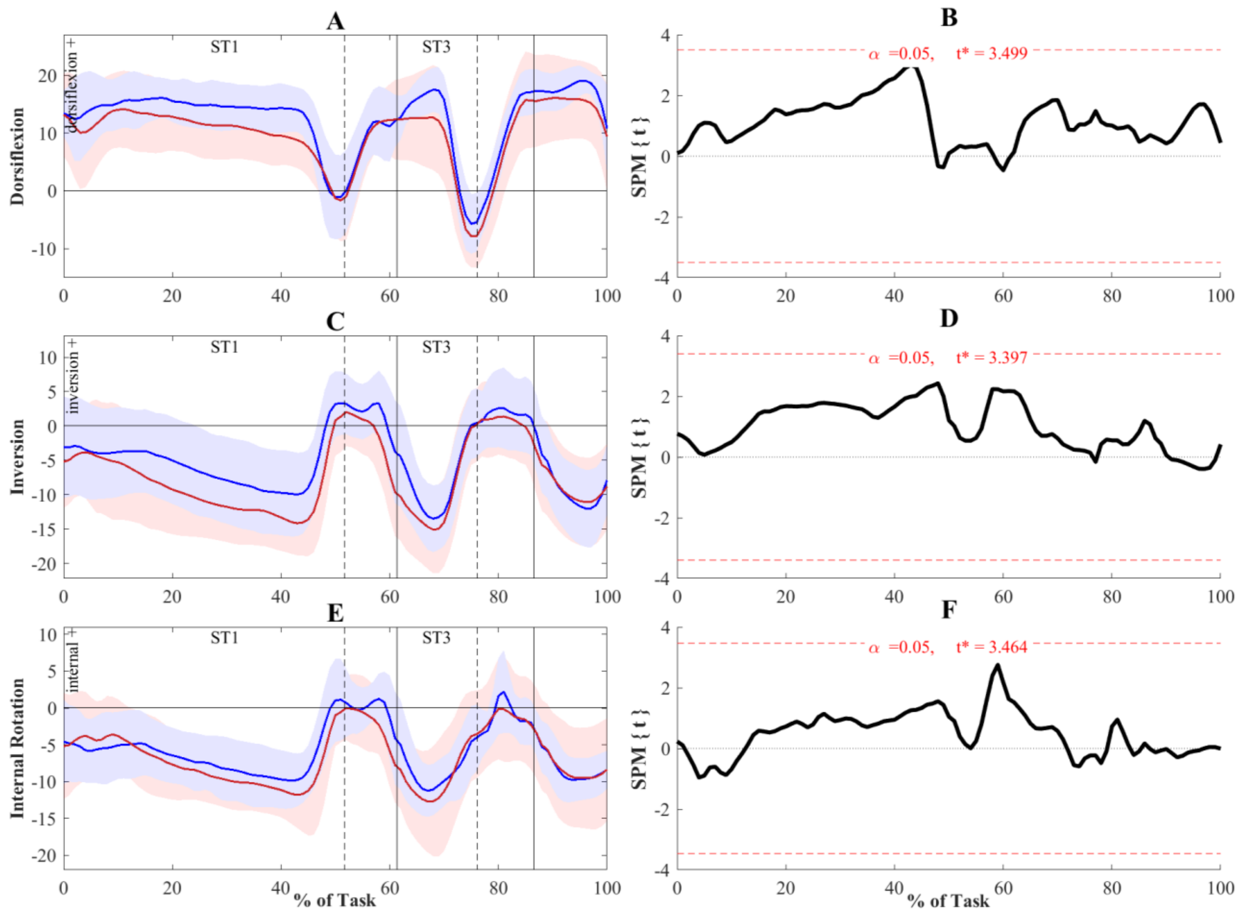

Note. (A) Ankle dorsi/plantar flexion, (C) ankle inversion/eversion, (E) ankle internal/external rotation for the outside leg. Angles are represented in degrees, where dorsiflexion, inversion, and internal rotation are positive. Angles are expressed as a percentage of the right turn task, where 0% represents the start of the turn event. Associated SPM plots are positioned to the right of each joint angle waveform graph ((B), (D), (F)). Red lines represent mean angle for females, blue lines represent mean angle for males. Red (female) and blue (male) shaded regions denote standard deviations. Vertical lines indicate skate ON (solid) and skate OFF (dotted) events. Stance phases are labelled within their respective skate ON and OFF events. Regions where the scalar output statistic (SPM{t}) surpassed the critical threshold (t*) indicate a significant difference in joint angle between males and females. These regions are shaded in grey with significance levels marked as * $p < 0.05$.

Figure 24

Inside leg ankle dorsi/plantar flexion, inversion/eversion, and internal/external rotation angles during right turns

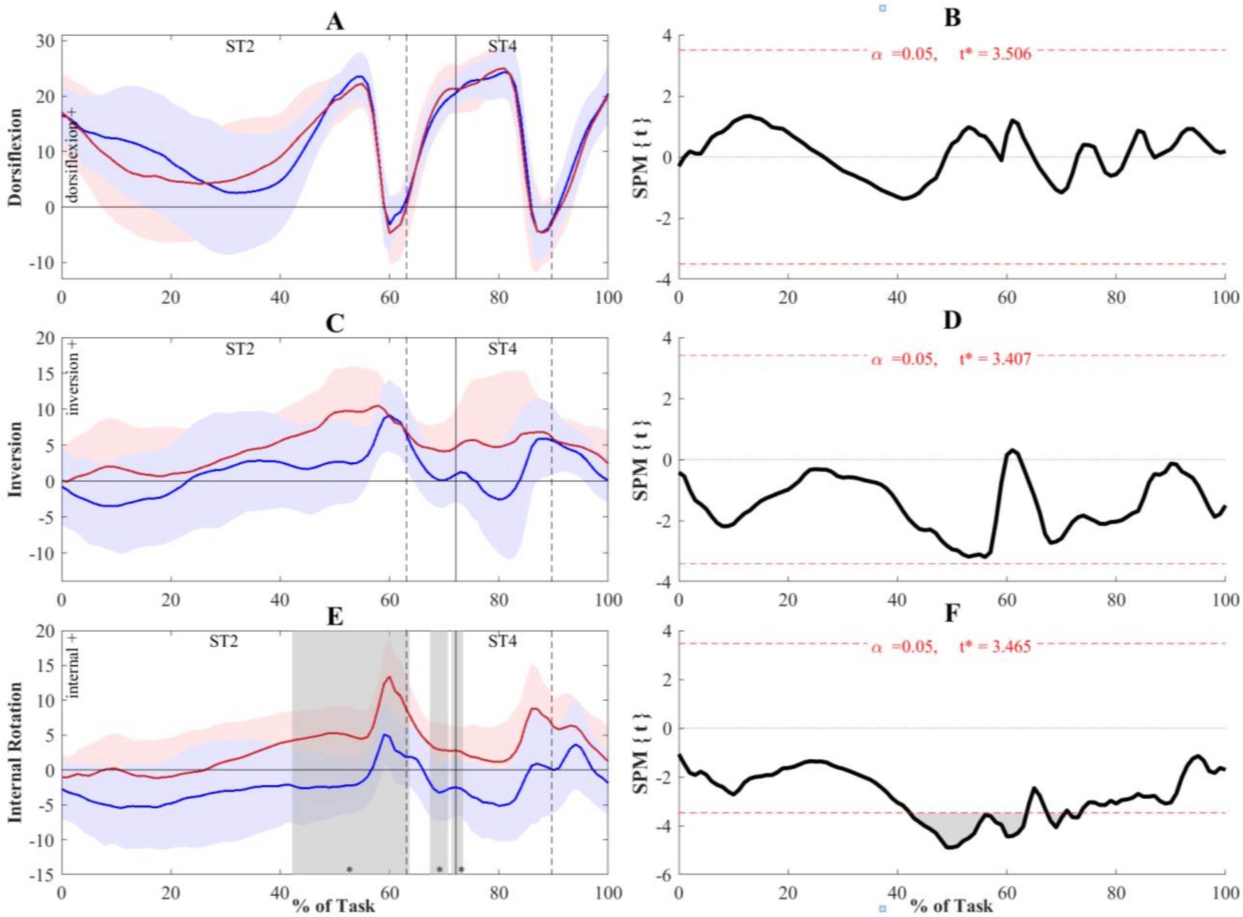

Note. (A) Ankle dorsi/plantar flexion, (B) ankle inversion/eversion, (C) ankle internal/external rotation for the inside leg. Angles are represented in degrees, where dorsiflexion, inversion, and internal rotation are positive. Angles are expressed as a percentage of the right turn task, where 0% represents the start of the turn event. Associated SPM plots are positioned to the right of each joint angle waveform graph ((B), (D), (F)). Red lines represent mean angle for females, blue lines represent mean angle for males. Red (female) and blue (male) shaded regions denote standard deviations. Vertical lines indicate skate ON (solid) and skate OFF (dotted) events. Stance phases are labelled within their respective skate ON and OFF events. Regions where the scalar output statistic (SPM{t}) surpassed the critical threshold (t*) indicate a significant difference in joint angle between males and females. These regions are shaded in grey with significance levels marked as * $p < 0.05$.

Figure 25

Inside leg ankle dorsi/plantarflexion, inversion/eversion, and internal/external rotation angles between blade conditions, during right turns

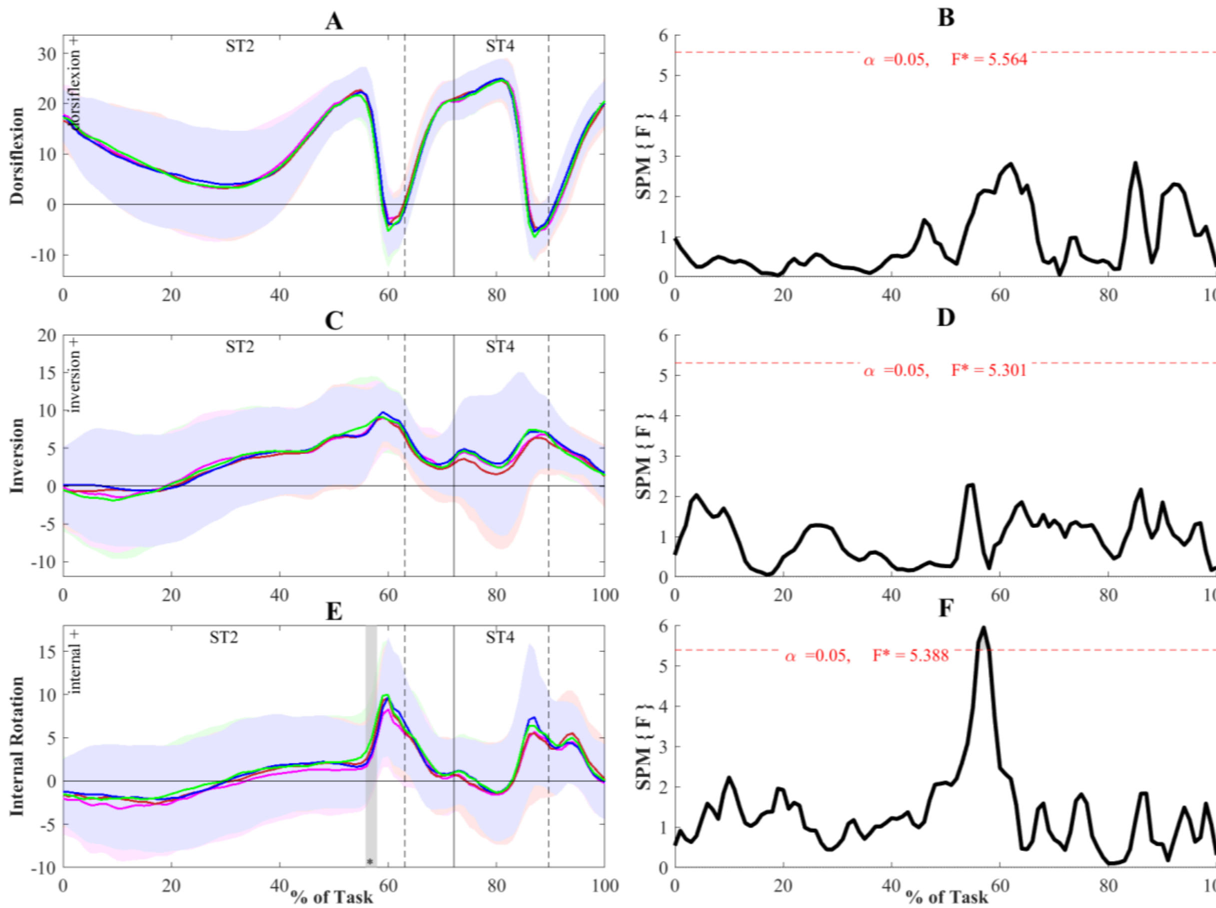

Note. (A) Ankle dorsi/plantarflexion, (C) ankle inversion/eversion, (E) ankle internal/external rotation for the inside leg. Angles are represented in degrees where dorsiflexion, inversion, and internal rotation are positive. Angles are expressed as a percentage of the right turn task, where 0% marks the beginning of the turn event. Associated SPM {F} plots are positioned to the right of each joint angle waveform graph ((B), (D), (F)). Each coloured line represents blade conditions Single Radius (red), Triple Radius (magenta), Quadruple Radius (green), and Ellipse (blue). Shaded regions denote standard deviations with respective colours for each blade. Vertical lines indicate skate ON (solid) and skate OFF (dotted) events. Stance phases are labelled within their respective skate ON and OFF events. Regions where the scalar output statistic (SPM{F}) surpassed the critical threshold (F) indicate a significant difference in joint angle between blade conditions. These regions are shaded in grey with significance levels marked as * $p < 0.05$.

4.3 Perception Scores

Differences between the average rating scores were not statistically significant, indicating that participants' ratings were similar across conditions (Table 12). Specifically, the Friedman tests revealed no significant differences in VAS score between blade conditions for the forward scale ($\chi^2 = 0.152$, $p = 0.99$), turn scale ($\chi^2 = 0.233$, $p = 0.97$), and the overall scale ($\chi^2 = 0.822$, $p = 0.84$). Additional written commentary was focused on several aspects of blade perception, such as comfortability, ease of glide, confidence, and control. Based on anecdotal observations and written commentary, participants were able to distinguish a difference in the "feel" of each blade condition.

Table 12

Means (standard deviations) for Visual Analog Scale (VAS) rating scores by blade condition

	VAS score (mm)			
	Blade Condition			
VAS scale type	**Single**	**Triple**	**Quadruple**	**Ellipse**
Forward	69 (15)	70 (13)	70 (20)	71 (16)
Turn	65 (19)	66 (17)	68 (22)	69 (20)
Overall	66 (18)	67 (12)	67 (21)	69 (19)

5. Discussion

The primary findings from the analysis indicated that blade condition had no significant effect on any measured spatiotemporal, kinematic, or perception variable during forward skating and tight turns on ice. Significant sex differences in joint angles were revealed in forward skating, and in a task not previously examined – tight turns. Primary sex differences observed during skating included hip adduction and knee flexion during forward skating, as well as hip and ankle internal rotation during turns. Only a few studies have examined the impact of blade profile on skating, and no study has compared turns between males and females.

5.1 Blade Effects

Blade effect hypotheses were not supported as blade condition had no significant effect on any spatiotemporal or kinematic variable for any task. However, there was one significant SPM ANOVA result, observed for inside ankle rotation for the right turn task (Figure 25E). Post-hoc analysis, though not statistically significant after Bonferroni correction, indicated greater ankle internal rotation in the Quadruple Radius profile compared to the Triple Radius profile, at the first inside leg push off out of the turn. Caution is warranted in interpreting these results due to the simplicity of current SPM post-hoc testing methods (Pataky, 2022). If this trend were significant, it may be explained by the reduced blade contact at the toe region of the Triple Radius profile, impacting player stability while turning and therefore limited internal rotation of the ankle during the crossover undercut. However, this effect was not observed in other stances nor in the left turn task.

Blade condition may not have significantly affected lower limb joint angles due to a lack of familiarity and period for adaptation. Similar cross-sectional studies on skate modification and skating mechanics report non-significant results speculating that changes in skating technique from modified skates may require a familiarization period and deliberate practice (Culhane, 2013; Robert-Lachaîne, 2011). This could be evaluated with longitudinal studies testing the effect of blade condition over an extended intervention period. Additionally, effects may have been too subtle to detect a significant difference. In a related study on ROC conditions, subtle hip flexion variations during backwards crossovers were reported between blade conditions, with differences up to 2.2 degrees in mean and push-off hip angles (Vienneau et al., 2017). Although this analysis examined a different task and different profile specifications, the comparable limited effects on joint angles suggest the need for a larger sample size in future studies to establish the significance of minor distinctions between conditions.

These findings highlight the importance of subjective comfort when altering blade profile, as spatiotemporal performance and skating mechanics were unaffected. Similar importance of comfort is observed in other footwear design such as running shoes, where uncomfortable shoes can limit kinematic variability by restricting runners to the least uncomfortable movement pattern (Meyer et al., 2018). In the context of blade alterations, discomfort from unfamiliar blades may have restricted skaters to the most comfortable skating pattern. This would be detrimental in game-scenarios where players must adapt their movement pattern in response to the open environment. Comfort should continue to play a role in blade profile design and future research should focus on quantifying its' relationship to kinematics or other biomechanical variables.

5.2 Sex Effects

5.2.1 Spatiotemporal

A main effect of sex was evident in task completion times, with males completing all tasks in less time than females. This aligns with previous sex comparison study findings in forward skating and transitional maneuvers (Hallihan, 2018; Shell et al., 2017). Male participants were significantly older and had more years of playing experience, factors often speculated to contribute to this disparity, alongside greater muscle strength and stride rate in males (Shell et al., 2017). Forward skating task completion times were greater overall compared to previous findings, likely attributed to the longer distance covered and the influence of fatigue, as the quantity of trials performed was substantial due to multiple blade conditions.

5.2.2 Forward Skating Joint Angles

Consistent with the hypothesis, females maintained a more adducted position of the hip and extended position of the knee throughout the task, suggesting a more upright body positioning overall. For Side 1, the disparity in hip adduction became significantly different at distinct regions of each stride cycle, just prior to ice-contact, continuing through ice contact and into the midpoint of each stance phase (Figure 7C). Males were significantly more flexed at the knee extension plateau of ST1, and ST5 – ST8 (Figure 9A and 10A).

These disparities between sexes are consistent with previous literature (Budarick et al., 2020; Shell et al., 2017). Reduced hip abduction in females is speculated to be a strategy for reducing the stretch of the adductor muscles and potential for injury (Budarick et al., 2020; Shell et al., 2017). At blade contact, the muscles of the thigh display a peak in activity required for stabilization, followed by eccentric activity of the hip adductors during the stance phase and into the late push-off phase (Chang et al., 2009). Greater hip adduction in females may have reduced the stretch on the adductors as they stabilized at blade contact, and began to load eccentrically (Shell et al., 2017). Alternatively, anatomical sex differences may play a role, as pelvis width is typically relatively greater in females, which may affect the amount of abduction they could engage in (Brinckmann et al., 1981). In previous studies, the elongated knee extension period during stance, known as the knee extension plateau, was found to be more emphasized in females, as males extend their knee throughout the stance with less pause while maintaining an overall more flexed position throughout (Budarick et al., 2020; Shell et al., 2017). It is speculated that this difference is related to disparities in muscle strength and stiffness, which allows males to better absorb the force of blade contact and continue through knee extension (Budarick et al., 2020; Shell et al., 2017). From visual observation, the difference in plateau between sexes was not as pronounced compared to previous research, other than the greater magnitude of knee flexion angle in males during this period (Figure 9A and 10A).

5.2.3 Tight Turn Joint Angles

Several joint angle disparities between sexes were present in both the right and left turn tasks. Males displayed a more flexed knee position for both leg sides throughout the task, which was significant at the start of the turn for the outside knee, as well as later stance phases out of the turn for both knees (Figure 15A, 16A, and 21A and 22A). Females also exhibited greater hip adduction in the inside hip at the blade contact of the first step out of the right turns (Figure 20C). In the transverse plane, males were significantly more internally rotated at the outside hip at the first OFF event out of the turn and into the swing phase, and more externally rotated at the inside ankle at the end of the turn event and at the first ON event after the step (Figure 13E, 19E, 18E and 24E). Overall, relatively large standard deviations were observed, potentially influenced by individual variations in technique, which could be linked to factors such as leg dominance, turn side preference, or stick side.

Rapid change of direction (COD) tasks are known for their heightened risk of knee injuries, particularly among female athletes, as increased knee valgus and internal rotation moments are introduced with rapid turning (Ford et al., 2005; Sigward & Powers, 2007).

Reduction in knee flexion may have been a strategy to mitigate this risk (Shell et al., 2017). For transverse plane angles, greater outside hip internal rotation and inside ankle external rotation angles in males may have positioned their legs at a more acute angle as they exited the turn, affording males a “sharper” turn exit. This may have improved their positioning to accelerate in the forward direction post-turn and effectively decrease their task completion time (Haché, 2002; McGrail, 2006).

Implications for these results highlight the need for training interventions that emphasize eccentric loading and stabilization, especially for the hip adductors, and knee stabilizing muscles of the thigh for females. In other sports, eccentric training has shown to help female athletes tolerate greater loads during COD tasks (Jones et al., 2022; Jones et al., 2017). Turn technique training should focus on rotational range of motion in the transverse plane particularly at the hip and ankle to optimize turn cutting angle.

5.3 Double Support Effects

Double support (DS) phase times generally increased with the progression of DS phases across all tasks. In turns, the DS phase times reached up to 0.1 seconds by the second phase, whereas in forward skating, this duration was not reached until the seventh or eighth phase. During forward skating starts of elite skaters, the initial DS phases are typically short or may even transition into a flight phase, resembling ‘run-like’ push-off steps that facilitate acceleration from zero velocity (Renaud et al., 2017). In contrast, during turn exit steps, the initial DS phases were elongated, possibly due to the skater’s existing motion and the undercut from the crossover steps. Force propulsion occurs during the DS phase of a stride cycle, and studies suggest maximizing force propulsion is most successful by maximizing propulsive phase rate (Culhane, 2013; Marino, 1977). Despite the overall trend of elongated DS phases in turns, it was observed that some participants did employ techniques similar to that of the forward skating start – utilizing short, quick steps and DS phases out of the turn. Future studies should compare turn exit techniques (i.e., step and DS phase rate/duration) to determine the most effective way to maximize acceleration out of a turn.

5.4 Perception

Perception scores from the VAS were diverse across all blade conditions, with average scores ranging between 65 – 71 mm, out of 100, for each task, and standard deviations between 12 – 22 mm. No significant differences were observed between blade condition ratings, indicating that no blade condition was consistently rated higher than another. The Single Radius profile received the highest overall VAS rating from six participants, the Triple Radius profile from five participants, the Quadruple Radius profile from seven participants, and the Ellipse profile from eight participants. Based on anecdotal observations and participant comments, it was clear that the participants could distinguish a difference in the "feel" between blade conditions. Participant comments touched on their perception of blade contact, comfortability, and the ability to glide or be agile; however, opinions were not unanimous and did not always align with the intended characteristics of each profile. For example, the Triple Radius profile intended to improve agility due to less blade contact and a more forward leaning pitch, received mixed feedback. Some participants felt difficulty turning whereas others experienced an enhanced feel during turns (based on written commentary). This may be attributed to factors such as how the blades compared to the individual's normal condition, or the effect of individual skating styles. While this commentary was not considered for formal interpretation, it provides a valuable subjective perspective on the impact of blade condition.

5.5 Limitations

The study presents with several limitations. The elite population may limit the generalizability of the results to other populations, such as recreational or developing hockey players. Results also lack generalizability to other skating tasks. Blade effects could become more apparent in tasks with greater length and a broader range of transitional skills. Participants did not use the same skate model. It was decided that skaters would wear their own skates to ensure accurate perceptions of comfort and "feel" between blade conditions. If skate model was to be controlled, players may not have been able to attribute differences in feel solely to the blade condition. This approach was also more feasible in terms of resource requirements for this study. Profile "size" or ROC dimensions and pitches were not the same for a given blade condition between participants due to differences in foot sizes. This decision was based on the standardized profile sizes currently recommended by the manufacturer. ROC and ROH of the blade conditions were not quantitatively measured for size validation or edge quality but were assumed to be sharpened and profiled correctly by the manufacturers. The current blade characteristics of the participants were self-reported and not quantitatively measured, which may have limited the accuracy of the identification of these metrics. The level of familiarity as well as the level of "newness" or "differentness" with each profile may have differed across participants depending on what blade they currently use, which may have influenced their perceptions of or their adaptations to each profile. Although, most participants had very limited familiarization to other blade conditions besides the Single Radius prior to this testing. The data were collected in a controlled, non-game environment which was most effective for the use of biomechanical measurement equipment. Results may therefore not be perfectly game-applicable, as the experiment did not involve game elements such as full protective equipment, the presence of other players, or a puck. The conditions of the ice may have fluctuated across participants. This limitation was mitigated as much as possible by visually inspecting the ice quality prior to collection, and by adjusting the on-ice position of the task course after several consecutive trials.

5.6 Future Directions

Future research should compare blade profile conditions through additional biomechanical measurement methods including force and plantar pressure, center of mass, and muscle activation. Some research suggests blade ROC can affect regional plantar pressure during backwards crossovers and is theorized to influence the general location of the center of pressure (Broadbent, 1985, as cited in Cadeau, 2017; Vienneau et al., 2017). Further biomechanical investigation could help identify factors that contribute to differences in “feel” and explore ways to optimize this more objectively. Additionally, it would be valuable to analyze other tasks such as backward skating and stopping, and to compare forward acceleration with maximal speed skating, as this may provide deeper insights into how each profile enhances different skating aspects of the game.

Coaches and players may benefit from a more individualized analysis approach. For example, correlations between individual factors (e.g., height, weight, position, biomechanical variables) and blade profile preferences could be explored. Within the study’s cohort, all participants except one did not know their current blade profile condition or had never adjusted it. As this area of blade alteration is relatively new and developing, more practical recommendations are warranted. Future studies should implement blade condition comparisons in game-like scenarios and include other populations such as developing players, to improve the applicability of the results.

Findings may offer comprehensive insights to integrate into the blade design process. Skate manufacturers should consider the optimal techniques and ranges of motion identified in these results and acknowledge the differences between sexes. As more sex differences in kinematic and spatiotemporal characteristics of skating are uncovered, the necessity for inclusion of female participants in ice hockey biomechanics becomes increasingly apparent. Many aspects of skating mechanics should be explored in female skaters including kinetic analyses (i.e., force and pressure), exploration of other skating tasks (e.g., backwards skating and pivots), and the effect of skate design on skating mechanics.

6. Conclusion

The effect of skate blade profile on spatiotemporal and joint angles during forward skating and turning was non-significant, highlighting the importance of subjective experience when adapting blade profile. Sex-specific kinematic differences were revealed in forward skating and tight turn technique. In forward skating, males maintained a more flexed knee positioning and greater hip abduction at blade contact. In turning, males showed greater internal rotation of the outside hip and external rotation of the inside ankle which may have optimized turn cutting angle. Males also showed greater knee flexion during turns. As the popularity of blade profile adaptation rises, a scientific approach is important for optimizing skater performance and comfort. This study provides a foundation for skate manufacturers to explore other profile shapes and radii dimensions and their effects on biomechanical variables and perception. Players should continue to employ trial-and-error methods and prioritize comfort when experimenting with blade profiles. The results have implications for sex-specific training and equipment design that consider the differing technique, range of motion, and strength capacity between sexes. The study underscores the importance of continued involvement of female athletes in ice hockey skating biomechanics research, contributing to the expansion and strengthening of knowledge in the field as a whole.

References

Abkowitz, S., Abkowitz, S. M., Fisher, H., & Schwartz, P. J. (2004). CermeTi® discontinuously reinforced Ti-matrix composites: Manufacturing, properties, and applications. *JOM*, *56*, 37-41.

Bonci, C. M. (1999). Assessment and evaluation of predisposing factors to anterior cruciate ligament injury. *Journal of Athletic Training*, *34*(2), 155.

Bowden, F. P., & Hughes, T. (1939). The mechanism of sliding on ice and snow. *Proceedings of the Royal Society of London. Series A. Mathematical and Physical Sciences*, *172*(949), 280-298.

Brinckmann, P., Hoefert, H., & Jongen, H. T. (1981). Sex differences in the skeletal geometry of the human pelvis and hip joint. *Journal of Biomechanics*, *14*(6), 427-430.

Broadbent, S. (1985). *Skateology: Iceskate Conditioning Equipment*. Littleton, CO.

Budarick, A. R., Shell, J. R., Robbins, S. M., Wu, T., Renaud, P. J., & Pearsall, D. J. (2020). Ice hockey skating sprints: Run to glide mechanics of high calibre male and female athletes. *Sports Biomechanics*, *19*(5), 601-617.

Cadeau, L. (2017). *The Effect of Recommended Sharpening Characteristics on Skating Speed*. [Master's thesis, Brock University]. Brock University Digital Repository

Chang, R., Turcotte, R., & Pearsall, D. (2009). Hip adductor muscle function in forward skating. *Sports Biomechanics*, *8*(3), 212-222.

Culhane, L. (2013). *Acceleration characteristics of forward skating.* [Master's thesis, McGill University]. eScholarship @ McGill

Denroche, S. K. (2020). *Evaluating the use of inertial measurement unit technology during an ice hockey shooting task*. [Master's thesis, McGill University]. eScholarship @ McGill

Dixon, P. C., Loh, J. J., Michaud-Paquette, Y., & Pearsall, D. J. (2017). biomechZoo: An open-source toolbox for the processing, analysis, and visualization of biomechanical movement data. *Computer Methods and Programs in Biomedicine*, *140*, 1-10.

Donnelly, N. (2010). *Improvement of the sharpening style of ice hockey skate blades.* [Unpublished Thesis].

Faul, F., Erdfelder, E., Lang, A.-G., & Buchner, A. (2007). G* Power 3: A flexible statistical power analysis program for the social, behavioral, and biomedical sciences. *Behavior Research Methods*, *39*(2), 175-191.

Federolf, P., & Nigg, B. (2012). Skating performance in ice hockey when using a flared skate blade design. *Cold Regions Science and Technology*, *70*, 12-18.

Federolf, P., & Redmond, A. (2010). Does skate sharpening affect individual skating performance in an agility course in ice hockey? *Sports Engineering*, *13*(1), 39-46.

Federolf, P. A., Mills, R., & Nigg, B. (2008). Ice friction of flared ice hockey skate blades. *Journal of Sports Sciences*, *26*(11), 1201-1208.

Ford, K. R., Myer, G. D., Toms, H. E., & Hewett, T. E. (2005). Gender differences in the kinematics of unanticipated cutting in young athletes. *Medicine & Science in Sports & Exercise*, *37*(1), 124-129.

Formenti, F., & Minetti, A. E. (2007). Human locomotion on ice: The evolution of ice-skating energetics through history. *Journal of Experimental Biology*, *210*(10), 1825-1833.

Gagnon, M., & Dore, R. (1983). Testing procedures and modeling for the evaluation of skating blade characteristics. *Scandinavian Journal of Sports Science*, *5*(1), 29-33.

Haché, A. (2002). *The physics of hockey*. JHU Press.

Hallihan, A. (2018). *Analysis of Male and Female Hockey Players during a Stop and Go Skating Task*. [Master's thesis, McGill University]. Proquest Dissertations & Theses @ McGill

Jones, P. A., Dos'Santos, T., McMahon, J. J., & Graham-Smith, P. (2022). Contribution of eccentric strength to cutting performance in female soccer players. *Journal of Strength and Conditioning Research*, *36*(2), 525-533.

Jones, P. A., Thomas, C., Dos'Santos, T., McMahon, J. J., & Graham-Smith, P. (2017). The role of eccentric strength in 180 turns in female soccer players. *Sports*, *5*(2), 42.

Khandan, A., Fathian, R., Carey, J. P., & Rouhani, H. (2022). Measurement of temporal and spatial parameters of ice hockey skating using a wearable system. *Scientific Reports*, *12*(1), 22280.

Lever, J. H., & Lines, A. P. (2023). Ice-rich slurries can account for the remarkably low friction of ice skates. *Journal of Glaciology*, *69*(274), 217-236.

Lever, J. H., Lines, A. P., Taylor, S., Hoch, G. R., Asenath-Smith, E., & Sodhi, D. S. (2022). Revisiting mechanics of ice–skate friction: from experiments at a skating rink to a unified hypothesis. *Journal of Glaciology*, *68*(268), 337-356.

Lockwood, K. (2003). *What are NHL players really skating on.* [Conference presentation] SPHEM/PHATS Annual Conference.

Lockwood, K., & Frost, G. (2009). When metal meets ice: Potential for performance or injury. *Journal of ASTM International*, *6*(2), 1-8.

MacCormick, L., Best, T. M., & Flanigan, D. C. (2014). Are there differences in ice hockey injuries between sexes? A systematic review. *Orthopaedic Journal of Sports Medicine*, *2*(1), 2325967113518181.

Marino, G. W. (1977). Kinematics of ice skating at different velocities. *Research Quarterly. American Alliance for Health, Physical Education and Recreation*, *48*(1), 93-97.

McGrail, J. S. (2006). *Skate boot pressure analysis of elite and recreational ice hockey skaters during the execution of tight turns* [Master's thesis, McGill University]. eScholarship @ McGill

McKenzie, A. (2012). *The Effect of Skate Blade Radius of Contour and Radius of Hollow on Skating Performance in Male Ice Hockey Players*. [Master's thesis, Brock University]. Brock University Digital Repository

Meyer, C., Mohr, M., Falbriard, M., Nigg, S. R., & Nigg, B. M. (2018). Influence of footwear comfort on the variability of running kinematics. *Footwear Science*, *10*(1), 29-38.

Panagodage Perera, N. K., Joseph, C., Kemp, J. L., & Finch, C. F. (2018). Epidemiology of injuries in women playing competitive team bat-or-stick sports: A systematic review and a meta-analysis. *Sports Medicine*, *48*(3), 617-640.

Pataky, T. C. (2012). One-dimensional statistical parametric mapping in Python. *Computer Methods in Biomechanics and Biomedical Engineering*, *15*(3), 295-301.

Pataky, T. C. (2022). *ANOVA post hoc analysis*. spm1d. https://spm1d.org/doc/PostHoc/anova.html?highlight=post+hoc

Pearsall, & Robbins, S. (2019). Design and materials in ice hockey. *Materials in Sports Equipment* (pp. 297-322). Elsevier.

Pearsall, Turcotte, R. A., Levangie, M. C., & Forget, S. (2013). Biomechanical adaptation in ice hockey skating. *Routledge Handbook of Ergonomics in Sport and Exercise* (pp. 51-60). Routledge.

Prosharp-Bauer. (2021). *AS2001 Instruction Manual.*

Renaud, P. J., Robbins, S. M., Dixon, P. C., Shell, J. R., Turcotte, R. A., & Pearsall, D. J. (2017). Ice hockey skate starts: A comparison of high and low calibre skaters. *Sports Engineering*, *20*(4), 255-266.

Reynolds, O. (1899). On the slipperiness of ice. *Memoirs and proceedings of the Manchester Literary and Philosophical Society, 43*(5 Pt 2*)*.

Robert-Lachaîne, X. (2011). *Force measurement and ankle motion of the forward skating and crossovers with a standard hockey skate and a modified hockey skate.* [Master's thesis, McGill University]. eScholarship @ McGill

Schick, D. M., & Meeuwisse, W. H. (2003). Injury rates and profiles in female ice hockey players. *The American Journal of Sports Medicine*, *31*(1), 47-52.

Shell, J. R., Robbins, S. M., Dixon, P. C., Renaud, P. J., Turcotte, R. A., Wu, T., & Pearsall, D. J. (2017). Skating start propulsion: Three-dimensional kinematic analysis of elite male and female ice hockey players. *Sports Biomechanics*, *16*(3), 313-324.

Sigward, S. M., & Powers, C. M. (2007). Loading characteristics of females exhibiting excessive valgus moments during cutting. *Clinical Biomechanics*, *22*(7), 827-833.

van den Berg, R. G. (2023). *SPSS ANOVA - Levene's Test "Significant"*. SPSS Tutorials. https://www.spss-tutorials.com/spss-anova-levenes-test-significant/

Vienneau, J., Smith, A., Nigg, S., & Nigg, B. (2017). *Modified hockey skate blade profiles affect skating biomechanics and performance* [Conference presentation abstract]. 41st annual meeting of the American Society of Biomechanics, Boulder, Colorado, USA.

Winchester, A. (2007). *Anaerobic performance in ice hockey: The effect of skate blade radius of hollow.* [Master's thesis, Brock University]. Brock University Digital Repository

Appendix A
Ethics Certification

McGill

Research Ethics Board Office
James Administration Bldg.
845 Sherbrooke Street West. Rm 325
Montreal, QC H3A 0G4

Tel: (514) 398-6831

Website: https://mcgill.ca/research/research/compliance/human/reb-i-ii-iii

Research Ethics Board 2
Certificate of Ethical Acceptability of Research Involving Humans

REB File #: 22-08-025

Project Title: A biomechanical analysis of ice hockey skate blade design

Principal Investigator: Laura Holman

Department: Kinesiology and Physical Education

Status: Master's Student

Supervisor: Professor Shawn Robbins

Independent Researcher: Professor David Pearsall

Funding: NSERC

Approval Period: October 17, 2022 – October 16, 2023

The REB 2 reviewed and approved this project by delegated review in accordance with the requirements of the McGill University Policy on the Ethical Conduct of Research Involving Human Participants and the Tri-Council Policy Statement: Ethical Conduct for Research Involving Humans.

Georgia Kalavritinos
Ethics Review Administrator

---

* Approval is granted only for the research and purposes described.
* Modifications to the approved research must be reviewed and approved by the REB before they can be implemented.
* A Request for Renewal form must be submitted before the above expiry date. Research cannot be conducted without a current ethics approval. Submit 2-3 weeks ahead of the expiry date.
* When a project has been completed or terminated, a Study Closure form must be submitted.
* Unanticipated issues that may increase the risk level to participants or that may have other ethical implications must be promptly reported to the REB. Serious adverse events experienced by a participant in conjunction with the research must be reported to the REB without delay.
* The REB must be promptly notified of any new information that may affect the welfare or consent of participants.
* The REB must be notified of any suspension or cancellation imposed by a funding agency or regulatory body that is related to this study.
* The REB must be notified of any findings that may have ethical implications or may affect the decision of the REB.

Appendix B

Participant Consent Form

Participant Consent Form

Principal Investigator:
Laura Holman, M.Sc. Candidate
Department of Kinesiology and Physical Education, McGill University
Email: laura.holman@mail.mcgill.ca; Phone: 416-997-7189

Supervisor:
Dr. Shawn Robbins, Associate Professor
School of Physical and Occupational Therapy, McGill University
Email: shawn.robbins@mcgill.ca; Phone: 514-398-4400 ext. 00720

Co-Investigator:
Dr. David Pearsall, Independent Researcher
Email: david.pearsall@mcgill.ca

Title of Project: A biomechanical analysis of ice hockey skate blade design
Sponsor: Natural Sciences and Engineering Research Council of Canada

Purpose of the Study: The purpose of this research project is to explore the effects of ice hockey skate blade design on foot pressure, joint motion, and player preferences during skating in elite ice hockey players. Altering the shape and design of skate blades can affect skating performance but little is known about the specific effect on skating motion.

This study has three objectives: 1) To analyze the effect of skate blade design on skating, specifically across four specific blade designs. 2) To compare males and females in their blade preferences and skating performance. 3) To quantify factors that impact blade design preference.

Study Procedures: The approximate time commitment of the study is 2 hours in one study visit. You will be required to bring and wear athletic shorts and t-shirt, track pants and jacket as well as your hockey skates, stick, and gloves for the study visit. All other equipment will be provided by the researcher. For the data collection visit, you will arrive at the McConnell arena on the McGill University campus and be escorted to a private change room in the arena building. If you are a female, you will be accompanied by a female researcher. Vice versa for males. You will be asked to fill out a form regarding your ice hockey playing history, age, injury history and information about the equipment you use. You will then have several body measurements taken such as your weight and height. These measurements are required for calibration of the materials used in the study.

The study contains an off-ice and an on-ice procedure. During the off-ice procedure, you will be asked to perform trials of a stationary standing pose and a hockey stance “ready position” pose. You will perform these trials standing barefoot on pressure sensing footwear insoles placed flat on the ground. Each trial will consist of 10 seconds standing in each pose. You will complete 2 trials of each pose.

You will then have 17 small sensors attached to the major segments of your body, which track the position of your body as you skate. The sensors will be placed on your skin with double sided tape and secured with a layer of medical tape. The feet sensors will be placed on the laces of your skates and secured with duct tape. You will wear a headband that contains the head sensor. You will wear small gloves which will secure the hand sensors. The pressure insoles you stood on during the off-ice portion of the study will be placed into your skates. You will be provided with socks to ensure uniformity in sock thickness among participants. You will put on your gloves, skates, and carry your stick. You will then be escorted to the ice surface.

On the ice surface, the sensors will be calibrated to the computer system. To calibrate, you will walk forward four meters one direction, turn 180˚, and walk four meters in the opposite direction. This will be done on a carpet laid out on the ice. You will have five minutes to warm up between each blade condition.

You will then be asked to perform 4 types of skating tasks. These will be repeated with each of the 4 blade conditions. This includes forward skating, backwards skating, and tight turns (clockwise and counterclockwise). Adequate rest time and water breaks will be given when needed in between trials. You will perform 3 trials of each task in each blade condition which totals to 48 skating trials.

1) *Forward Skating:* You will start at the goal line, accelerate forward at full speed toward the far blue line and stop at the far blue line finishing area (34 m).
2) *Backwards Skating:* You will start at the goal line. You will perform a backwards start to accelerate backwards towards the far blue line at full speed and stop at the far blue line finishing area (34 m).
3) *Tight turns*: You will start at the blue line. You will skate forward at full speed toward the opposite blue line (15 m). You will perform as tight of a turn as possible (180˚) around a cone at the opposite blue line without stopping to return to the initial starting location. You will perform 3 trials clockwise, and 3 trials counterclockwise.

The blade conditions in this study will vary in their radius of contour (ROC) design which is the longitudinal shape of the blade. A blade can contain one or multiple contours. See examples below:

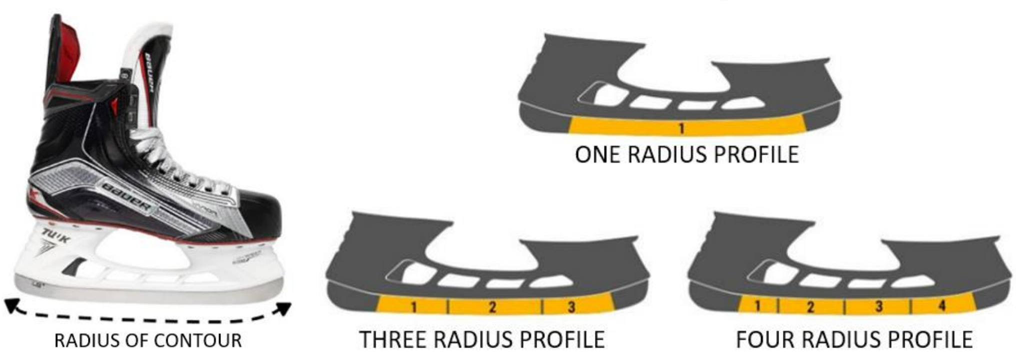

The following blade conditions are used in the study:

1) Quad – Profile with four differently contoured regions.
2) Zuperior – Profile with three differently contoured regions.
3) Ellipse – An ellipse shaped single contour.
4) Standard: Profile with one contour, the manufacturer's standard contour.

Between trials, you will be asked to fill out a questionnaire about your perception of your performance and preference. You will rate the blade condition on speed, control, and overall preference.

Voluntary Participation: Participation in this research is voluntary. You may refuse to participate in any part of the study, decline to answer any question and may withdraw from the study at any time, for any reason. Data collected up to the point of withdrawal will be destroyed if you do choose to withdraw from the study during or right after participating unless you permit (at the time of withdrawal) that all or some of the data may be kept. Once the data has been combined for publication, it may not be possible to withdraw the data in its entirety. We can only remove it from further analysis and from use in future publications. The data will be de-identified after the completion of the data collection and analysis (i.e., 31/08/2023) after which the data can no longer be linked to you.

Potential Risks: You may experience minimal discomfort when removing the sensors with attached medical tape from your skin and may experience brief redness where the tape was placed, which will disappear within a few hours after the study. You may become fatigued throughout the testing session; however, you will be given adequate rest and water breaks and will not be asked to perform at an effort level higher than your normal level of physical exertion during a game.

Potential Benefits: Participating in this study may not directly benefit you; however, results may provide insight into the effect of blade shape/profile on skating, and how it may affect males and females differently. Results may support and direct future guidelines for individualized blade profiling and in-store recommendations.

Compensation: You will be compensated $40 in cash for your participation in this study.

Confidentiality: All personal information (i.e., name, date of birth, height, weight, sex etc.) collected during the study will be kept on a password protected computer to maintain your confidentiality. Your personal information will not be disclosed in any manner in the dissemination of the results. During data collection, your data will be labelled using an identification code. De-identified data will be stored on the internal hard drive on the computer for further analysis and will be kept confidential by the research team (i.e., principal investigator, faculty supervisors and lab technician). With your consent, all de-identified data will be kept permanently in the Ice Hockey Biomechanics Laboratory database by Dr. Shawn Robbins and published online for use by other researchers for unspecified purposes.

Trials will be video recorded for visual analysis, solely for the use of the researcher. The footage will be kept on a password protected computer accessible only by the PI, supervisors, and co-investigators/lab technician.

With your consent, the researcher may take pictures with a camera while you perform the off-ice and on-ice protocols. This may be included in the final thesis report for visual reference to demonstrate the tasks and methods used. With your consent, video recordings may also be used in the dissemination of the results. When used for this purpose, in both photo and video captures, your face, or any secondary identifiable information such as tattoos, piercings, birthmarks, or any identifiable clothing (such as your name, team name and number on team apparel) will NOT be shown. To maintain confidentiality, both pictures and videos will be stored on the hard drive on the password protected computer of the lab.

Please check Yes or No to the following statements:

Yes: ___ No: ___ You consent to have pictures taken during testing and used in the dissemination of the results (no face or secondary identifiable information shown)

Yes: ___ No: ___ You consent for use of video recorded material by the principal investigator in dissemination of results (no face or secondary identifiable information shown)

Yes: ___ No: ___ You consent for your de-identified data to be used for future, unspecified purposes

Dissemination of Results: Results will be included in a thesis document which will be available on McGill University's digital thesis repository - eScholarship. The results may also be disseminated through an academic journal publication, at academic conference presentations, and presented to our industry partner, Bauer Hockey Ltd.

If you have any questions, concerns, or complaints at any time, please contact the PI – (Laura Holman; laura.holman@mail.mcgill.ca) or the faculty supervisor (Dr. Shawn Robbins; shawn.robbins@mcgill.ca).

If you have any ethical concerns or complaints about your participation in this study, and want to speak with someone not on the research team, please contact the Associate Director, research Ethics at 514-398-6831 or lynda.mcneil@mcgill.ca citing REB file number 22-08-025.

Please sign below once you have read the above document and if you consent to participate in this research project. A copy of this consent form will be kept by the researcher.

Please sign below if you have read the above information and consent to participate in this study. Agreeing to participate in this study does not waive any of your rights or release the researchers from their responsibilities. To ensure the study is being conducted properly, authorized individuals, such as a member of the Research Ethics Board, may have access to your information. A copy of this consent form will be given to you and the researcher will keep a copy.

Participant's Name: (please print) ____

Participant's Signature: ______________________________________*Date*______________

Participant's Email: ____

Appendix C

Participant Information Form

Participant ID#: ___________________________________

Date of Birth: ___________________________________

Sex: ___________________________________

Years of hockey playing experience: ___________________________________

Highest level played: ___________________________________

Current Team: ___________________________________

Position(F/D): ___________________________________

Skate size: ___________________________________

Shot handedness: ___________________________________

Dominant leg: ___________________________________

Height: ___________________________________

Weight: ___________________________________

Stick Brand/Model: ___________________________________

Skate Brand/Model: ___________________________________

Blade Holder Model: ___________________________________

Skate blade characteristics (typically used):

Radius of Hollow: ______________________

Radius of Contour: ______________________

Height of blade at: 25%_______75%_______

If applicable:

Approximate time using the performance profiles (number of games/practices/days):_______________

Of the performance profiles, which one do you currently prefer (if any)? _________________________

Do you currently wear insoles in your skates? If so, which ones? _______________________________

Injury History:

1. In the past year, have you suffered any injuries to your hip, knee, or ankle? Has it prevented you from playing hockey? Explain.

____

____

____

2. In the past year have you experienced any other lower body injuries? (i.e., broken bones, torn ligaments etc.) Have they prevented you from playing hockey? Explain.

____

____

____

3. In the past year, have you experienced any injury to your nervous system? (e.g., concussion, damage to a nerve etc.) Has it prevented you from playing hockey? Explain.

____

____

____

4. Is there any other reason why you believe you should not participate in this study? Explain.

____

____

____

Appendix D

Participant Blade Information

Table D1

Participant blade information

Participant	Skate Model	Skate Size	ROH	ROC or profile	Insoles
1	Vapor 1X	L:8.75, R:9.25	5/8”	Unknown	Y
2	Vapor X Shift Pro	9.5	5/8”	Unknown	N
3	Supreme	7.5	Flat bottom V	Unknown	N
4	Supreme 2S	9	5/8”	Unknown	N
5	Supreme Mach	7.5	5/8”	Unknown	N
6	Supreme M4	4	1/2”	Unknown	N
7	Supreme Mach	8	3/4”	Unknown	N
8	Vapor APX	8	1/2”	Unknown	Y
9	Vapor	8	5/8”	Unknown	N
10	Vapor Hyperlite	4.5	1/2"	Unknown	N
11	Supreme	9.5	5/8”	Unknown	N
12	Supreme Mach	9	1/2"	Unknown	N
13	Vapor Hyperlite	9.5	5/8”	Unknown	N
14	Vapor Hyperlite	5.5	1/2"	Unknown	Y
15	Vapor	6.5	5/8”	Prosharp Quad	Y
16	Supreme Mach	4.5	1/2"	Unknown	N
17	Supreme 2S Pro	5	11/16”	Unknown	Y
18	Supreme S180	4	9/16”	Unknown	N
19	Vapor	5.5	1/2"	Unknown	N
20	Vapor	9	5/8”	Unknown	Y
21	Vapor X700	7	5/8”	Unknown	N
22	Supreme Mach	8	1/2"	Unknown	N
23	Supreme Mach	4	5/8”	Unknown	Y
24	Supreme	6.5	1/2”	Unknown	N
25	Vapor Hyperlite	4.5	1/2"	Unknown	N
26	Supreme Total One MX3	10.5	5/8” or 1/2"	Unknown	Y

Note. As information was self-reported some information may be missing. In the Insoles column, Y indicates “yes” to wearing insoles, N indicates “no” to wearing insoles.

Appendix E
Visual Analog Scale

Participant Feedback Questionnaire

Participant ID#: ___________________________________

Blade Code: ____________________________________

Please rate this blade condition from least ideal to most ideal on the following criteria by placing a vertical mark along each scale where you feel best fits your experience.

1. **Forward skating**

|——————————————————————————|

Least ideal for forward skating — Most ideal for forward skating

2. **Tight turn**

|——————————————————————————|

Least ideal for tight turns — Most ideal for tight turns

3. **Backward skating**

|——————————————————————————|

Least ideal for backward skating — Most ideal for backward skating

4. **Overall Rating**

Make a mark along the line regarding the following statement:
These blades are the ideal blade condition for me

|——————————————————————————|

Least ideal overall — Most ideal overall

Additional Comments

Appendix F

ANOVA Results

Table F1

2-way mixed ANOVA results for all task completion, and turn times

Measure	Source	F	Sig	Partial Eta Squared
Forward Completion Time	Blade*	0.189	0.854	0.008
	Sex	**40.01**	**0.000**	**0.625**
	Blade.sex	0.624	0.559	0.025
Left Turn Completion Time	Blade	1.349	0.265	0.053
	Sex	**15.764**	**0.001**	**0.396**
	Blade.sex	1.845	0.147	0.071
Left Turn Time	Blade	0.097	0.961	0.004
	Sex	0.021	0.886	0.001
	Blade.sex	1.647	0.187	0.070
Right Turn Completion Time	Blade*	1.780	0.159	0.072
	Sex	**25.731**	**0.000**	**0.528**
	Blade.sex	2.011	0.120	0.008
Right Turn Time	Blade	0.542	0.613	0.023
	Sex	0.933	0.344	0.039
	Blade.sex	0.267	0.801	0.011

Note. Significant results are denoted in bold text. Effects adjusted using Greenhouse Geisser correction are indicated with an asterisk (*).

Table F2

3-way mixed ANOVA results for all skating task double support phase times

Measure	Source	F	Sig	Partial Eta Squared
Forward Double Support Phase Time	**DS***	**13.178**	**0.000**	**0.364**
	Blade	0.313	0.816	0.013
	Sex	1.365	0.255	0.056
	DS.blade*	1.395	0.144	0.057
	DS.sex	0.580	0.771	0.025
	Blade.sex	0.337	0.798	0.014
	DS.blade.sex	0.597	0.921	0.025
Left Turn Double Support Phase Time	**DS***	**561.144**	**0.000**	**0.962**
	Blade*	0.432	0.678	0.019
	Sex	0.096	0.759	0.004
	DS.blade*	0.348	0.777	0.016
	DS.sex	0.142	0.732	0.006
	Blade.sex	1.468	0.239	0.063
	DS.blade.sex	1.492	0.227	0.064
Right Turn Double Support Phase Time	**DS***	**685.859**	**0.000**	**0.968**
	Blade*	0.624	0.553	0.026
	Sex	1.460	0.239	0.060
	DS.blade*	0.681	0.559	0.029
	DS.sex	0.674	0.433	0.028
	Blade.sex	0.420	0.677	0.018
	DS.blade.sex	0.458	0.702	0.020

Note. DS stands for Double Support Phase. Significant results are denoted in bold text. Effects adjusted using Greenhouse Geisser correction are indicated with an asterisk (*).

Table F3

Matrix of mean time differences (95% confidence intervals) between double support phase times for the forward skating task

	Mean difference (seconds)						
Phase	DS1	DS2	DS3	DS4	DS5	DS6	DS7
DS1	-						
DS2	-0.020 (-.043, .003)	-					
DS3	-0.003 (-.024, .018)	0.017 (.005, .029)	-				
DS4	0.009 (-.015, .032)	0.029* (.018, .040)	0.012 (.003, .021)	-			
DS5	0.022 (-.002, .046)	0.042* (.027, .057)	0.025* (.017, .033)	0.013 (.004, .023)	-		
DS6	0.024 (-.002, .051)	0.044* (.029, .059)	0.027* (.015, .040)	0.016* (.007, .024)	0.002 (-.011, .015)	-	
DS7	0.034 (.010, .059)	0.054* (.039, .070)	0.037* (.028, .047)	0.026* (.016, .036)	0.012* (.006, .019)	0.010 (-.001, .021)	-
DS8	0.042 (.011, .072)	0.061* (.044, .079)	0.045* (.026, .063)	0.033* (.019, .047)	0.019 (.001, .038)	0.017* (.008, .027)	0.007 (-.008, .022)

Note. Negative differences indicate that the column-listed variable had shorter double support times compared to the row-listed variable for all comparisons. Significant differences are marked as **p* < 0.001 following adjustment for multiple comparisons using the Bonferroni correction.

Table F4

Matrix of mean time differences (95% confidence intervals) between double support phase times for left and right turn task

	Left Turn Task			*Right Turn Task*	
	Mean difference (seconds)			Mean difference (seconds)	
Variable	DS1	DS2	Variable	DS1	DS2
DS1	-		DS1	-	
DS2	0.056* (0.034, 0.077)	-	DS2	0.048* (0.033, 0.063)	-
DS3	0.048* (0.033, 0.063)	-0.008 (-0.032, 0.017)	DS3	0.037* (0.018, 0.056)	-0.011 (-0.033, 0.010)

Note. Negative differences indicate that the column-listed variable had shorter double support times compared to the row-listed variable for all comparisons. Significant differences are marked as **p* < 0.01 following adjustment for multiple comparisons using the Bonferroni correction.

Appendix G
SPM ANOVA figures

Figure G1

Side 1 leg hip flexion/extension, adduction/abduction, and internal/external rotation angles during forward skating

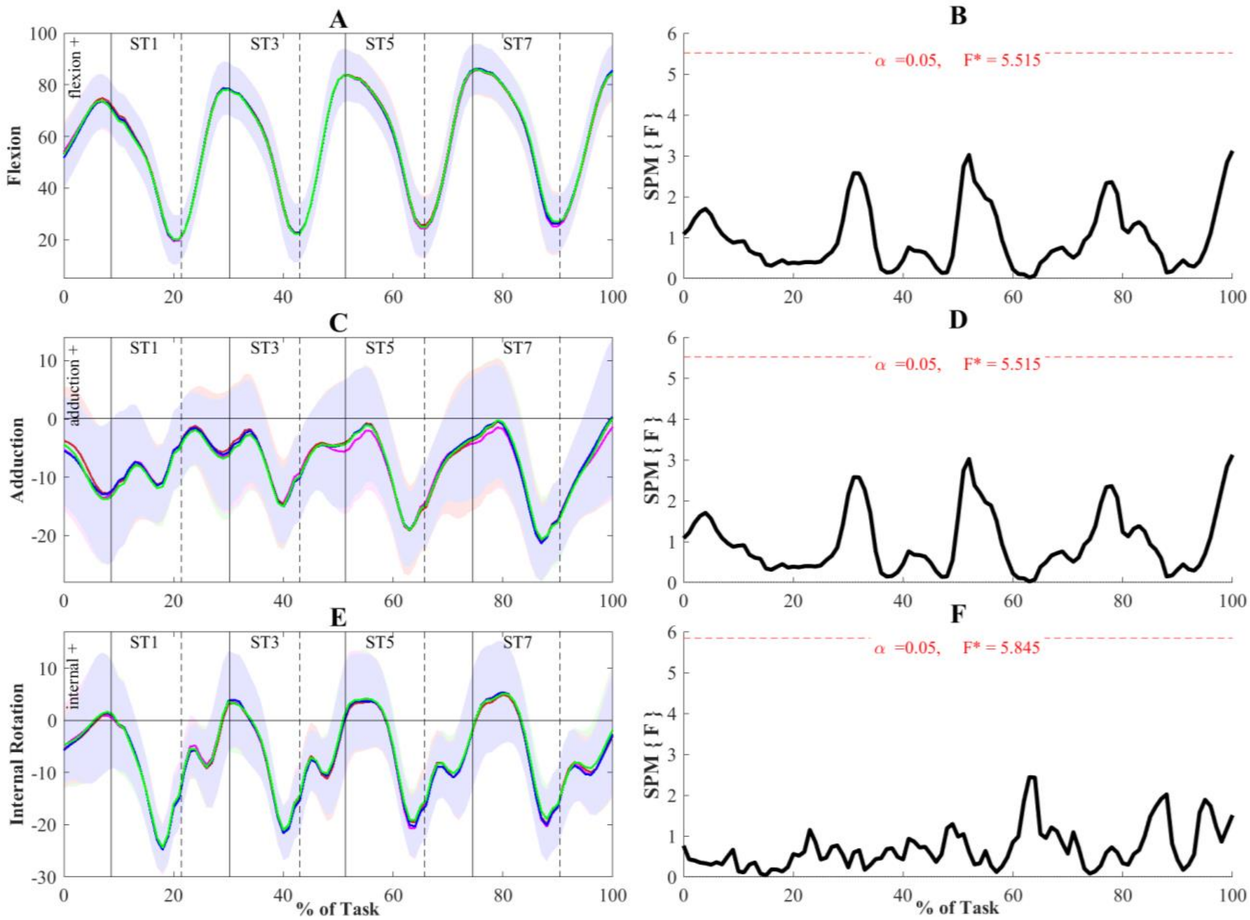

Note. (A) Hip flexion/extension, (C) hip adduction/abduction, (E) hip internal/external rotation for side 1. Angles are represented in degrees, where flexion, adduction and internal rotation are positive. Angles are expressed as a percentage of the forward skating task. Associated SPM {F} plots are positioned to the right of each joint angle waveform graph ((B), (D), (F)). Each coloured line represents blade conditions: Single Radius (red), Triple Radius (magenta), Quadruple Radius (green), and Ellipse (blue). Shaded regions denote standard deviations with respective colours for each blade. Vertical lines indicate skate ON (solid) and skate OFF (dotted) events. Stance phases are labelled within their respective skate ON and OFF events. Regions where the scalar output statistic (SPM{F}) surpassed the critical threshold (F) indicate a significant difference in joint angle between blade conditions. These regions are shaded in grey with significance levels marked as * $p < 0.05$.

Figure G2

Side 2 leg hip flexion/extension, adduction/abduction, and internal/external rotation angles during forward skating

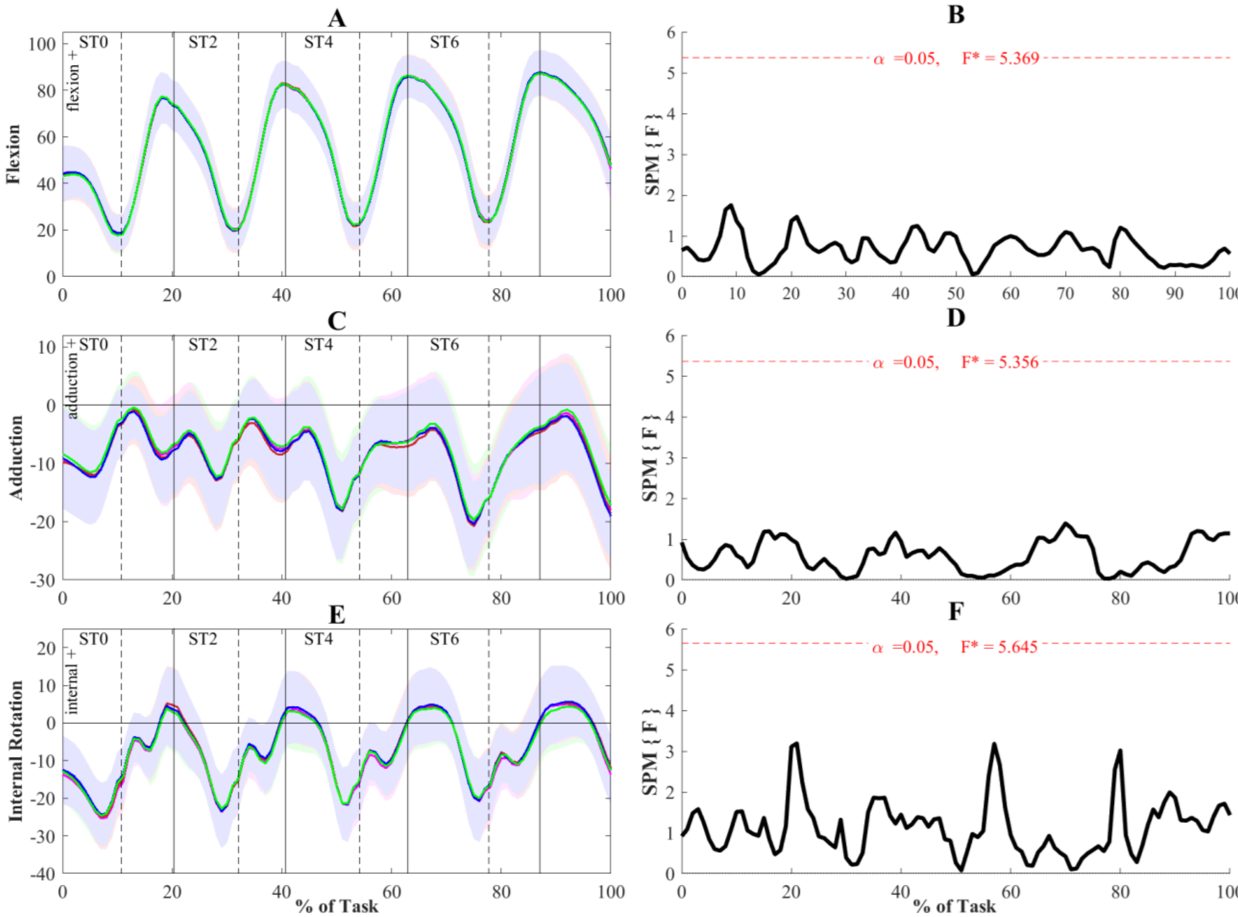

Note. (A) Hip flexion/extension, (C) hip adduction/abduction, (E) hip internal/external rotation for side 2. Angles are represented in degrees, where flexion, adduction and internal rotation are positive. Angles are expressed as a percentage of the forward skating task. Associated SPM {F} plots are positioned to the right of each joint angle waveform graph ((B), (D), (F)). Each coloured line represents blade conditions Single Radius (red), Triple Radius (magenta), Quadruple Radius (green), and Ellipse (blue). Shaded regions denote standard deviations with respective colours for each blade. Vertical lines indicate skate ON (solid) and skate OFF (dotted) events. Stance phases are labelled within their respective skate ON and OFF events. Regions where the scalar output statistic (SPM{F}) surpassed the critical threshold (F) indicate a significant difference in joint angle between blade conditions. These regions are shaded in grey with significance levels marked as * $p < 0.05$.

Figure G3

Side 1 knee flexion/extension and internal/external rotation angles during forward skating

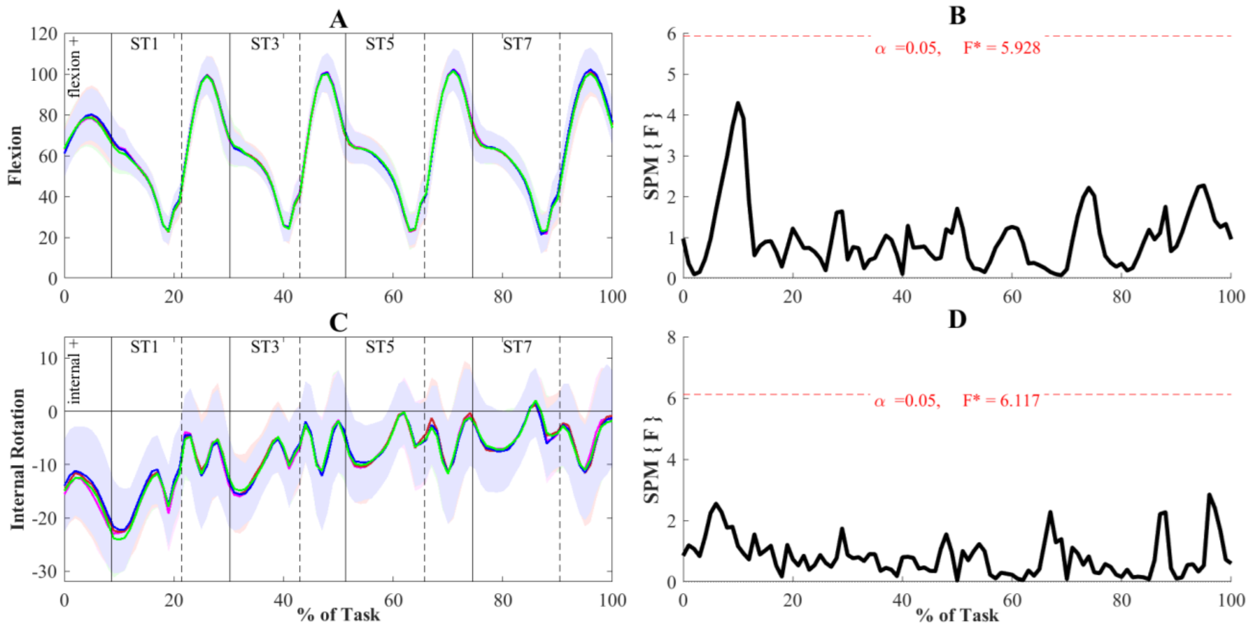

Note. (A) Knee flexion/extension, (C) knee internal/external rotation for side 1. Angles are represented in degrees, where flexion and internal rotation are positive. Angles are expressed as a percentage of the forward skating task. Associated SPM {F} plots are positioned to the right of each joint angle waveform graph ((B), (D)). Each coloured line represents blade conditions Single Radius (red), Triple Radius (magenta), Quadruple Radius (green), and Ellipse (blue). Shaded regions denote standard deviations with respective colours for each blade. Vertical lines indicate skate ON (solid) and skate OFF (dotted) events. Stance phases are labelled within their respective skate ON and OFF events. Regions where the scalar output statistic (SPM{F}) surpassed the critical threshold (F) indicate a significant difference in joint angle between blade conditions. These regions are shaded in grey with significance levels marked as * $p < 0.05$.

Figure G4

Side 2 knee flexion/extension and internal/external rotation angles during forward skating

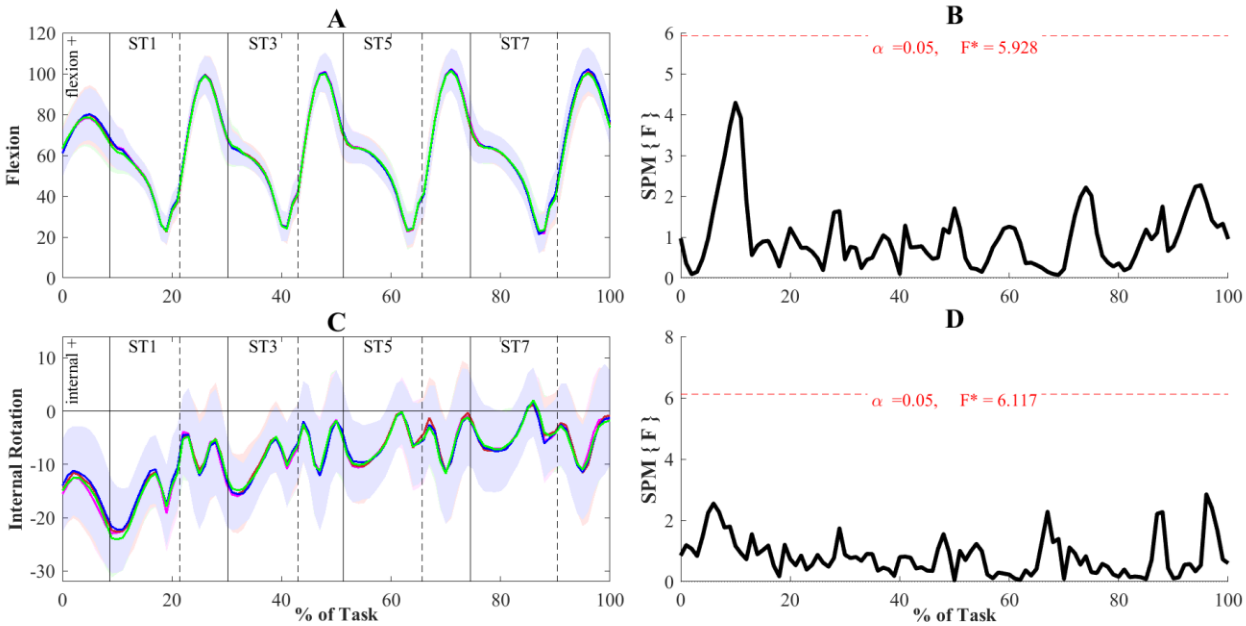

Note. (A) Knee flexion/extension, (C) knee internal/external rotation for side 2. Angles are represented in degrees, where flexion and internal rotation are positive. Angles are expressed as a percentage of the forward skating task. Associated SPM {F} plots are positioned to the right of each joint angle waveform graph ((B), (D)). Each coloured line represents blade conditions Single Radius (red), Triple Radius (magenta), Quadruple Radius (green), and Ellipse (blue). Shaded regions denote standard deviations with respective colours for each blade. Vertical lines indicate skate ON (solid) and skate OFF (dotted) events. Stance phases are labelled within their respective skate ON and OFF events. Regions where the scalar output statistic (SPM{F}) surpassed the critical threshold (F) indicate a significant difference in joint angle between blade conditions. These regions are shaded in grey with significance levels marked as * $p < 0.05$.

Figure G5

Side 1 ankle dorsi/plantar flexion, inversion/eversion, and internal/external rotation angles during forward skating

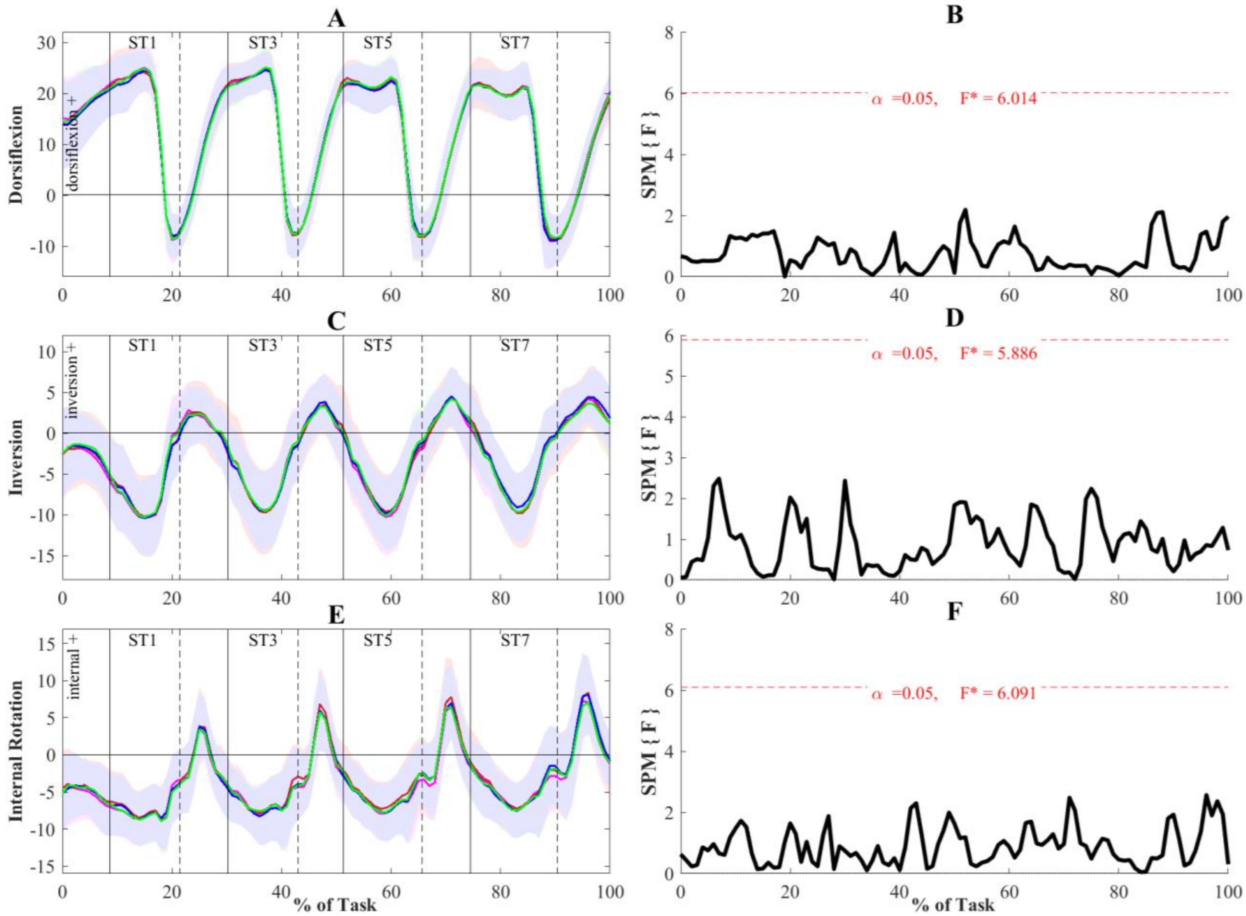

Note. (A) Ankle dorsi/plantarflexion, (C) ankle inversion/eversion, (E) ankle internal/external rotation for side 1. Angles are represented in degrees, where dorsiflexion, inversion, and internal rotation are positive. Angles are expressed as a percentage of the forward skating task. Associated SPM {F} plots are positioned to the right of each joint angle waveform graph ((B), (D), (F)). Each coloured line represents blade conditions Single Radius (red), Triple Radius (magenta), Quadruple Radius (green), and Ellipse (blue). Shaded regions denote standard deviations with respective colours for each blade. Vertical lines indicate skate ON (solid) and skate OFF (dotted) events. Stance phases are labelled within their respective skate ON and OFF events. Regions where the scalar output statistic (SPM{F}) surpassed the critical threshold (F) indicate a significant difference in joint angle between blade conditions. These regions are shaded in grey with significance levels marked as * $p < 0.05$.

Figure G6

Side 2 ankle dorsi/plantar flexion, inversion/eversion, and internal/external rotation angles during forward skating

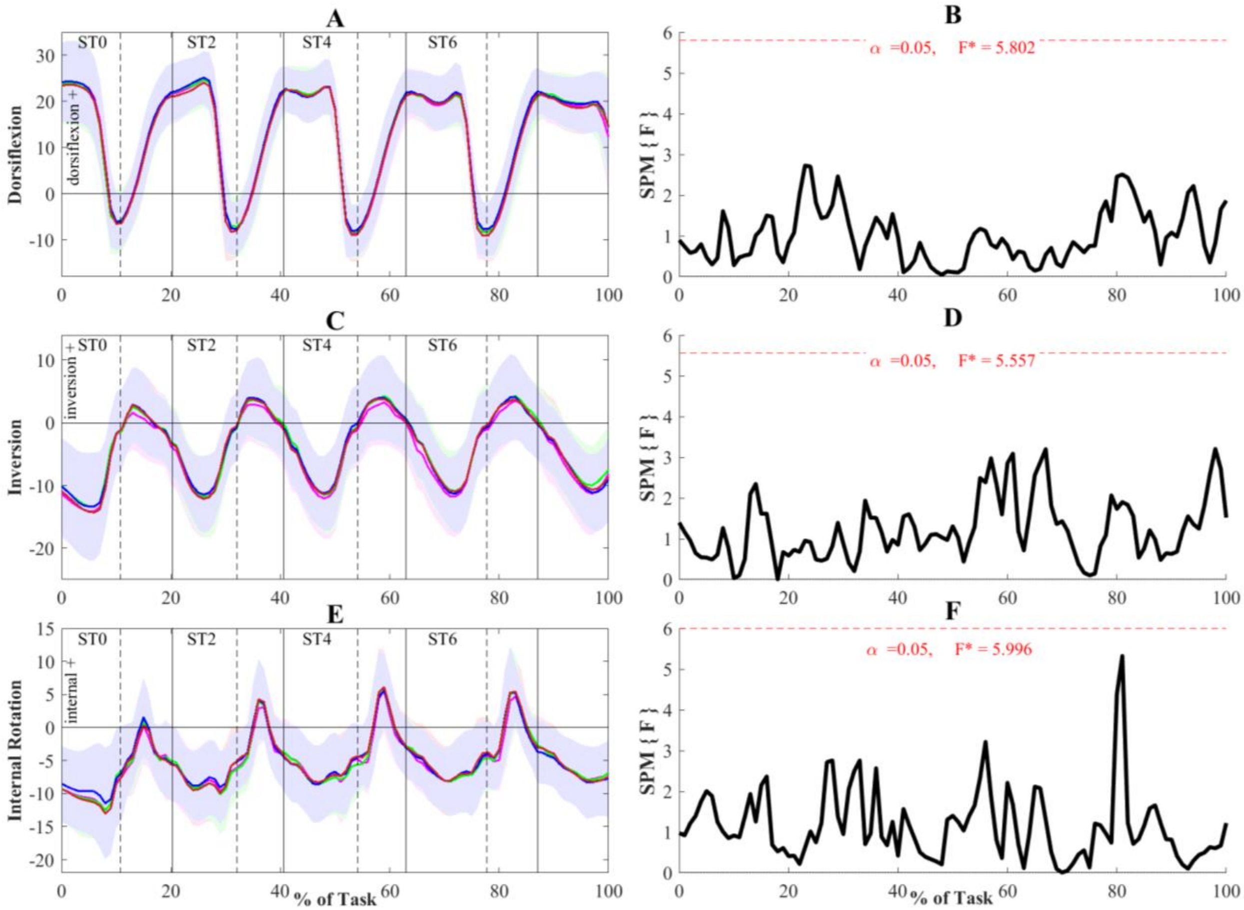

Note. (A) Ankle dorsi/plantarflexion, (C) ankle inversion/eversion, (E) ankle internal/external rotation for side 2. Angles are represented in degrees, where dorsiflexion, inversion, and internal rotation are positive. Angles are expressed as a percentage of the forward skating task. Associated SPM {F} plots are positioned to the right of each joint angle waveform graph ((B), (D), (F)). Each coloured line represents blade conditions Single Radius (red), Triple Radius (magenta), Quadruple Radius (green), and Ellipse (blue). Shaded regions denote standard deviations with respective colours for each blade. Vertical lines indicate skate ON (solid) and skate OFF (dotted) events. Stance phases are labelled within their respective skate ON and OFF events. Regions where the scalar output statistic (SPM{F}) surpassed the critical threshold (F) indicate a significant difference in joint angle between blade conditions. These regions are shaded in grey with significance levels marked as * $p < 0.05$.

Figure G7

Outside leg hip flexion/extension, adduction/abduction, and internal/external rotation angles during left turns

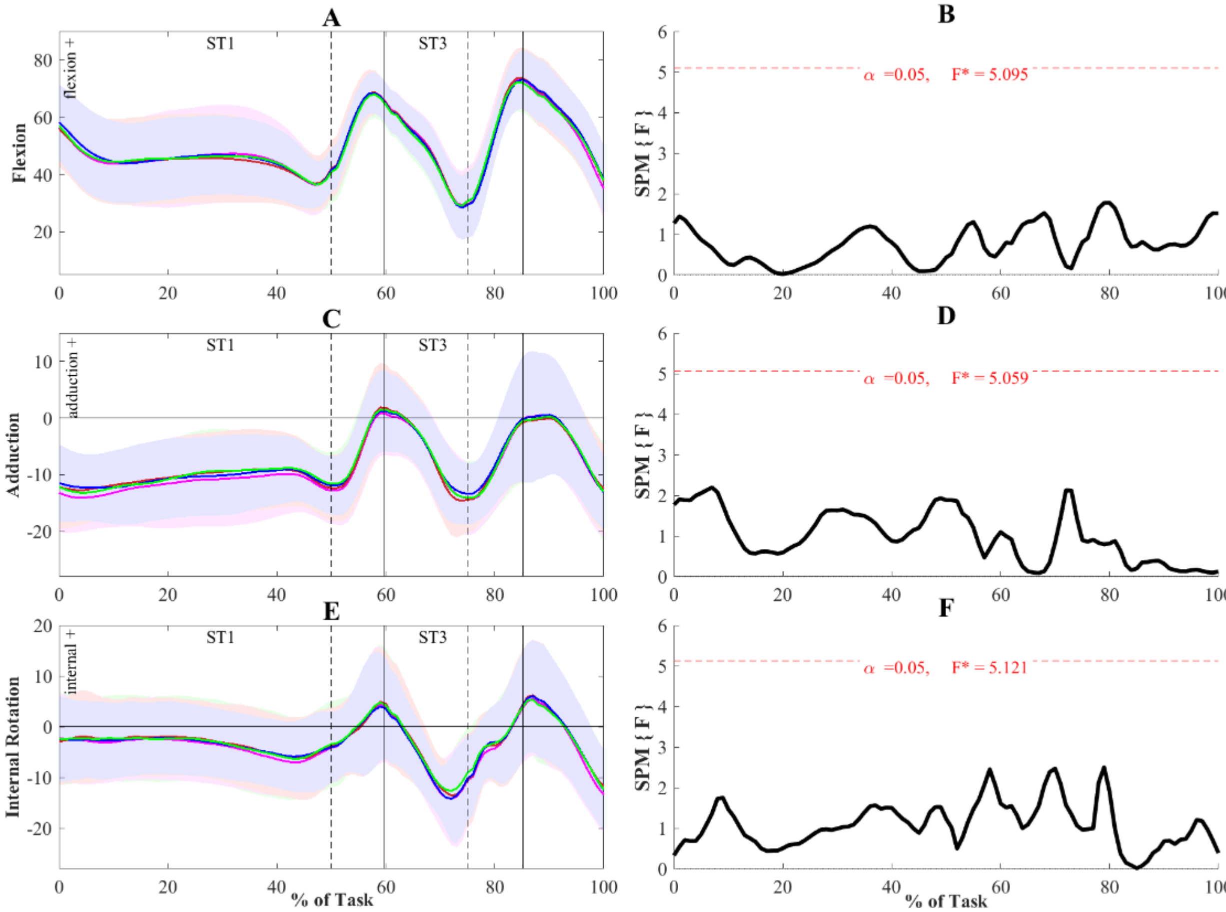

Note. (A) Hip flexion/extension, (C) hip adduction/abduction, (E) hip internal/external rotation for the outside leg. Angles are represented in degrees where flexion, adduction, and internal rotation are positive. Angles are expressed as a percentage of the left turn task, where 0% marks the start of the turn event. Associated SPM {F} plots are positioned to the right of each joint angle waveform graph ((B), (D), (F)). Each coloured line represents blade conditions Single Radius (red), Triple Radius (magenta), Quadruple Radius (green), and Ellipse (blue). Shaded regions denote standard deviations with respective colours for each blade. Vertical lines indicate skate ON (solid) and skate OFF (dotted) events. Stance phases are labelled within their respective skate ON and OFF events. Regions where the scalar output statistic (SPM{F}) surpassed the critical threshold (F) indicate a significant difference in joint angle between blade conditions. These regions are shaded in grey with significance levels marked as * $p < 0.05$.

Figure G8

Inside leg hip flexion/extension, adduction/abduction, and internal/external rotation angles during left turns

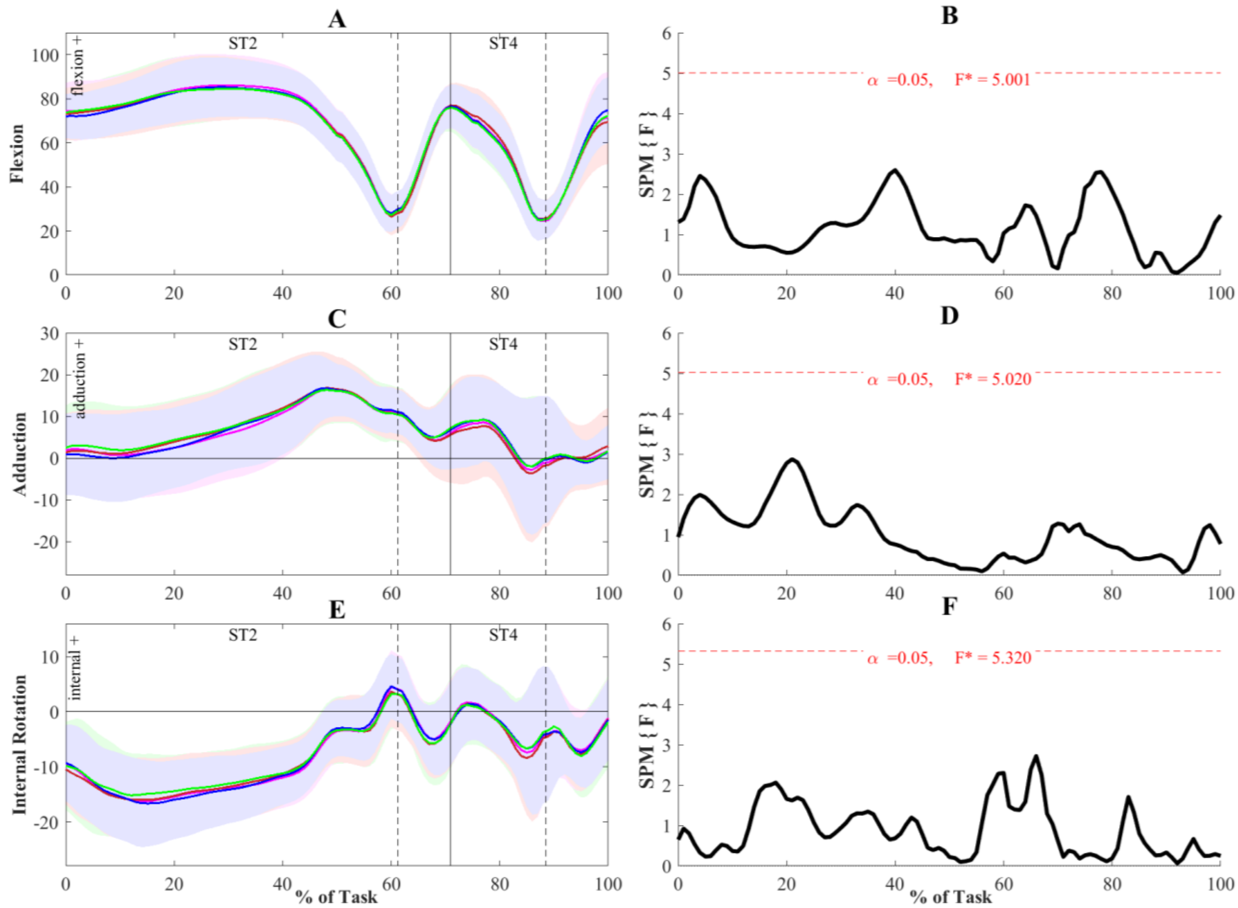

Note. (A) Hip flexion/extension, (C) hip adduction/abduction, (E) hip internal/external rotation for the inside leg. Angles are represented in degrees where flexion, adduction, and internal rotation are positive. Angles are expressed as a percentage of the left turn task, where 0% marks the start of the turn event. Associated SPM {F} plots are positioned to the right of each joint angle waveform graph ((B), (D), (F)). Each coloured line represents blade conditions Single Radius (red), Triple Radius (magenta), Quadruple Radius (green), and Ellipse (blue). Shaded regions denote standard deviations with respective colours for each blade. Vertical lines indicate skate ON (solid) and skate OFF (dotted) events. Stance phases are labelled within their respective skate ON and OFF events. Regions where the scalar output statistic (SPM{F}) surpassed the critical threshold (F) indicate a significant difference in joint angle between blade conditions. These regions are shaded in grey with significance levels marked as * $p < 0.05$.

Figure G9

Outside leg knee flexion/extension, internal/external rotation angles during left turns

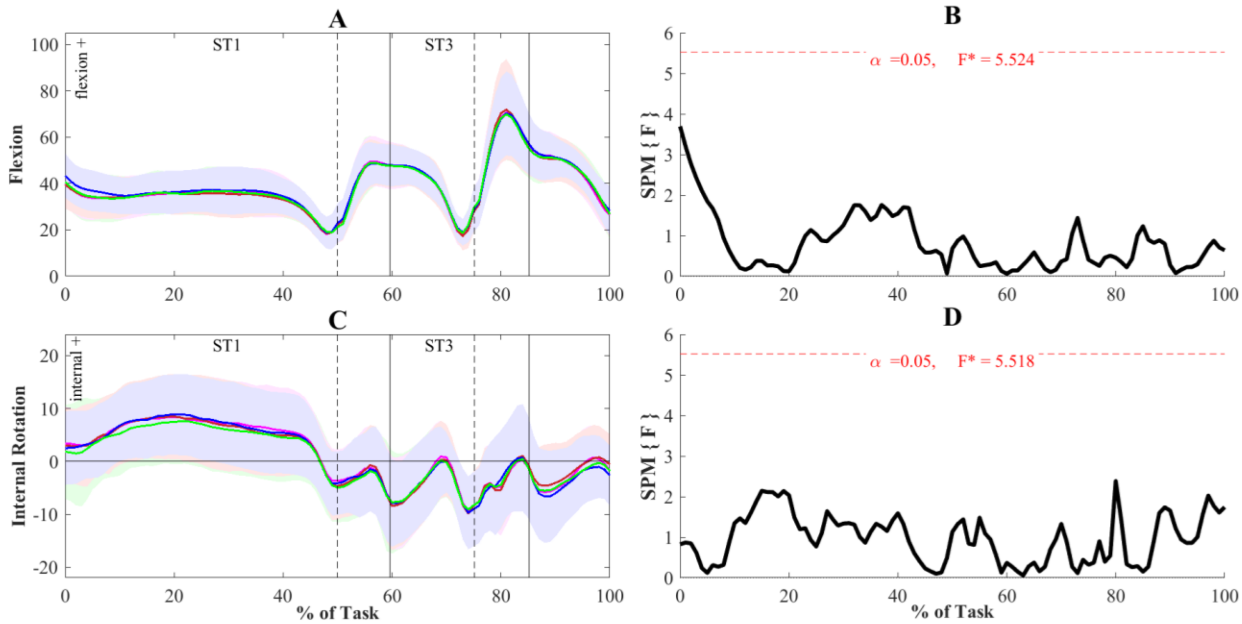

Note. (A) Knee flexion/extension, (C) knee internal/external rotation for the outside leg. Angles are represented in degrees where flexion and internal rotation are positive. Angles are expressed as a percentage of the left turn task, where 0% marks the beginning of the turn event. Associated SPM {F} plots are positioned to the right of each joint angle waveform graph ((B), (D)). Each coloured line represents blade conditions Single Radius (red), Triple Radius (magenta), Quadruple Radius (green), and Ellipse (blue). Shaded regions denote standard deviations with respective colours for each blade. Vertical lines indicate skate ON (solid) and skate OFF (dotted) events. Stance phases are labelled within their respective skate ON and OFF events. Regions where the scalar output statistic (SPM{F}) surpassed the critical threshold (F) indicate a significant difference in joint angle between blade conditions. These regions are shaded in grey with significance levels marked as * $p < 0.05$.

Figure G10

Inside leg knee flexion/extension, internal/external rotation angles during left turns

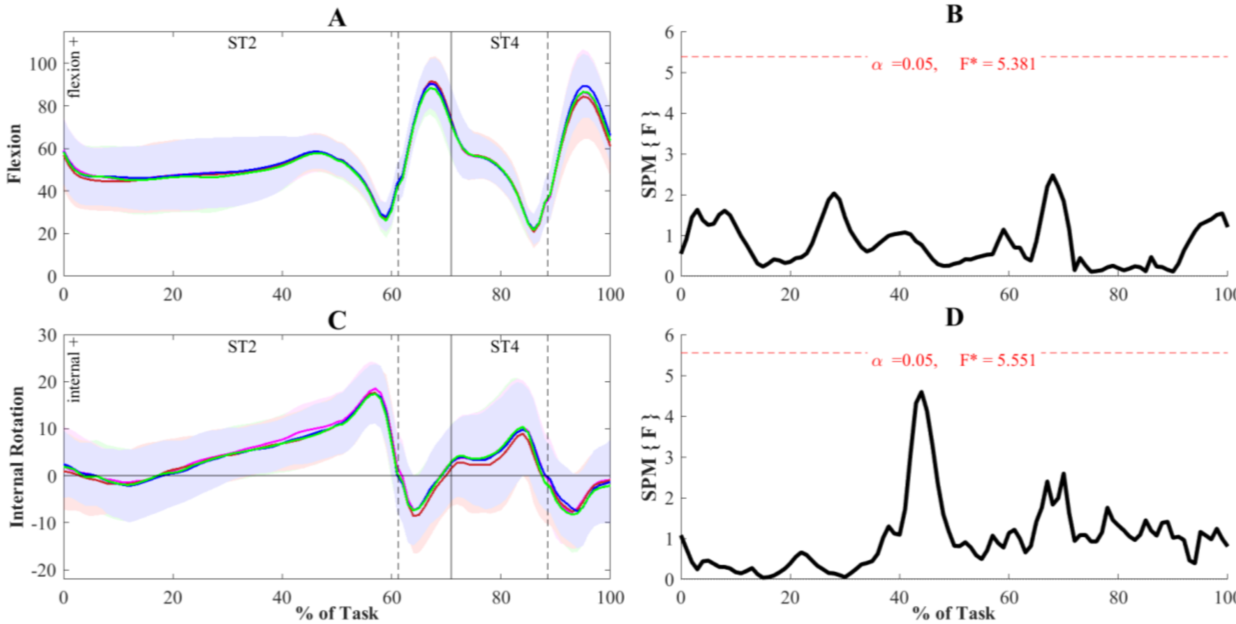

Note. (A) Knee flexion/extension, (C) knee internal/external rotation for the inside leg. Angles are represented in degrees where flexion and internal rotation are positive. Angles are expressed as a percentage of the left turn task, where 0% marks the beginning of the turn event. Associated SPM {F} plots are positioned to the right of each joint angle waveform graph ((B), (D)). Each coloured line represents blade conditions Single Radius (red), Triple Radius (magenta), Quadruple Radius (green), and Ellipse (blue). Shaded regions denote standard deviations with respective colours for each blade. Vertical lines indicate skate ON (solid) and skate OFF (dotted) events. Stance phases are labelled within their respective skate ON and OFF events. Regions where the scalar output statistic (SPM{F}) surpassed the critical threshold (F) indicate a significant difference in joint angle between blade conditions. These regions are shaded in grey with significance levels marked as * $p < 0.05$.

Figure G11

Outside leg ankle dorsi/plantar flexion, inversion/eversion, and internal/external rotation angles during left turns

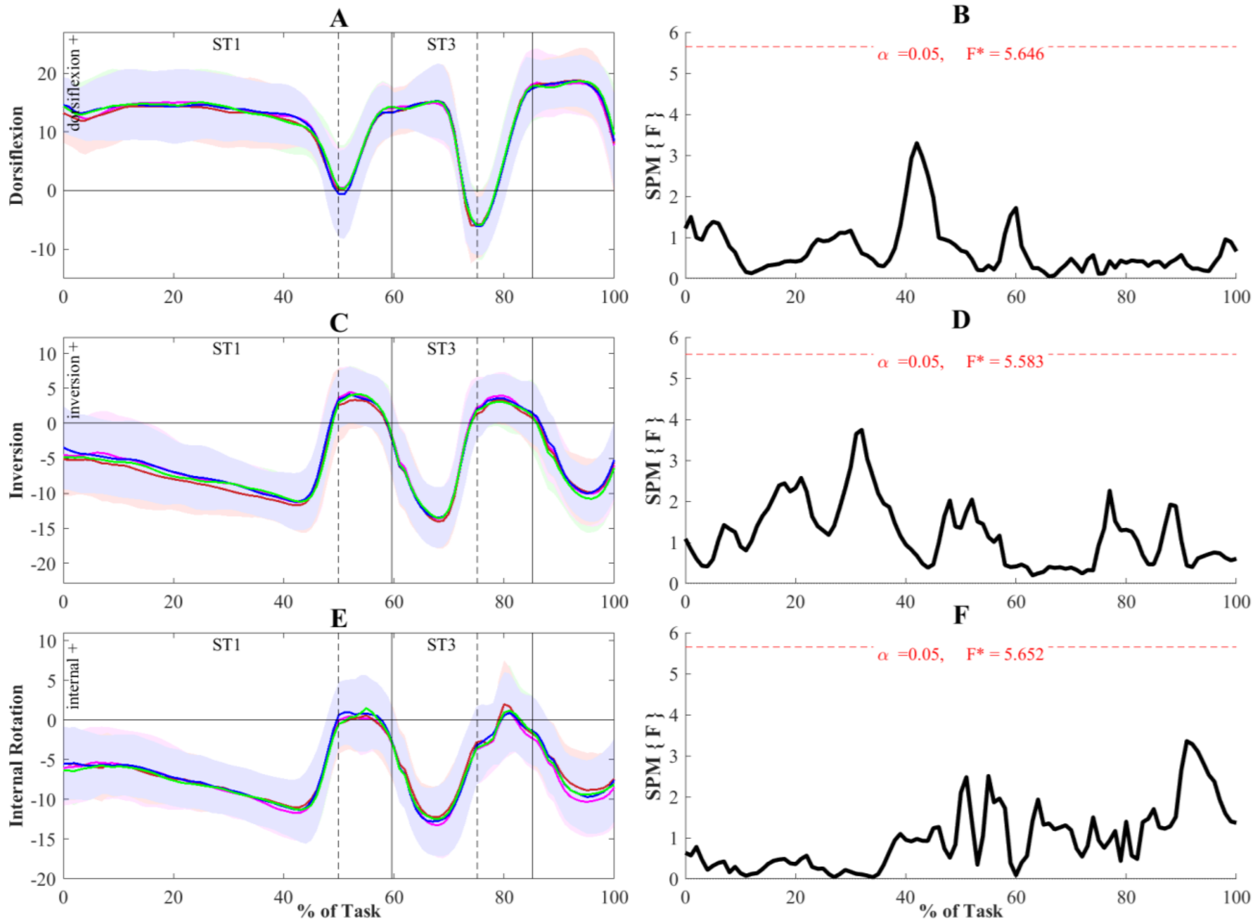

Note. (A) Ankle dorsi/plantarflexion, (C) ankle inversion/eversion, (E) ankle internal/external rotation for the outside leg. Angles are represented in degrees where dorsiflexion, inversion, and internal rotation are positive. Angles are expressed as a percentage of the left turn task, where 0% marks the beginning of the turn event. Associated SPM {F} plots are positioned to the right of each joint angle waveform graph ((B), (D), (F)). Each coloured line represents blade conditions Single Radius (red), Triple Radius (magenta), Quadruple Radius (green), and Ellipse (blue). Shaded regions denote standard deviations with respective colours for each blade. Vertical lines indicate skate ON (solid) and skate OFF (dotted) events. Stance phases are labelled within their respective skate ON and OFF events. Regions where the scalar output statistic (SPM{F}) surpassed the critical threshold (F) indicate a significant difference in joint angle between blade conditions. These regions are shaded in grey with significance levels marked as * $p < 0.05$.

Figure G12

Inside leg ankle dorsi/plantar flexion, inversion/eversion, and internal/external rotation angles during left turns

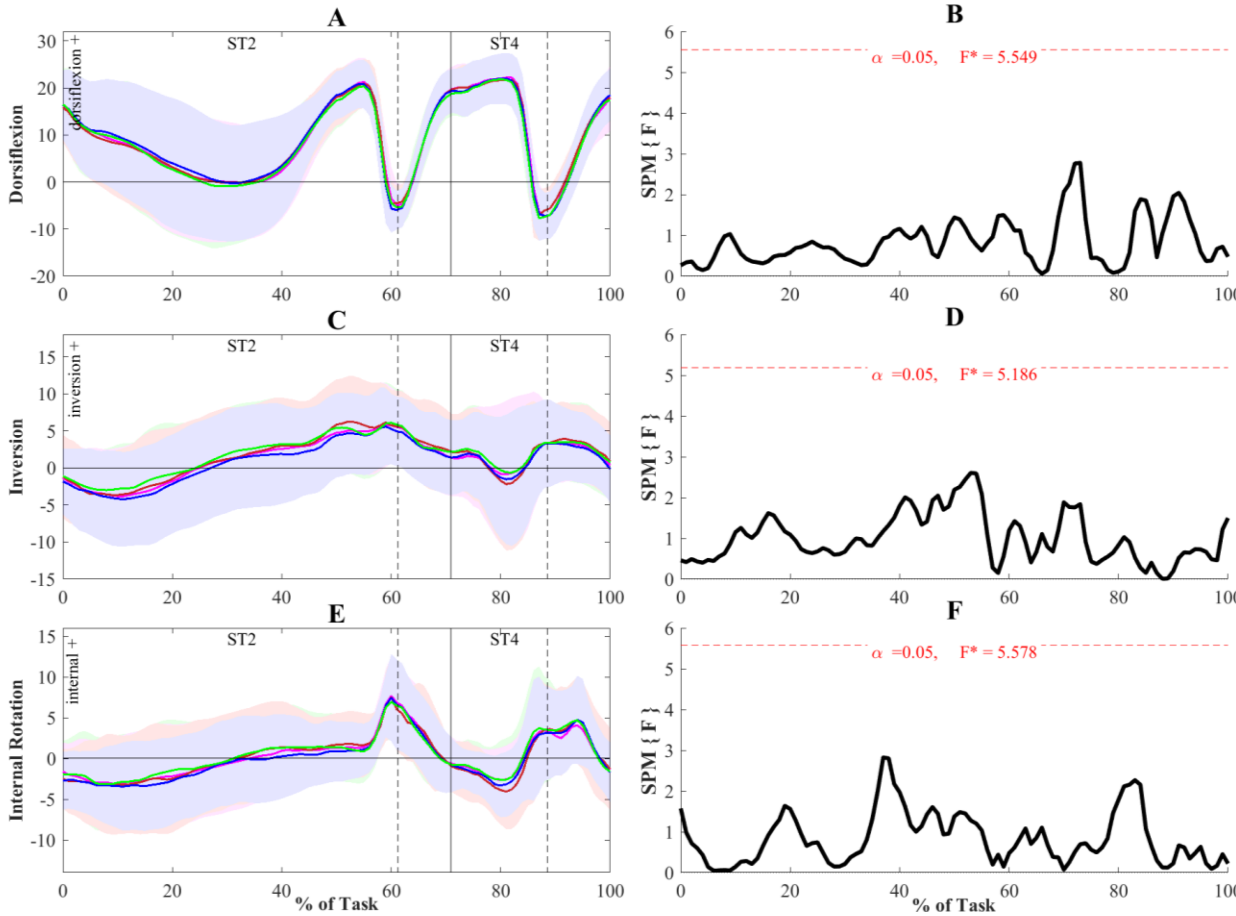

Note. (A) Ankle dorsi/plantarflexion, (C) ankle inversion/eversion, (E) ankle internal/external rotation for the inside leg. Angles are represented in degrees where dorsiflexion, inversion, and internal rotation are positive. Angles are expressed as a percentage of the left turn task, where 0% marks the beginning of the turn event. Associated SPM {F} plots are positioned to the right of each joint angle waveform graph ((B), (D), (F)). Each coloured line represents blade conditions Single Radius (red), Triple Radius (magenta), Quadruple Radius (green), and Ellipse (blue). Shaded regions denote standard deviations with respective colours for each blade. Vertical lines indicate skate ON (solid) and skate OFF (dotted) events. Stance phases are labelled within their respective skate ON and OFF events. Regions where the scalar output statistic (SPM{F}) surpassed the critical threshold (F) indicate a significant difference in joint angle between blade conditions. These regions are shaded in grey with significance levels marked as * $p < 0.05$.

Figure G13

Outside leg hip flexion/extension, adduction/abduction, and internal/external rotation angles during right turns

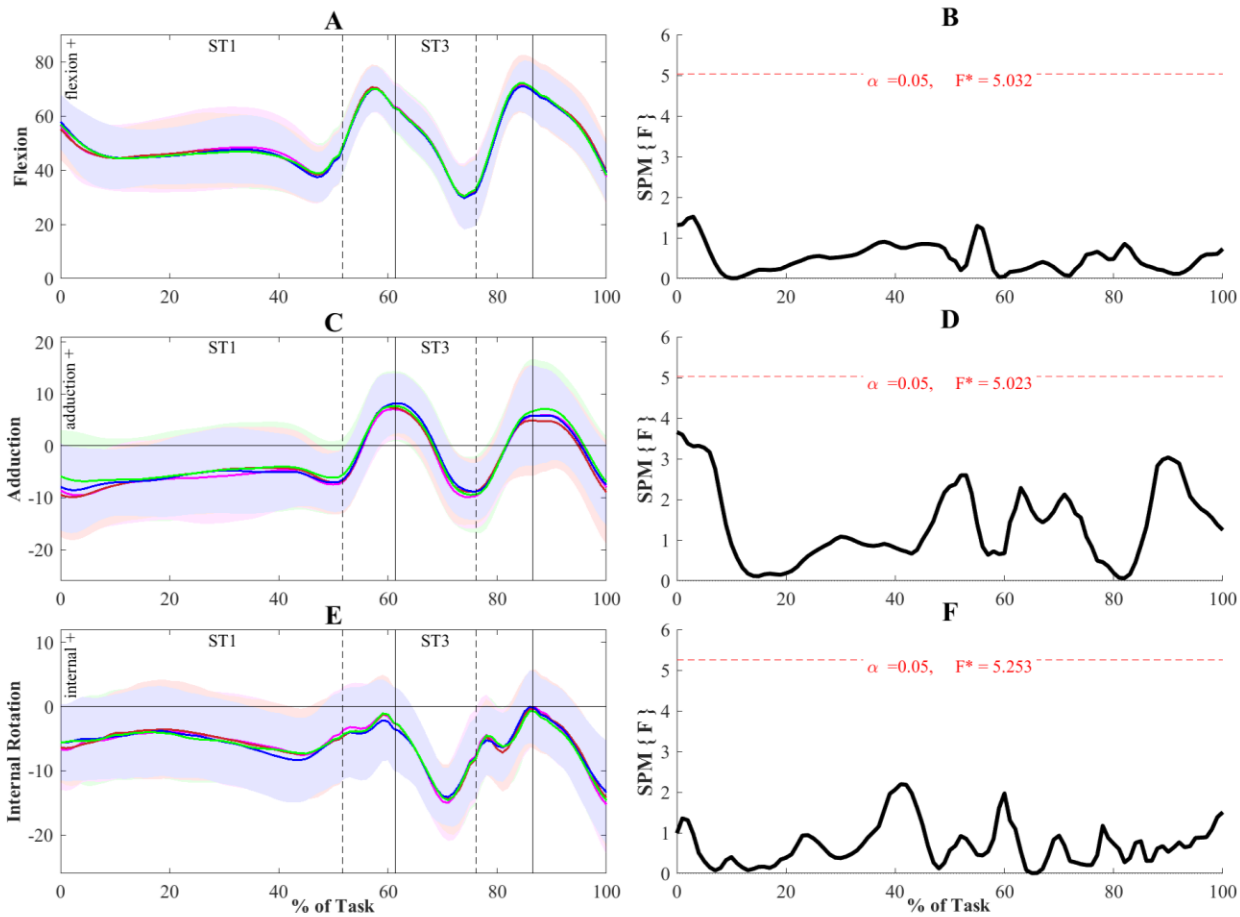

Note. (A) Hip flexion/extension, (C) hip adduction/abduction, (E) hip internal/external rotation for the outside leg. Angles are represented in degrees where flexion, adduction, and internal rotation are positive. Angles are expressed as a percentage of the right turn task, where 0% marks the beginning of the turn event. Associated SPM {F} plots are positioned to the right of each joint angle waveform graph ((B), (D), (F)). Each coloured line represents blade conditions Single Radius (red), Triple Radius (magenta), Quadruple Radius (green), and Ellipse (blue). Shaded regions denote standard deviations with respective colours for each blade. Vertical lines indicate skate ON (solid) and skate OFF (dotted) events. Stance phases are labelled within their respective skate ON and OFF events. Regions where the scalar output statistic (SPM{F}) surpassed the critical threshold (F) indicate a significant difference in joint angle between blade conditions. These regions are shaded in grey with significance levels marked as * $p < 0.05$.

Figure G14

Inside leg hip flexion/extension, adduction/abduction, and internal/external rotation angles during right turns

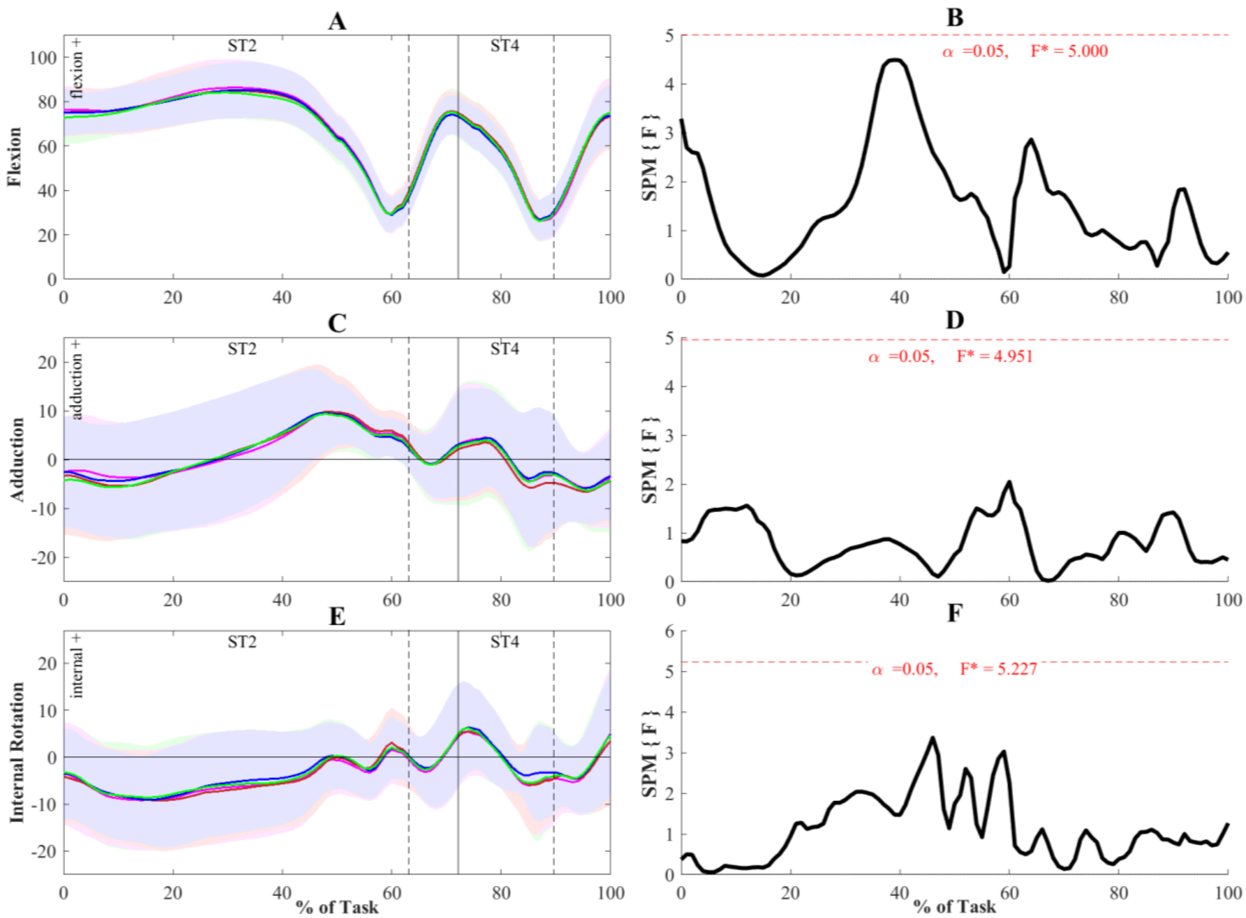

Note. (A) Hip flexion/extension, (C) hip adduction/abduction, (E) hip internal/external rotation for the inside leg. Angles are represented in degrees where flexion, adduction, and internal rotation are positive. Angles are expressed as a percentage of the right turn task, where 0% marks the beginning of the turn event. Associated SPM {F} plots are positioned to the right of each joint angle waveform graph ((B), (D), (F)). Each coloured line represents blade conditions Single Radius (red), Triple Radius (magenta), Quadruple Radius (green), and Ellipse (blue). Shaded regions denote standard deviations with respective colours for each blade. Vertical lines indicate skate ON (solid) and skate OFF (dotted) events. Stance phases are labelled within their respective skate ON and OFF events. Regions where the scalar output statistic (SPM{F}) surpassed the critical threshold (F) indicate a significant difference in joint angle between blade conditions. These regions are shaded in grey with significance levels marked as * $p < 0.05$.

Figure G15

Outside leg knee flexion/extension, and internal/external rotation angles during right turns

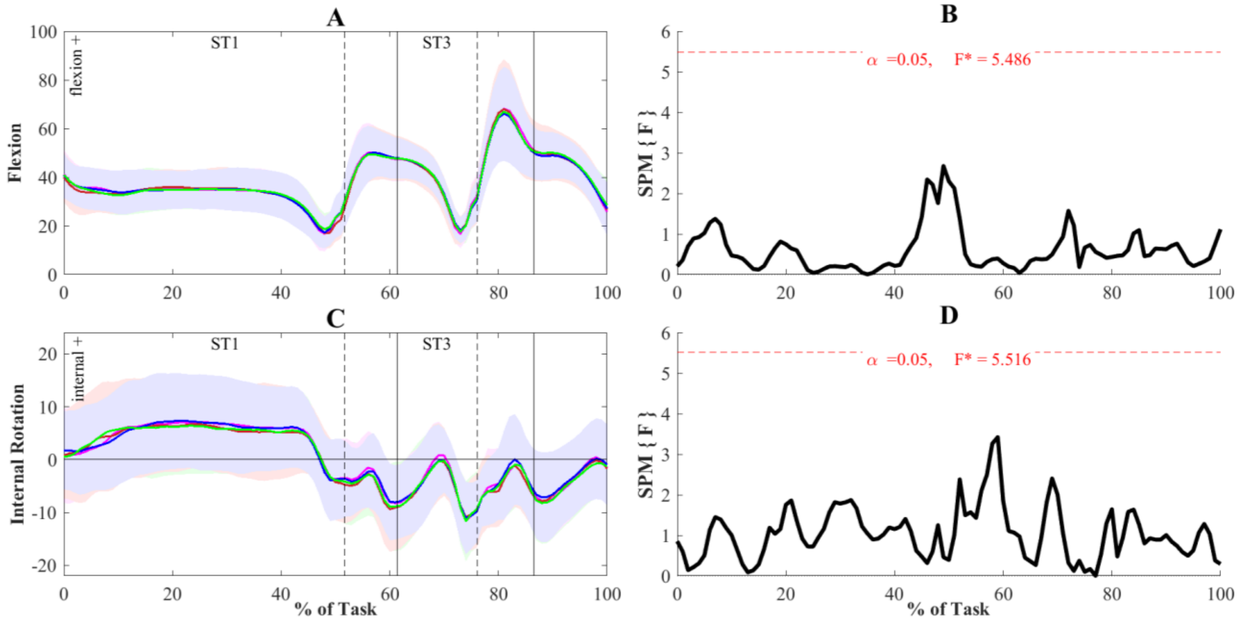

Note. (A) Knee flexion/extension, (C) knee internal/external rotation for the outside leg. Angles are represented in degrees where flexion and internal rotation are positive. Angles are expressed as a percentage of the right turn task, where 0% marks the beginning of the turn event. Associated SPM {F} plots are positioned to the right of each joint angle waveform graph ((B), (D)). Each coloured line represents blade conditions Single Radius (red), Triple Radius (magenta), Quadruple Radius (green), and Ellipse (blue). Shaded regions denote standard deviations with respective colours for each blade. Vertical lines indicate skate ON (solid) and skate OFF (dotted) events. Stance phases are labelled within their respective skate ON and OFF events. Regions where the scalar output statistic (SPM{F}) surpassed the critical threshold (F) indicate a significant difference in joint angle between blade conditions. These regions are shaded in grey with significance levels marked as * $p < 0.05$.

Figure G16

Inside leg knee flexion/extension, and internal/external rotation angles during right turns

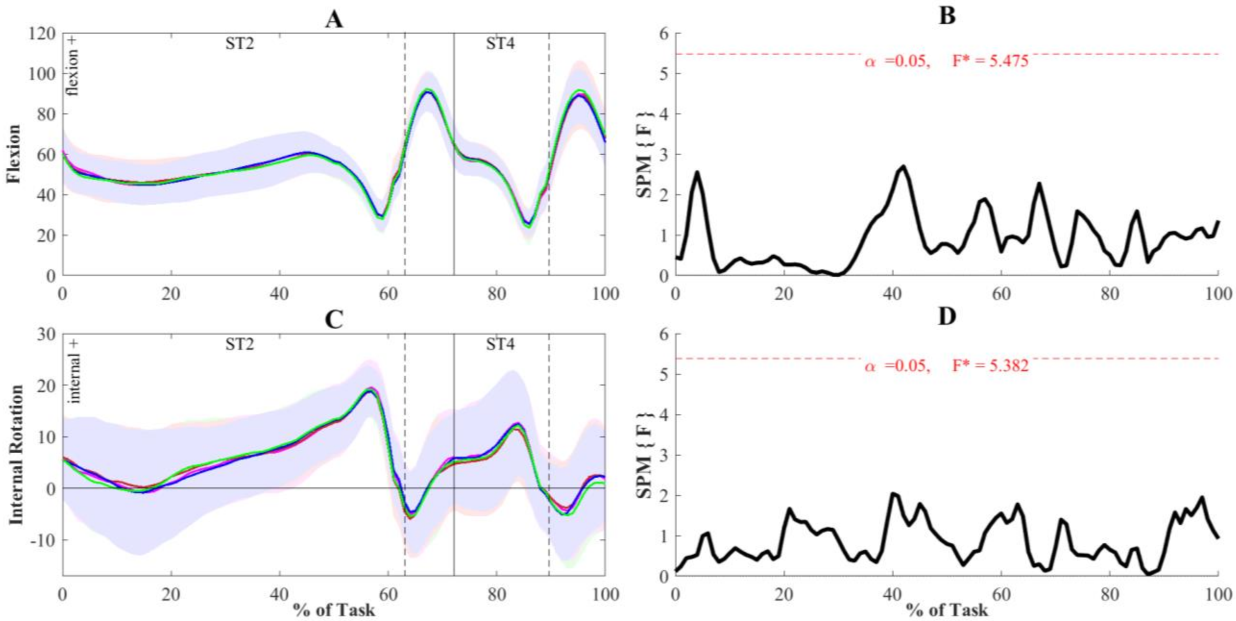

Note. (A) Knee flexion/extension, (C) knee internal/external rotation for the inside leg. Angles are represented in degrees where flexion and internal rotation are positive. Angles are expressed as a percentage of the right turn task, where 0% marks the beginning of the turn event. Associated SPM {F} plots are positioned to the right of each joint angle waveform graph ((B), (D)). Each coloured line represents blade conditions Single Radius (red), Triple Radius (magenta), Quadruple Radius (green), and Ellipse (blue). Shaded regions denote standard deviations with respective colours for each blade. Vertical lines indicate skate ON (solid) and skate OFF (dotted) events. Stance phases are labelled within their respective skate ON and OFF events. Regions where the scalar output statistic (SPM{F}) surpassed the critical threshold (F) indicate a significant difference in joint angle between blade conditions. These regions are shaded in grey with significance levels marked as * $p < 0.05$.

Figure G17

Outside leg ankle dorsi/plantarflexion, inversion/eversion, and internal/external rotation angles during right turns

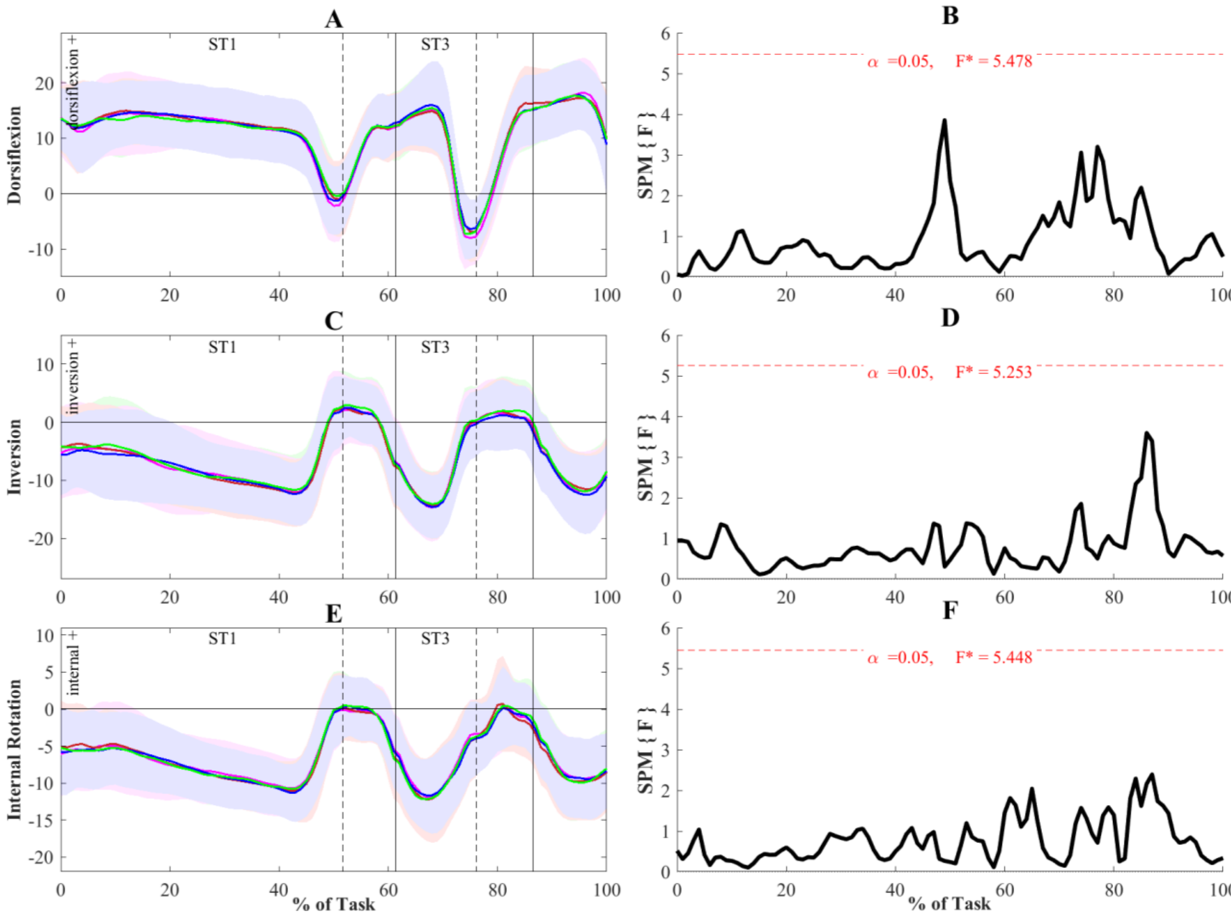

Note. (A) Ankle dorsi/plantarflexion, (C) ankle inversion/eversion, (E) ankle internal/external rotation for the outside leg. Angles are represented in degrees where dorsiflexion, inversion, and internal rotation are positive. Angles are expressed as a percentage of the right turn task, where 0% marks the beginning of the turn event. Associated SPM {F} plots are positioned to the right of each joint angle waveform graph ((B), (D), (F)). Each coloured line represents blade conditions Single Radius (red), Triple Radius (magenta), Quadruple Radius (green), and Ellipse (blue). Shaded regions denote standard deviations with respective colours for each blade. Vertical lines indicate skate ON (solid) and skate OFF (dotted) events. Stance phases are labelled within their respective skate ON and OFF events. Regions where the scalar output statistic (SPM{F}) surpassed the critical threshold (F) indicate a significant difference in joint angle between blade conditions. These regions are shaded in grey with significance levels marked as * $p < 0.05$.